ROLE OF NUCLEAR RECEPTOR-INDEPENDENT PATHWAYS IN THE MECHANISM OF ACTION OF PEROXISOME PROLIFERATORS

Courtney Georgette Woods

A dissertation submitted to the faculty of the University of North Carolina at Chapel Hill in partial fulfillment of the requirements for the degree of Doctor of Philosophy in the Department of Environmental Sciences and Engineering, School of Public Health

Chapel Hill
2007

Approved by:

Ivan Rusyn, M.D., Ph.D.

Michael Cunningham, Ph.D.

Rebecca Fry, Ph.D.

James Swenberg, D.V.M., Ph.D.

David Threadgill, Ph.D.

ABSTRACT

COURTNEY G WOODS: Role of Nuclear Receptor–Independent Pathways in the Mechanism of Action of Peroxisome Proliferators
(Under the direction of Dr. Ivan Rusyn)

Peroxisome proliferators are a structurally diverse group of chemicals that are non-genotoxic hepatocarcinogens in rodents. For decades there has been controversy surrounding these compounds because of the uncertainty of human risk, high potential for exposure and insufficient understanding of their mechanism of action in rodents. Two key molecular pathways are thought to be important in the mode of action: activation of the nuclear receptor PPARα in liver parenchymal cells, and activation of Kupffer cells, which do not express PPARα. In hepatocytes, PPARα mediates peroxisome induction, increased fatty acid metabolism and alterations in gene expression. Furthermore, activation of the PPARα is required for peroxisome proliferator-induced carcinogenesis. In Kupffer cells, acute administration of peroxisome proliferators stimulates oxidant production and mitogenic cytokine release, as well as activation of NFκB, a transcription factor implicated in cell proliferation and apoptosis. The role that Kupffer cells play in chronic effects of peroxisome proliferators is not yet known. We hypothesized that peroxisome proliferators activate Kupffer cells to produce oxidants that may be involved in oxidative cellular damage, and that mediate cytokine production. The cytokines stimulate proliferative and anti-apoptotic effects of these chemical agents. To test this hypothesis, we first evaluated whether peroxisome proliferators cause a sustained increase in reactive oxygen species (ROS) in rodent liver. *In*

vivo measurements of ROS in *PPARα* -null or NADPH oxidase-deficient (*p47*^{phox}-null) mice following sub-acute treatment with di-(2-ethylhexyl) phthalate (DEHP) or 4-chloro-6-(2,3-xylidino)-2-pyrimidinylthio acetic acid (WY-14,643), both model peroxisome proliferators revealed a persistent elevation in oxidant production with parenchymal cells, not Kupffer cells as the primary molecular source. Next, the role of Kupffer cell oxidants and PPARα in mediating proliferative, apoptotic and oxidative stress responses was assessed. Findings from a five month WY-14,643 feeding study suggest that NADPH oxidase is not required for increased hepatocellularl proliferation or DNA damage, but may be important to anti-apoptotic effects. Finally, gene expression profiling revealed a temporal shift from Kupffer cell to PPARα-dependence of peroxisome proliferator-induced changes. Collectively, our findings demonstrate that Kupffer cell-mediated events play an important role in early responses, but are short-lived and likely not required for chronic effects of peroxisome proliferators, including hepatocarcinogenesis.

ACKNOWLEDGEMENTS

I greatly appreciate the training and guidance that my advisor, Dr. Ivan Rusyn, has provided over the course of my graduate studies. I trust that the skill sets that I have obtaining while in Dr. Rusyn's laboratory will serve me well in my career. I am continually inspired by him to become a mentor to young researchers. I am very thankful for having worked with supportive, constructive committee members, Dr. James Swenberg, Dr. David Threadgill, Dr. Rebecca Fry, and Dr. Michael Cunningham. Their advice and input was invaluable to the completion of this research project.

I must also acknowledge several other researchers and scientists whose contributions were important to my research:

- Dr. Ronald Mason, Dr. Maria Kadiiska, Dr. Henry Conner, Dr. Jinjie Jiang, and Jean Corbett of the National Institute of Environmental Health Sciences;
- Dr. Jeffery Peters and Dr. Jack vanden Heuval of Pennsylvania State University;
- Dr. Akira Maki, Dr. Wonyoung Tak and Robert Schoonhoven, former employees of University of North Carolina at Chapel Hill

I am very grateful for having been surrounded by lab mates who gave willingly of their time and fun-loving spirit and did not hestitate to offer their assistance. It was truly a joy to work with them all. Miss Amanda Burns, Mrs. Oksana Kosyk, Miss Pamela Ross and Mrs. Svitlana Shymonyak provided a helping hand with experiments. Ms. Blair Bradford also was a valuable source of information, guidance and encouragement. Miss Christine Powell was a wonderful office mate who provided much support and encouragement each day.

Thanks to the staff of the Research Education Support (RES) program, Dr. Henry Frierson and Kathy Wood, for providing my first year of graduate funding and travel allowance to attend conferences. I also appreciate the many efforts they have made to change the landscape of doctoral programs across the country by providing underrepresented minorites with opportunities to conduct undergraduate and graduate research.

I would be remiss if I did not acknowledge the many friends and family who were constant cheerleaders during my graduate studies. Lastly, I could not have completed this journey had it not been for the unconditional love and inspiration from my mother, Doris Woods Baskett, who continues to be a source of strength for me. She was my biggest fan and with her support I felt like anything was possible.

TABLE OF CONTENTS

LIST OF FIGURES

LIST OF TABLES

LIST OF ABBREVIATIONS AND SYMBOLS

ALT	alanine aminotransferase
ACO	acyl-coA oxidase
BrdU	5-Bromo-2'-deoxyuridine
CDK	cyclin dependent kinase
CYP	cytochrome P450
DEHP	di(2-ethylhexyl)phthalate
ESR	electron spin resonance
FDR	false discovery rate
GO	gene ontology
H_2O_2	hydrogen peroxide
•L	lipid centered radical
CO_2^{-}•	carbon dioxide radical anion
NFκB	nuclear factor kappa B
POBN	α-(4-pyridyl-1-oxide)-*N*-tert-butylnitrone
PPAR	peroxisome proliferator activated receptor
PPRE	peroxisome proliferator response element
ROS	reactive oxygen species
RT-PCR	reverse transcriptase-polymerase chain reaction
SAM	significance analysis of microarrays
TNF	tumor necrosis factor
WY-14,643	[4-Chloro-6-(2,3-xylidino)-2-pyriminylthio]acetic acid

CHAPTER I

INTRODUCTION

A. PEROXISOME PROLIFERATORS

1. General Use, Exposure and Risk Assessment

Peroxisome proliferators are a structurally diverse group of chemicals that have been identified as non-genotoxic hepatocarcinogens in rodents. Members of this class, include naturally occurring steroids, such as leukotriene B_4 (LTB4), and 8(S)-hydroxyeicosatetraenoic acid (8(S)-HETE), fatty acids, such as ω-3 polyunsaturated fatty acids, very long chain fatty acids, as well as synthetic compounds, such as hypolipidemic drugs (fibrates), industrial plasticizers, such as di-(2-ethylhexyl)phthalate (DEHP), some pesticides, and halogenated solvent, trichloroethylene (TCE) [1]. Within the peroxisome proliferator class, phthalate esters are one of the most important chemical groups. The widespread use of phthalates in consumer products, medical devices, food packaging, automotives and other applications has greatly increased the potential for occupational and environmental exposure. Common exposure routes for the general population include inhalation, ingestion, intravenous and dermal contact [2]. Children, blood-transfusion patients and dialysis patients represent two segments of the population at high risk of exposure, due to the use of phthalates in children's toys and medical tubing and containers. Intravenous exposure levels in patients can range from 1-2 mg/kg/day and infants may ingest 10-100 μg /kg/ day from chewing on toys containing phthalates [3]. In 2005, the European Union approved a permanent ban (to update the temporary ban issued in 1999) on use of phthalates in children's toys. The US currently does not restrict its use in any products.

In 2000, the International Agency for Research on Cancer (IARC) downgraded DEHP to a category reserved for chemicals with no evidence of cancer causing potential in humans on the basis that "the mechanism (peroxisome proliferation) by which DEHP

increases the incidence of hepatocellular tumours (*sic*) in rats and mice is not relevant to humans" [4]. Several other peroxisome proliferators, including clofibrate, and gemfibrozil are also categorized by IARC in Group 3, as not classifiable with regard to human carcinogenicity. The US Environmental Protection Agency (US EPA) classifies the DEHP and other phthalate esters as a probable carcinogen, with the qualifier that there is inadequate data to provide a causal link between human exposure and cancer.

The dearth of epidemiological data and unknown human relevance of mechanisms of action of peroxisome proliferators in laboratory animals makes it challenging to determine human risk of cancer by phthalates and other peroxisome proliferators. A limited amount of human data from long term, large scale studies investigating the effects of peroxisome proliferators is available. The few epidemiological studies that have been conducted failed to observe a correlation between peroxisome proliferator exposure and cancer incidence [5-7]. In addition to gathering human data, there remains a considerable amount of work to be done in the way of elucidating the mechanism of carcinogenesis in rodents and understanding the relevance of animal data to human risk.

2. Pathophysiological changes and carcinogenesis in rodent liver following peroxisome proliferator treatment

Many of the effects of peroxisome proliferators are mediated by nuclear receptor peroxisome proliferator activated receptor (PPAR)α. Ligand binding of PPARα by peroxisome proliferator compounds leads to transcriptional activation of genes encoding peroxisomal enzymes [8]. Peroxisome proliferators, as the name implies, also cause a marked increase in the number and size of peroxisomes [9]. Peroxisomes are ubiquitous

organelles that are largely responsible for fatty acid β-oxidation of very long chain fatty acids, oxidation of cholesterol derivatives, D- and L- amino acid oxidation, and purine catabolism. In rat liver, an array of H_2O_2 -generating oxidases are present in peroxisomes, including urate oxidase, acyl-coA oxidase (ACO), along with H_2O_2-degrading enzyme catalase. While peroxisome proliferation and induction of fatty acid metabolism are hallmarks of peroxisome proliferator treatment, a causal link between this response and tumor formation has yet to be identified [10].

Exposure to peroxisome proliferators causes a range of acute and chronic pleiotropic responses in rodent liver. Gross and histological hepatic changes observed following treatment with peroxisome proliferators include hepatomegaly, hepatocellular hyperplasia and hypertrophy [11]. Peroxisome proliferators also cause a significant reduction in adiposity and lower serum triglyceride levels, a characteristic for which it has been exploited as a therapeutic agent for hyperlipidemic patients. Lipid lowering effects of perioxisome proliferator pharmaceutical compounds are a result of increased lipid metabolism and transport [12]. Peroxisome proliferators also contribute to increased oxidant production in cells through induction of peroxisomal, mitochondrial and microsomal and enzymes, and reduction in glutathione S-transferase and superoxide dismutase [13-15].

Chronic exposure to peroxisome proliferators in rodents leads to the formation of hepatocellular neoplasia. The tumors are generally multiple in liver and have been known to metastasize to the lungs. Nafenopin was the first peroxisome proliferators proven to cause hepatocellular carcinomas in mice [16]. Subsequently, WY-14,643 and DEHP were shown to induce liver tumors in rats and mice [17,18]. Potent peroxisome proliferators such as ciprofibrate, WY-14643 and tibric acid induced liver tumors in 100% of the rats and mice

that were given dietary treatment for 50-60 weeks [19]. Less potent peroxisome proliferator, DEHP requires at least 70 weeks for tumor development [17]. Interestingly, studies have shown that most of the effects of peroxisome proliferators are reversible [20]. Even adenomas can regress when peroxisome proliferator administration ceases. As stated previously, PPARα-null mice are resistant to peroxisome proliferator-induced tumorigenesis [21]. Surprisingly, naïve acyl-coA oxidase null mice have been shown to develop spontaneous tumors [22].

Peroxisome proliferator-induced tumors histologically can be trabecular to poorly differentiated in appearance. These tumors do not express the classical liver markers gamma-glutamyltranpeptidase (GGT) or glutathione-S-transferase (GST-π) [23,24]. Protein profiling confirmed reduction of, GST-π, which suggests that PPARα may be a negative regulator of this enzyme [25].

3. Species Differences in response to peroxisome proliferators

Across species, there is a significant difference in response to peroxisome proliferators. While mice and rats appear to be a very susceptible species, with long-term peroxisome proliferator administration resulting in liver carcinomas and adenomas, there is no evidence to date that chronic administration of these agents leads to tumors in non-human primates or humans [11]. In fact, humans, and non-human primates appear to be refractory to many of the pleiotropic responses associated with these compounds, including hepatoceulluar and hepatic peroxisome proliferation for many peroxisome proliferator compounds. Gemfibrozil, fenofibrate and nafenopin cause hepatic peroxisomal proliferation and significant induction of peroxisomal enzymes is rodents, but cause only a slight increase or no change in enzyme activity or peroxisome abundance in the non-human primates and dogs.

Conversely, potent peroxisome proliferator ciprofibrate has been shown to increase peroxisome number and activity in marmosets and rhesus monkeys [26,26]. *In vitro* studies have demonstrated that cell proliferation has been identified as a correlative marker of species sensititivy to peroxisome proliferators, over anti-apoptotic effects [27].

Expression of PPARα is at least 10–fold less in humans than in rodents [28]. It is possible that the low level of PPARα expression in humans is sufficient to mediate peroxisome proliferator-induced hypolipidemia, but not adequate to activate the numerous genes associated with rodent peroxisome proliferation and cancer. In addition to differences in expression, there also appears to be a difference in the genes regulated by rodent PPARα and human PPARα. *In vitro* experiments have shown that genes responsive to PPARα in rodent liver were not responsive in human liver cell lines, even when human PPARα was overexpressed [29,30]. The comparison between rodent and human peroxisome proliferators response element (PPRE) sensitivity/responsiveness have also been made. It has been shown that acyl-coA oxidase in rats responds to peroxisome proliferators via its PPRE, whereas the human acyl-coA oxidase fails to respond because its PPRE is inactive [31]. Finally, species differences in metabolism are also being investigated. A study investigated enzyme activity in DEHP-treated microsomes from rats, mice and marmoset [32]. The most prominent species differences were most evident in lipase activity, the enzyme responsible for converting DEHP to mono (2-ethylhexyl) phthalate (MEHP). A 150 to 350-fold difference was observed with mice exhibiting the highest activity and marmosets exhibiting the lowest. To help determine susceptibility of humans to peroxisome proliferators, determining which molecular events are important for rodent carcinogenicity of these agents is necessary.

B. KEY EVENTS IN THE MODE OF ACTION OF PEROXISOME PROLIFERATORS AND THE MOLECULAR MEDIATORS INVOLVED

1. Induction of peroxisomal proliferation by peroxisome proliferators

Induction of peroxisomes is thought to be important in the mode of action of peroxisome proliferators because of their role in mediating oxidative stress which may be responsible for DNA damage and altered cell turnover. While PPARα activation is responsible for transcriptional regulation of peroxisomal genes, evidence for PPARα-independent peroxisome proliferation by WY-14,643 and fenofibrate exists [33,34]. In fact, compounds with high specificity for PPARγ over PPARα display a high degree of peroxisome proliferation (DeLuca et al., 2000). These findings suggest that cross-talk between PPAR isoforms may occur and contribute to peroxisome proliferation and some of the pleiotropic effects of peroxisome proliferation. Though the weight of evidence for peroxisome proliferation by peroxisome proliferators is very strong, there is uncertainty of a causal link to cell proliferation and tumor formation. Previous studies have shown a poor correlation between peroxisome proliferation and hepatocellular proliferation (Marsman et al., 1988).

2. Increased cell proliferation and suppression of apoptosis by peroxisome proliferators

Induction of cell proliferation is an important event in the mode of action of nongenotoxic carcinogens. Increased cell replication facilitates the fixation of DNA damage and silencing of tumor suppressor genes. These conditions promote clonal expansion of mutated cells and development of focal lesions in the liver. Peroxisome proliferators appear

to induce mitogenic, not compensatory cell proliferation [35]. Several compounds have been identified as possessing mitogenic properties, including nafenopin, WY-14, 643, ciprofibrate and clofibric acid [35-38]. Also peroxisome proliferator-induced increases in expression of proliferating cell nuclear antigen (PCNA), cyclin dependent kinases (CDKs), cyclins, and other cell cycle regulatory proteins in mouse liver have been reported [39], although the mechanism for this regulation remains unknown. A strong correlation between replicative DNA synthesis and hepatocarcinogenecity has been demonstrated using peroxisome proliferators, DEHP and WY-14,643. Cell replication, which varies greatly between DEHP and WY-14,643 was the better determinant of the two compound's tumorigenic potency, than peroxisomal proliferation, which is comparable between both compounds [38]. This and other studies also demonstrated a rapid induction of cell proliferation, within several hours of treatment. Despite continued treatment, the proliferative response was diminished to control levels for DEHP and slightly above control for WY-14,643 by 4 weeks of treatment. These findings point to the importance of cell proliferation in the carcinogenic mechanism of these compounds.

Suppression of apoptosis is another important cellular event that contributes to non-genotoxic carcinogenesis. Just as cell proliferation is critical to clonal expansion of initiated cells, apoptosis is equally as important in removing DNA-damaged cells that could potentially be tumorigenic. Viability assays have shown that peroxisome proliferator-treated rat hepatocytes can be maintained for at least 4 weeks, compared to 8 days for control-treated cells. Also signs of apoptosis (i.e. condensed or fragmented nuclei) were less frequently observed in peroxisome proliferator-treated cultures [40]. A role for tumor necrosis factor

(TNF)α in anti-apoptotic effects of peroxisome proliferators has been previously demonstrated [41].

3. Induction of oxidative stress and DNA damage by peroxisome proliferators

Oxidative stress is another important mechanism of action of non-genotoxic carcinogens. Peroxisome proliferators are well known for their induction of metabolizing enzymes. H_2O_2 generation from these enzymes has been implicated an important event in the mechanism of action of these compounds. Peroxisomal oxidases and cytochrome P450 (CYP) enzymes are the two main sources of H_2O_2 in parenchymal cells. Under normal physiologic conditions they account for about 80% of the H_2O_2 in the liver [42]. Acyl-coA oxidase and the 4A family of CYPs are associated with the degradation of long chain and very long chain fatty acids by β-oxidation and ω-oxidation, respectively. CYP4A has also been identified as a primary route for metabolism of lipid peroxidation product, trans-4-hydroxy-2-nonenal (HNE) [42,43]. Expression of CYP4A and acyl-coA oxidase enzymes can increase by 20- to 40-fold when induced by peroxisome proliferators, thus increasing the H_2O_2 load on the cell considerably [44,45]. Other sources of peroxisome proliferator-induced oxidants include Kupffer cells. These cells produce highly reactive superoxide and nitric oxide radicals which may be involved in second messenger signaling and/or macromolecular damage. Previous studies have demonstrated that NADPH oxidase in nonparenchymal cells is essential for early oxidant production by peroxisome proliferators [46].

There is still uncertainty as to whether there is a significant increase in oxidant production by peroxisomes. The H_2O_2 generating enzymes are balanced with induction of oxidant scavenging enzymes, such as catalase [44,47]. Though the induction of catalase is

not proportional to that of acyl-coA oxidase, catalase has a high capacity for scavenging H_2O_2. Furthermore, there are conflicting data regarding the level of damage inflicted upon macromolecules by peroxisome proliferator-induced oxidants. In parenchymal cells, conversion of H_2O_2 to reactive hydroxyl radicals (following Haber-Weiss chemistry) that immediately react with surrounding lipid membranes is one hypothesized mechanism of intra-hepatic oxidative stress. Lipid radicals and other by-products of peroxidation can cause oxidative damage to DNA. Several studies have reported increases in lipid peroxidation products such as conjugated dienes, aldehydes, and HNE as a result of peroxisome proliferators treatment in rats [48,49]. However, there are an equal number of studies that have failed to detect any increases. F_2-isoprostanes, a sensitive marker of arachidonic acid peroxidation were not significantly elevated in WY-14,643 treated mice. These experiments were however conducted relatively low dose of WY-14,643 (100 ppm) [50], which may have been insufficient for inducing oxidative damage. Oxidation of DNA bases, resulting in formation of 8-hydroxy deoxyguanosine (8-OHdG) has also been detected in livers of rats chronically exposed to peroxisome proliferators [51,52]. These adducts, if unrepaired, can be fixed into gene mutations during DNA replication. Other studies in rats have either failed to demonstrate increases in 8-OHdG in treated versus control liver DNA, or have been unable to link the magnitude of 8-OHdG levels to tumor multiplicity [53,54].

With regards to peroxisome proliferator –mediated changes in cell turnover, a great deal of uncertainty in the role of reactive oxygen species still exists. Oxidants (produced in parenchymal and nonparenchymal cells) are thought to act as signaling molecules to recruit mitogenic cytokines which cause increased cell turnover.

4. PPARα as a mediator of lipid metabolism and peroxisome proliferator-induced hepatocarcinogenesis

PPARα is a transcription factor involved in regulating expression of genes, largely involved in fatty acid metabolism (Figure 1.1). PPARα activation by peroxisome proliferators leads to transcription of genes that encode proteins involved in fatty acid metabolism and transport. Enzymes such as peroxisomal acyl-coA oxidase are increased 15-fold or greater in liver tissue that exhibits peroxisome proliferation [19,47]. Also ω-oxidation enzyme activity (i.e. CYP4A superfamily) is significantly elevated by PPARα agonists [55,56]. It is suspected that PPARα-mediated induction of lipid metabolism and reverse transport of cholesterol is what contributes to a reduction in serum cholesterol and triglyceride levels resulting from PPARα adminstration [12]. PPARα-null mice exhibit significantly higher serum lipid levels than their wild type counterparts and are refractory from peroxisome prolierator-induced reductions in serum lipids [57]. Indeed, the role of PPARα in transcriptional activation of many mediators in fatty acid metabolism clearly points to its importance physiologically in lipid homeostasis. The relevance of peroxisome proliferation and induction of lipid metabolism to the mechanism of carcinogenesis, however is still unknown. Metabolizing enzymes are an important source of oxidants which may be involved in mediating the effects of peroxisome proliferators (i.e through signaling) and may be involved in oxidative DNA, protein or lipid damage.

Activation of PPARα is required for peroxisome proliferator-induced tumorigenesis [21]. An 11-month WY-14,643 feeding study resulted in hepatocellular adenomas or carcinoma development in all wild type mice, while PPARα-null mice given the same treatment did not develop tumors, nor did they exhibit any of the pleiotropic responses

associated with peroxisome proliferator treatment. Though the mechanism of carcinogenesis is still largely unknown, this single study demonstrates the importance of PPARα in mediating the carcinogenicity by peroxisome prolifertators. Studies where PPARα wild type and knockout mice were fed different PPARα agonists have shown similar results [58].

PPARα activation and perturbation of cell proliferation and apoptosis are all causally linked to peroxisome proliferator-induced liver carcinogenesis, but the molecular mechanisms by which these events occur and how PPARα is involved remains to be shown. DNA replication and proliferation in hepatocytes are PPARα dependent, though there is no evidence of direct transcriptional regulation on cell-cycle genes by PPARα. It is clear that cyclin and CDK expression is elevated by PPARα agonists [39], but these genes do not possess a PPRE. It has been suggested that these mRNA are indirectly regulated by PPARα and more directly regulated by PPARα specific target genes. Previous studies have shown that PPARα is critical for cytokine-induced cell proliferation through mediating Ras and RhoA prenylation [59]. One hypothesis is that activation of PPARα results in the formation of various by-products of lipid metabolism, which facilitate membrane binding of small GTPases (i.e. Ras, RhoA). Once membrane-bound, these GTPases can stimulate cell proliferation in response to mitogenic signals.

PPARα also appears to play a role in inhibiting apoptosis. *In vitro* studies with WY-14,643, nafenopin and methylclofenapate showed suppression of spontaneous hepatocyte apoptosis and TGFβ1-induced apoptosis with peroxisome proliferators administration [60,61]. One study shows that the inhibition of apoptosis by PPARα can be eliminated by introducing a negative effector regulator of the nuclear receptor [62].

5. Role of Kupffer cells in pleiotropic effects of peroxisome proliferators

In vitro studies using peroxisome proliferators in pure hepatocytes fail to replicate the proliferative reponses observed *in vivo* [38]. This observation led to the hypothesis that nonparenchymal cells may be involved in peroxisome proliferator-induced cell replication. While the importance of PPARα in peroxisome proliferator-induced carcinogenesis is undisputable, many studies have revealed PPARα-independent responses in rodent liver that may be just as important. The role of Kupffer cells in peroxisome proliferator-induced responses has been studied extensively over the last 10 years.

When activated, Kupffer cells, which are the resident macrophages of the liver release mitogenic cytokines and chemotactic mediators (e.g. tumor necrosis factor-alpha epidermal growth factor, hepatocyte growth factor) which can influence cell growth. Both *in vitro* and *in vivo* experiments demonstrate that peroxisome proliferators are capable of activation Kupffer cells [63]. This activation is independent of PPARα, as Kupffer cells do not express this isoform of the PPAR [64]. While a putative mechanism of Kupffer cell activation has yet to be determined, it is hypothesized that these compounds either diffuse into membranes due to their lipophilicity or peroxisome proliferators incorporate into low density lipoproteins (LDL) and binding of the modified lipoprotein on the LDL receptors causes activation of Kupffer cells.

Kupffer cell inhibitors have been used extensively to demonstrate the role of nonparenchymal cells in cell proliferation. WY-14,643–induced increases in hepatocyte proliferation were abrogated by inactivating Kupffer cells with methyl palmitate or glycine [65,66]. Increases in mRNA expression of mitogenic cytokine, TNFα were also blocked. These findings point to the importance of Kupffer cells in hepatocyte growth and also

implicate TNFα as a mediator of cell proliferation. The importance of TNFα to peroxisome proliferator-induced cell proliferation was proven when WY-14,643-induced increases in cell turnover were completely blocked by pre-treatment with anti- TNFα antibodies [67]. It should be noted that peroxisome proliferators induce levels of TNFα production by Kupffer cells that are well below levels necessary to cause inflammation or apoptosis, as these are not responses associated with peroxisome proliferator exposure [68,69]. *In vitro* studies demonstrated that absence of nonparenchymal cells prevents hepatic proliferation by WY-14, 643 or nafenopin [70,71]. Collectively, these findings clearly demonstrate a dependence on Kupffer cells for proliferative responses observed following peroxisome proliferator treatment. More specifically, it can be concluded that there is a causal relationship between TNFα from nonparenchymal cells and the proliferative effect of WY-14, 643.

NFκB is also an important mediator of cellular responses to peroxisome proliferator in rodent liver. This transcription factor has been shown to regulate genes involved in cell growth and differentiation, apoptosis and inflammation [72]. Peroxisome proliferators, WY-14,643 and ciprofibrate can increase NFκB [73,74] DNA binding activity. Furthermore, it has been demonstrated that the active form of NFκB, is almost exclusively localized in nonparenchymal cells at levels that are 20-fold greater than in parenchymal cells following acute treatment with WY-14,643 [74]. NFκB has been previously demonstrated to be sensitive to cellular redox state in a manner such that increases in intracellular oxidants cause NFκB activation [75]. Therefore, oxidant production by peroxisome proliferators may play a role in NFκB induction.

Like hepatocytes, a number of oxidant producing enzymes are present, including NAPDH oxidase, inducible nitric oxide and xanthine oxidase. Oxidants from these sources

can play a role in signaling and activation of downstream mediators of cell proliferation. Activation of NADPH oxidase and production of superoxide occurs as a result of Kupffer cell activation [69]. As a result, peroxisome proliferator treatment in rodents was suspected to cause an increase in Kupffer cell-derived oxidants. When measured *in vitro*, superoxide production in Kupffer cells was found to be elevated in a dose-dependent manner by WY-14,643 and DEHP metabolite, monoethylhexyl phthalate (MEHP) [76]. This response was inhibited when Kupffer cells were inactivated with glycine. *In vivo* measurements unequivocally point to NADPH oxidase in Kupffer cells as being the source of early oxidants production caused by peroxisome proliferators. Increased levels of α-[4-Pyridyl-1-oxide] N-tert-butylnitrone (POBN) /radical adducts were detected in rat bile by electron spin resonance (ESR) two hours after DEHP administration and pre-treatment with dietary glycine abrogated DEHP-induced free radical production [46]. Furthermore, when this study was repeated in NADPH oxidase deficient ($p47^{phox}$ –null) and *PPARα*-null mice, NADPH oxidase not PPARα was identified as the source of early oxidant production. A link between Kupffer cell-derived oxidants and events leading to hepatocellular proliferation was made when inhibition of NADPH oxidase with diphenyleniodonium (DPI) blocked WY-14,643-induced cell proliferation and NFκB activity [77]. These responses, along with TNFα mRNA expression were also suppressed in $p47^{phox}$ –null mice.

When considered collectively, these studies provide strong evidence for the involvement of Kupffer cells in cell proliferation by peroxisome proliferators. In particular, oxidant activation of NFκB, leading to TNFα production appears to be an early response that may be important to the mechanism of action of these compounds.

C. RATIONALE AND SPECIFIC AIMS

1. Rationale

The mechanism of carcinogenesis by peroxisome proliferators in rodents is not completely understood but is hypothesized to involve the following: (i) induction of hepatic peroxisomes, (iI) activation of nuclear receptor PPARα and Kupffer cells, independent of each other, (iii) induction of oxidant generating enzymes and production of reactive oxygen species that can act as second messangers and cause DNA damage, (iv) release of mitogenic cytokines by Kupffer cells and (v) increased proliferation of hepatocytes and decreased apoptosis. Figure 1.2 shows a scheme with many of the key events mediated by Kupffer cells and parenchymal cells. A major task remains to fit these events together to understand the mechanism of carcinogenesis. The major premise of the specific aims below is to elucidate how these cellular and molecular pathways interact to bring about the changes that lead to cancer and in particular, whether PPARα-independent and dependent pathways are involved in long-term molecular changes caused by peroxisome proliferators.

2. Determine the effects of peroxisome proliferators on prolonged reactive oxygen species production.

Previous *in vivo* measurements revealed that the peroxisome proliferator, DEHP caused an increase in free radical generation in liver only 2 hr after it was administered [46]. We hypothesize that feeding mice a DEHP- or WY-14,643-containing diet will cause a sustained increase in oxidants, which will correlate with the tumorigenic potency of the peroxisome proliferator agent. In this aim, we will further test this hypothesis by

investigating oxidant production over a range of time points and determining the molecular source of free radicals by using knockout mice. *PPARα* -null and NADPH oxidase –deficient (*p47*^{phox}-null) mice and corresponding wild type mice will be fed DEHP or WY-14,643 (0.05% w/w) for 3 days, 1 week or 3 weeks. Following administration of a spin trap, α-(4-pyridyl-1-oxide)-*N*-tert-butylnitrone (POBN) bile samples will be collected and measured by electron spin resonance (ESR). This experimental approach is novel, as it provides direct evidence of radical generation, as opposed to extrapolating this data from markers of oxidative stress. We expect that WY-14,643 but not DEHP will have a sustained effect on production of oxidants for up to 3 weeks. Furthermore, we expect that NADPH oxidase will contribute to observed increases in oxidant production.

3. Investigate PPARα-dependent and -independent mechanisms involved in peroxisome proliferator-induced cell proliferation, apoptosis and DNA damage

While it is clear that Kupffer cell-derived oxidants play a critical role in the initial peroxisome proliferator-induced proliferation in rodent liver, little is known about the potential for the long-term effects of Kupffer cell activation and whether this plays a role in carcinogenesis. To address this important question, we will conduct a long-term dietary study in *p47*^{phox}-null mice, a mouse model that was used to conclusively demonstrate the role of NADPH oxidase in early oxidant production, mitogenic cytokine release and cell proliferation by peroxisome proliferator, WY-14,643 [77]. We expect that feeding WY-14,643, not DEHP will produce a sustained oxidant generation. For this reason, we will use WY-14,643 to further investigate phenotypic responses to peroxisome proliferators. WY-14,643 (0.1%)-containing diet will be administered for 1 week, 5 weeks, or 5 months to

p47^{phox}-null mice, *PPARα*-null mice. Cell proliferation, apoptosis and oxidative DNA damage endpoints will be measured, as these are key events for the mode of action of rodent carcinogenesis. Histological changes in liver and clinical chemistry will also be assessed.

Since Kupffer cell activation by peroxisome proliferators is PPARα-independent, these results will help differentiate receptor-mediated and –independent events in the mechanisms of hepatocarcinogenic action of peroxisome proliferators. We hypothesize that there will be a significant delay in proliferative effects of WY-14,643 in NADPH oxidase-deficient mice.

4. Understand the temporal role of PPARα-dependent and -independent pathways using gene expression profiling.

In this aim, we will identify variations in global transcriptional activation induced by WY-14,643 in our two knockout models. Because our preliminary studies suggest that there may be a temporal difference in the onset of Kupffer cell-mediated and PPARα-mediated events, we will select both acute and sub-chronic time points for these experiments. Computational analysis of the data will be carried out to establish common fingerprints characteristic of the exposure to these agents and whether these changes correlate with dose, time, strain and other variables. By assessing changes in the expression of genes involved in regulating cell growth, apoptosis and oxidative stress, we expect to determine genes with dose and/or time-dependent responses and also genes that are associated with PPARα -or Kupffer cell-dependent pathways. Findings from microarray experiments will be confirmed using RT-PCR. This is a well established technique for measuring mRNA levels and often

used to validate microarray findings. We expect that the results of this aim will reveal distinguishable "signature" profiles at each condition (dose, time, knockout gene).

Figure 1.1. Gene network regulated by PPARα consists primarily of lipid metabolism modulators.

On this and other figures, proteins involved in cell proliferation (denoted by "*" and highlighted yellow), apoptosis (denoted by "†" and highlighted blue) or oxidative stress (denoted by "‡" and highlighted red) were identified by searching for these terms in each proteins' GO Biological Processes using PathStudio software.

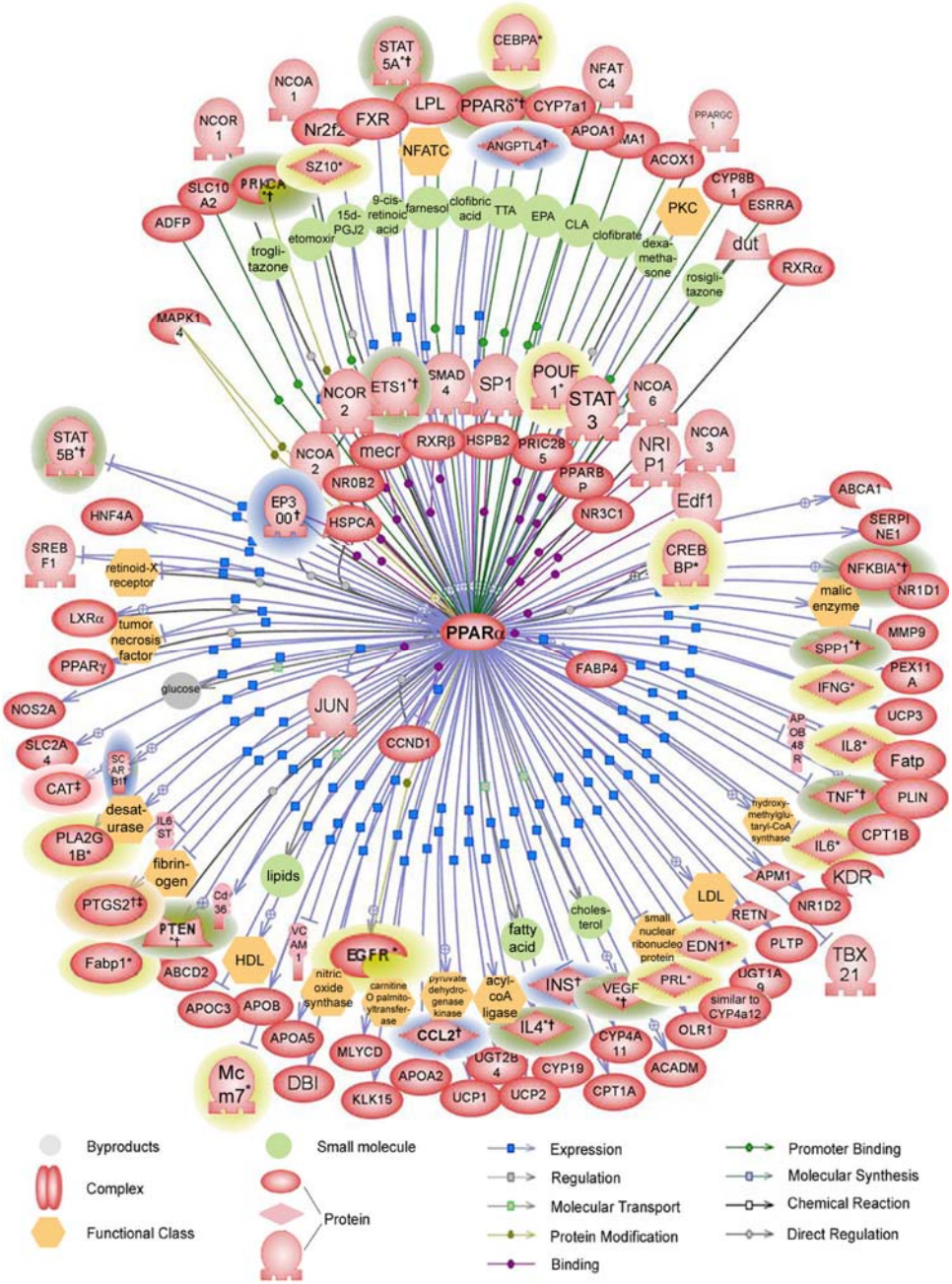
PPARα
STAT 5A*†
CEBPA*
NCOA 1
NFAT C4
LPL
PPARδ*†
CYP7a1
FXR
Nr2f2
NCOR 1
APOA1
ACOX1
NFATC
ANGPTL4†
SZ10*
SLC10 A2
PRKCA *†
ADFP
CYP8B 1
ESRRA
PKC
dut
RXRα
etomoxir
troglitazone
15d-PGJ2
9-cis-retinoic acid
farnesol
clofibric acid
TTA
EPA
CLA
clofibrate
dexamethasone
rosiglitazone
MAPK14
NCOR 2
ETS1*†
SMAD 4
SP1
POUF 1*
STAT 3
NCOA 6
NCOA 2
mecr
RXRβ
HSPB2
PRIC285
NRIP1
NCOA 3
PPARBP
NR0B2
NR3C1
Edf1
STAT 5B*†
EP300†
HSPCA
HNF4A
SREBF1
retinoid-X receptor
CREBBP*
ABCA1
SERPINE1
NFKBIA*†
NR1D1
malic enzyme
LXRα
tumor necrosis factor
PPARγ
glucose
FABP4
SPP1*†
MMP9
PEX11A
IFNG*
NOS2A
JUN
CCND1
UCP3
SLC2A4
SCARB1†
CAT‡
IL8*
Fatp
TNF*†
PLIN
desaturase
IL6ST
hydroxymethylglutaryl-CoA synthase
CPT1B
PLA2G1B*
IL6*
fibrinogen
lipids
APM1
KDR
PTGS2†‡
Cd36
PTEN*†
LDL
NR1D2
cholesterol
RETN
PLTP
small nuclear ribonucleoprotein
EDN1*
TBX21
Fabp1*
ABCD2
HDL
VCAM1
EGFR*
fatty acid
PRL*
UGT1A9
nitric oxide synthase
carnitine O palmitoytransferase
pyruvate dehydrogenase kinase
acyl-coA ligase
INS†
VEGF*†
similar to CYP4a12
APOC3
APOB
CCL2†
IL4*†
OLR1
APOA5
MLYCD
CYP4A11
ACADM
Mcm7*
DBI
APOA2
UGT2B4
CYP19
KLK15
UCP1
UCP2
CPT1A
Byproducts
Complex
Functional Class
Small molecule
Protein
Expression
Regulation
Molecular Transport
Protein Modification
Binding
Promoter Binding
Molecular Synthesis
Chemical Reaction
Direct Regulation

Figure 1.2. Key events in the hypothesized mechanism of hepatocarcinogenesis for peroxisome proliferators involve both Kupffer cells and hepatocytes.

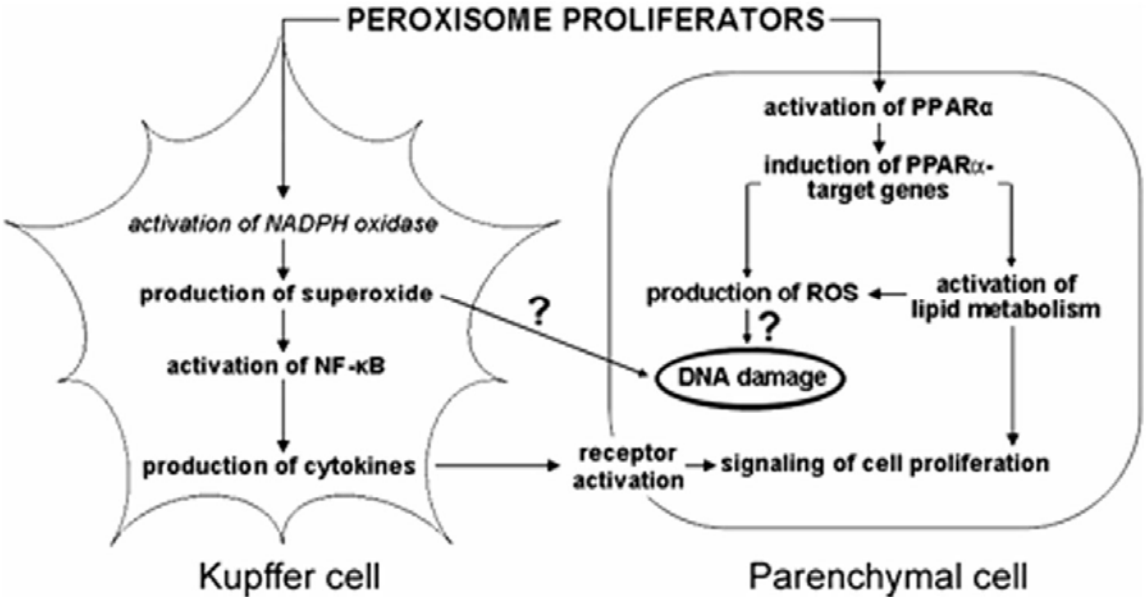

CHAPTER II

Sustained formation of POBN radical adducts in mouse liver by peroxisome proliferators is dependent upon PPARα, but not NADPH oxidase

A. ABSTRACT

Reactive oxygen species are thought to be crucial for peroxisome proliferator-induced liver carcinogenesis. Free radicals have been shown to mediate the production of mitogenic cytokines by Kupffer cells and cause DNA damage in rodent liver. Previous *in vivo* experiments demonstrated that acute administration of the peroxisome proliferator di-(2-ethylhexyl) phthalate (DEHP) led to an increase in production of free radicals in liver, an event that was dependent on Kupffer cell NADPH oxidase, but not peroxisome proliferator activated receptor (PPAR)α. Here, we hypothesized that continuous treatment with peroxisome proliferators will cause a sustained increase in free radicals in liver. Mice were fed diets containing either 4-chloro-6-(2,3-xylidino)-2-pyrimidinylthio acetic acid (WY-14,643, 0.05% w/w), or DEHP (0.6% w/w) for up to three weeks. Using α-(4-pyridyl-1-oxide)-*N*-*tert*-butylnitrone (POBN), liver-derived radical production was assessed in bile samples by measuring POBN-radical adducts using electron spin resonance. Our data indicate that WY-14,643 causes a sustained increase in free radicals in mouse liver and that this effect is greater than that of DEHP. To understand the molecular source of reactive oxygen species, NADPH oxidase-deficient ($p47^{phox}$-null) and *PPARα*-null mice were examined after treatment with WY-14,643. No increase in radicals was observed in *PPARα*-null mice that were treated with WY-14,643 for 3 weeks, while the response in $p47^{phox}$-nulls was similar to that of wild-type mice. These results show that PPARα, not NADPH oxidase, is critical for a sustained increase in radical production caused by peroxisome proliferators in rodent liver. Therefore, peroxisome proliferator-induced radical production in Kupffer cells may be limited to an acute response to these compounds in mouse liver.

B. INTRODUCTION

Peroxisome proliferators are a class of structurally diverse compounds that cause cancer in rodents by a non-genotoxic mechanism [78-80]. The high potential for human exposure and the known rodent carcinogenicity of these compounds has been the cause for intense debate for several decades regarding their potential adverse health effects in people [11]. The range of pleiotropic responses that these compounds induce in rodent liver includes increase in the size and number of peroxisomes in parenchymal cells, hepatomegaly, and induction of β-oxidation enzymes [38]. Considerable differences in metabolism and molecular changes induced by peroxisome proliferators in the liver, most predominantly the activation of the nuclear receptor peroxisome proliferator activated receptor (PPAR)α, have been identified between species [81]. In addition, PPARα-independent events that involve activation of Kupffer cells that involves production of reactive oxygen species have been also shown to occur after acute exposure to peroxisome proliferators in rodents [46].

Reactive oxygen species are implicated in the carcinogenesis mode of action of peroxisome proliferators. Oxidants have been shown to cause DNA damage, lipid peroxidation, and may also mediate signaling [82,83]. Within hepatocytes, these compounds activate transcription of genes encoding H_2O_2-generating enzymes, such as acyl-coA oxidase (ACO) and cytochrome P450 4A (CYP4A), and these events are known to be mediated by PPARα [42]. Studies using Kupffer cells demonstrated an increase in superoxide production *in vitro* 30 minutes after treatment with peroxisome proliferator, 4-chloro-6-(2, 3-xylidino)-2-pyrimidinylthio acetic acid (WY-14,643) [76]. *In vivo* studies of peroxisome proliferator-induced free radicals in rats using spin trap α-(4-pyridyl-1-oxide)-*N*-*tert*-butylnitrone (POBN) and electron spin resonance (ESR) detection reported an increase in radical adducts

in liver 2 hours following di-(2-ethylhexyl) phthalate (DEHP) treatment [46]. Furthermore, early reactive oxygen species generation as a result of DEHP administration was attributed to activation of NADPH oxidase in Kupffer cells, but not PPARα.

While many studies demonstrated a role for reactive oxygen species in the acute effects of peroxisome proliferators, it is not known whether Kupffer cell activation plays a role in radical generation during the long term exposure to peroxisome proliferators, and thus is a potential PPARα-independent mechanism of action of these compounds. The purpose of this study was to determine if peroxisome proliferator-derived reactive oxygen species production is in fact sustained and to identify the source of free radicals. These data provide direct evidence demonstrating that peroxisome proliferators cause a PPARα-dependent prolonged elevation in free radicals in rodent liver. Our findings suggest that Kupffer cell-derived free radical production is ephemeral and may be involved only in the acute phase of the response to these compounds in rodent liver.

C. MATERIALS AND METHODS

Animals

PPARα-null male mice (SV129 background; [33,84]), *p47*^{phox}-null male mice (C57BL/6J background; [85]) and corresponding wild-type counterparts (6-8 weeks of age) were used in these experiments. All animals used for this study were housed in sterilized cages in special facilities with a 12-hr night/day cycle. Temperature and relative humidity were held at 22 ± 2°C and 50 ± 5 %, respectively. The UNC Division of Laboratory Animal Medicine maintains these animal facilities, and veterinarians were always available to ensure animal health. All animals were given humane care in compliance with NIH and institutional guidelines and studies were performed according to approved protocols. Prior to experiments, animals were maintained on standard lab chow diet and purified water *ad libitum*.

Chemical Treatment

DEHP, WY-14,643, 2,2'-dipyridyl, and bathocuproinedisulfonic acid were obtained from Aldrich (Milwaukee, WI), and α-(4-pyridyl 1-oxide)-*N*-*tert*-butylnitrone (POBN) from Alexis (San Diego, CA). Control animals were given NIH-07 powdered diet. Treated animals were given the same diet blended with either DEHP or WY-14,643 at target concentrations of 0.6% w/w and 0.05% w/w, respectively. Diet was administered *ad libitum* for 3 days, 1 week or 3 weeks. Acutely treated mice were given one intragastric injection of either saline or DEHP at a dose of 1.2 g/kg.

Detection of Free Radicals in Bile

Animals were anesthetized with pentobarbital (75 mg/kg) and the spin trap POBN (1 g/kg, *i.p.*) was administered. The gallbladder was cannulated using a 10-cm long polyvinylchloride tube and bile samples were collected into Eppendorf tubes containing 50 μl of chelating agents, bathocupoinesulfonic acid (12 mM) and 2,2'-dipyridyl (30 mM) for 2 hrs. Bile samples were frozen immediately after collection and stored at -80°C until analyzed by electron spin resonance (ESR) spectroscopy. To consume endogenous ascorbic acid in bile which can act as reducing agent, an ascorbate oxidase spatula (Roche, Indianapolis, IN) was placed in the flat cell and O_2 and N_2 were bubbled through the sample in the flat cell for 10 minutes and 5 minutes, respectively. ESR spectra were recorded on a Bruker EMX ESR spectrometer with a super high Q cavity. Instrument settings were as follows: microwave power, 20 mW; modulation amplitude, 1 G; conversion time, 1.3 s; time constant, 1.3 s. Spectra were recorded on an IBM-compatible computer interfaced with the spectrophotometer and were analyzed to determine hyperfine coupling constants by computer simulation using EPR-WinSim software [86]. Graphical display of this data represents bile volume-corrected spectra amplitudes (peak-to-peak).

Acyl-coA Oxidase Activity and Expression

Acyl-coA oxidase (ACO) activity and expression are commonly used indicators of peroxisome induction [87]. The activity of ACO was determined by measuring formaldehyde, which is formed from oxidation of methanol by hydrogen peroxide. Liver tissue (100 mg) was homogenized in 10 volumes of 0.25 M sucrose buffer. A volume of 1.4 ml of reaction mixture (see [65] for details) was warmed at 37°C and mixed with 100 μl of

homogenate. The reaction was terminated after 5 minutes by adding 40% trichloroacetic acid. Blanks were prepared in parallel, in which 40% trichloroacetic acid was added before homogenate. Samples and blanks were centrifuged to pellet protein and 1.0 ml of the supernatant was added to 0.4 ml of Nash reagent containing acetyl acetone, which reacts with formaldehyde to form diacetyl-dihydrolutidine [88]. The concentration of formaldehyde was measured spectrophotometrically at $\lambda = 405$ nm. Protein concentration was determined using the BCA protein assay [89].

ACO protein expression was measured by western blot analysis. Nuclear extracts were prepared from liver samples obtained from mice fed control or WY-14,643-containing diet for 3 weeks. Hepatic proteins (10 μg/lane) were separated on an SDS-PAGE and transferred to a nitrocellulose membrane. Immunodetection of ACO was performed using an anti-ACO polyclonal antibody (a generous gift from Dr. Janaradan Reddy, Northwestern University), followed by conjugation with an HRP-labeled rabbit anti-mouse secondary antibody. Chemiluminescent detection of protein was employed.

Statistics

Data are represented as mean values plus or minus the standard error for three to six animals per group. One-way ANOVA was used for statistical comparison with control (*). In cases in which more than two treatments were used, two-way ANOVA with Tukey's multiple comparison test was employed for statistical comparisons of between control-(*) or DEHP-(†) treated groups. A p value less than 0.05 was selected prior to the study to determine statistical differences between groups.

D. RESULTS

DEHP and WY-14,643 cause a sustained increase in free radicals

Acute treatment with DEHP has been shown to cause an increase in liver free radical production *in vivo* [46], but it has not yet been determined by direct detection methods whether free radical production remains elevated for longer than 2 hrs. To investigate whether peroxisome proliferators cause a long-term increase in free radicals, mice were fed either control or DEHP-containing diet for 3 weeks. In order to establish if radical species that are produced after continuous treatment are similar to those that form after acute administration of DEHP, some mice were injected with either saline or DEHP (1.2 g/kg) intragastrically immediately before bile collection. Figure 2.1 shows that a DEHP-induced increase in free radicals is observed after both acute (2 hrs) and sub-chronic (3 weeks) treatment with the peroxisome proliferator compound. When injected *in vivo,* POBN forms a stable radical adduct (with a $t_{1/2}$ ranging from 10-15 hrs, data not shown). Thus, the rate of radical production is proportional to the ESR spectrum amplitude and the level of induction of free radical production (i.e., the amount of the radical species being produced) caused by treatment with DEHP is comparable at both time points (3.2- and 2.6-fold over control, respectively).

Computer simulations of the ESR spectra for DEHP-induced radicals produced at 2 hours and 3 weeks (Figure 2.1C and 2.1F, respectively) suggest that the radical species responsible for POBN adduct formation were similar. For both time points, the POBN-trapped radicals produced a composite six-line spectrum. Computer simulation of radical adducts produced following acute DEHP treatment (Figure 2.1C) possess hyperfine coupling

constants of (I) a^N = 15.6 G, a_β^H = 3.2 G and (II) a^N = 15.8 G, a_β^H = 2.7 G, and revealed a third species (III) a^H = 2.0 G due to the ascorbate radical (19). The relative amount of each adduct species was (I) 55%, (II) 35% and (III) 11%. The predominant radical species (I) appears to be derived from POBN/•CO_2^- [90], while species II likely originated from a lipid-centered radical [91]. Three week treatment with DEHP produces similar radical species with coupling constants (I) a^N = 15.7 G, a_β^H = 3.0 G, (II) a^N = 15.8 G, a_β^H = 2.7 G, and (III), a^H = 1.9 G derived from the same three species, POBN/•CO_2^- (49%), POBN/•L (41%), and the ascorbate radical III contributing 10%. The significant presence of formate-derived POBN/•CO_2^- radical adducts in both samples is likely caused by reactive species produced by oxidizing enzymes. In a Fenton-like reaction, endogenous formate is oxidized to form a carbon dioxide anion radical [91].

While our data indicates that DEHP is capable of invoking production of radical species in both acute (2 hrs) and sub-chronic (3 weeks) studies, it has been shown that DEHP is a relatively weak carcinogen that fails to produce a sustained induction of proliferative response in rodent liver [38]. To compare the level of free radical induction by two classical peroxisome proliferator compounds that differ in their carcinogenic potency, mice were fed a diet with either DEHP (0.6% w/w), or WY-14,643 (0.05% w/w) for 3 days, 1, or 3 weeks and radicals in bile were measured by ESR. Both DEHP and WY-14,643 caused a time-dependent increase in free radicals (Table 2.1 and Figure 2.2), with the latter treatment causing the most significant increase over control levels beginning at 1 week of treatment. These findings support the hypothesis that the carcinogenic potency of peroxisome proliferators is likely to be related to their ability to cause oxidative stress in liver [92].

PPARα is essential to long-term reactive oxygen species production by peroxisome proliferators

Earlier studies demonstrated that acute production of DEHP-induced radical species in rodent liver depends on Kupffer cell NADPH oxidase, but not PPARα [46]. To determine if long-term reactive oxygen species production is mediated by either Kupffer cell- or hepatocyte-related molecular events, *p47*^{phox}- and *PPARα*- null mice (along with their corresponding wild-types) were treated with WY-14,643 for 3 weeks. POBN trapped radicals were collected *in vivo* from liver using bile and quantitated using ESR. Though the knock-out mice used in this study were on different background strains (SV129 and C57BL/6J), no strain-associated differences in free radical production were observed. Both wild-type strains show a significant increase in radicals caused by dietary treatment with WY-14,643 for 3 weeks (Figure 2.3). Interestingly, induction of radical production by continuous treatment with WY-14,643 occurs in NADPH-oxidase deficient mice (*p47*^{phox}-null), but not in *PPARα*-null mice. These results clearly demonstrate that PPARα is required for prolonged reactive oxygen species production caused by peroxisome proliferators.

It has been hypothesized that induction of peroxisomal oxidases by peroxisome proliferators is important for the mode of action of these agents since it may lead to oxidative damage of DNA, proteins and lipids in rodent liver [93]. To determine if induction of peroxisomal enzymes correlates with sustained free radical production observed in this study, activity of acyl-CoA oxidase (ACO) was determined in liver homogenates from wild-type mice fed either DEHP or WY-14,643-containing diets for up to 3 weeks. ACO is widely used as a marker of peroxisomal β-oxidation [42,44] and increased expression or activity is hallmark to peroxisome proliferators. Both DEHP and WY-14,643 cause a progressive

increase in ACO activity, with more potent WY causing a greater increase of almost 30-fold over control as early as 3 days following diet initiation (Figure 2.4). Induction of ACO by DEHP and WY-14,643 persists for up to three weeks. These results corroborate that reactive oxygen species levels are sustained and progressively increase with the length of treatment. Measurements of ACO activity in liver from both knockout mouse strains revealed an induction in ACO in *p47*^{phox}-null mice (Figure 2.5A). No change of enzyme activity was observed in *PPARα*-null mice. ACO protein expression (Figure 2.5B) revealed a similar trend. When taken collectively, these results confirm that long term reactive oxygen species production is PPARα–dependent, and that peroxisomal enzymes are likely a primary source.

E. DISCUSSION

Involvement of reactive oxygen species in the mode of action of peroxisome proliferators

Reactive oxygen species are thought to be intimately associated with the mechanism of tumorigenesis by peroxisome proliferators. This assumption is based to a large degree on the fact that various proteins that are induced by these chemicals in liver parenchymal cells (peroxisomes, mitochondria and microsomes) are prone to formation of hydrogen peroxide and free radical species. Thus, it was hypothesized that such overproduction of oxidants might cause DNA damage and lead to mutations and cancer [42,93]. In addition, recent discoveries show that reactive oxygen species play an important signaling role in a rapid increase of parenchymal cell proliferation caused by peroxisome proliferators [94,94]. Collectively, it appears that oxidant-related molecular events are intertwined with other pathways activated by peroxisome proliferators *in vivo* in rodent liver.

It was initially hypothesized that fatty acyl-CoA oxidase in the peroxisome is the enzyme responsible for oxidative stress by peroxisome proliferators [47,95]; however, mice lacking this protein, instead of being protected from chemically induced liver cancer, develop liver tumors spontaneously, possibly as a result of a hyper-activation of PPARα by unmetabolized lipids [22]. A number of indirect confirmations for peroxisome proliferator-initiated increases in reactive oxygen species have been collected over past two decades; however, the causative relevance of some of this evidence to the carcinogenic effect of peroxisome proliferators has been questioned and contrasting views have been presented (reviewed in [96]). Therefore, we provide direct *in vivo* evidence for sustained production of oxidants after treatment with peroxisome proliferators, as well as information on whether

free radicals are produced by PPARα-dependent mechanisms, both of which are critical for understanding the mode of action of these agents.

Direct evidence for peroxisome proliferator-induced sustained production of free radicals in rodent liver

Despite the fact that few question a role of oxidative stress in the mechanism of action of these compounds, direct evidence that free radicals are produced under conditions of continuous exposure to peroxisome proliferators, as well as knowledge on precise molecular source(s) of reactive oxygen species that are involved were still lacking. It has been previously reported that PPARα is not required for generation of reactive oxygen species in mouse liver after ***acute*** exposure to peroxisome proliferators [46]. The same study demonstrated that Kupffer cell NADPH oxidase was the source of free radical production in rodent liver within hours after administration of DEHP. Thus, Kupffer cells have been suggested to be a potential source of free radicals in rat and mouse liver after treatment with peroxisome proliferators [46,97].

In this study, we provide the first direct evidence of peroxisome proliferator-induced ***sustained*** free radical production *in vivo* in mouse liver. It appears that ability of peroxisome proliferators to increase radical production in mouse liver correlates with the carcinogenic potency. Specifically, WY-14,643, which is known to be highly tumorigenic in rodents, causes greater radical production than DEHP, a weaker rodent liver carcinogen.

We also show that irrespective of the duration of treatment with peroxisome proliferators when the cellular source of radicals (i.e., Kupffer cell or hepatocyte) may differ (see below), the ultimate macromolecule-reactive species produced in mouse liver are similar

and consist of roughly equal amounts of $\bullet CO_2^-$ and •L. While Kupffer cell-derived radicals (e.g., superoxide anion) can either react directly with the surrounding lipid membrane (at low pHs [98]), or be converted to a hydroxyl radical that will react with lipids; in hepatocytes, excess peroxisomal H_2O_2 conversion to a reactive hydroxyl radical in the presence of iron is the presumed mechanism of formation of lipid peroxides [99]. While the utility of spin trapping with POBN for direct detection of hydroxyl radical itself is limited due to the instability of hydroxyl-radical adducts [100], the high reactivity of the hydroxyl radical, abundance of lipids in liver and the chain reaction nature of lipid peroxidation are likely to facilitate the formation of •L as a key terminal radical detected here by POBN.

Our results indicate that continuous treatment with peroxisome proliferators causes a time-dependent significant increase in free radicals in mouse liver. It is interesting, however, that the initial increase in POBN-radical adducts following acute exposure to DEHP was short-lived, as an appreciable increase in radical production is not observed until after 3 weeks of treatment with DEHP and after 1 week of treatment with WY-14,643. This result implies that the early, Kupffer cell-mediated, effect on increased reactive oxygen species is not sustained and we suggest that Kupffer cell activation by peroxisome proliferators is short lived (see below).

The peroxisome proliferator-induced PPARα-dependent (see below) prolonged free radical production in liver, detected here by ESR, may result from several sources in the parenchymal cell. A number of peroxisomal (e.g., fatty acyl-CoA oxidase) and microsomal (e.g., 4A superfamily of cytochrome P450 enzymes) oxidases are regulated by PPARα and are involved in the catabolism of long chain and very long chain fatty acids by β- and ω-oxidation, respectively. These enzyme systems are "leaking" electrons and are known to

generate considerable amounts of secondary reactive oxygen species even under normal physiologic conditions [42].

Disproportionately large increases in expression of hydrogen peroxide-generating fatty acyl-CoA oxidase, as compared to hydrogen peroxide-degrading catalase, have been reported following treatment with peroxisome proliferators in rodents [44,47]. However, given the extremely high rate at which peroxisomal catalase converts H_2O_2 into H_2O and O_2, it should not escape peroxisomes [101]. Furthermore, peroxisomal β-oxidation is limited by substrate availability. In fact, it has been shown that treatment with peroxisome proliferators increased H_2O_2 *in vitr*o, but not in the perfused liver because fatty acid supply is rate-limiting in intact cells [102,103]. Indeed, the timing of the increases in free radical production observed in this study did not correlate with that for the induction of ACO protein level and activity. However, peroxisomes devoid of catalase but capable of production of H_2O_2 via beta-oxidation of fatty acyl CoA compounds or via the activity of urate oxidase have been observed following clofibrate treatment and massive liver regeneration [104,105]. Thus, with continuous peroxisome proliferator treatment, it is still possible that catalase-deficient peroxisomes have less capability to scavenge the increasing pool of H_2O_2, resulting in the increase in POBN-radical adducts that were detected in bile. Marked induction of CYP4A [45] may be another likely source of oxidants under the condition of continuous treatment with peroxisome proliferators.

An alternative explanation for lack of increase in radicals until after 1 week of treatment could also be related to peroxisome proliferator-induced changes in iron homeostasis in rodent liver. Reactive species produced at early time points (2 hours or less) are presumably Kupffer-cell derived radicals (e.g., superoxide anion) that would not depend

on availability of excess transition metals for conversion to ESR-detectable species. However, a sufficient level of iron in the liver is critical for conversion of non-radical oxidants, like H_2O_2, to ESR-detectable radical species. Several studies have shown that dietary treatment with peroxisome proliferators in rodents creates a condition of iron overload in liver [106-108]. An increase in hepatic iron stores is thought to be one of the potential reasons for chronic oxidative stress in liver by peroxisome proliferators. In fact, an enhancement in lipid peroxidation as a result of hepatic iron overload after treatment with WY-14,643 was observed recently [108]. In addition to increased intracellular pools of iron, altered expression of proteins responsible for iron transport from the liver to plasma (i.e., transferrin receptors, ferritin, and iron regulatory protein 1) has been reported [106,109].

NADPH oxidase is not a source of free radicals under condition of chronic administration of peroxisome proliferators

Numerous reports in the past decade have suggested that Kupffer cells are involved in acute peroxisome proliferator-mediated pleiotropic responses in rodent liver. It was shown that Kupffer cell activation by peroxisome proliferators (i) is independent of PPARα, (ii) involves generation of reactive oxygen species, and (iii) leads to production of mitogenic cytokines (reviewed in [94]). Since it was not known whether Kupffer cell-specific events play a role in long-term effects of peroxisome proliferators, this study determined if this cell type may be involved in peroxisome proliferator-induced reactive oxygen species production when animals are administered these compounds for up to 3 weeks. We show here that radical species formation still occurs in the absence of active NADPH oxidase (as observed in *p47^{phox}*-null mice), but is PPARα-mediated. The importance of PPARα for

hepatocarcinogenicity of peroxisome proliferators is well known [21]. Importantly, here we demonstrate, by direct measurements of radical production in liver, that PPARα-dependent pathways are responsible for the long-term increase in oxidants after continuous treatment with peroxisome proliferators. This work, together with measurements of oxidative DNA damage under similar conditions [110], establishes a link between PPARα, free radical production and DNA damage, a key step in the mechanism of carcinogenesis.

In conclusion, this study is the first to provide direct *in vivo* evidence that increased free radical production in mouse liver is sustained following dietary treatment with peroxisome proliferators. Despite the apparent temporal shift in the cellular source of radicals (from Kupffer cells to hepatocytes) as peroxisome proliferator treatment is continued, there appears to be no difference in the radical species that are produced. Finally, we have demonstrated that long term reactive oxygen species production is mediated by PPARα and that NADPH oxidase-derived radicals may only be important as early responses to peroxisome proliferators.

Table 2.1. ESR spectra amplitudes for peroxisome proliferator-treated C57BL/6J mice.

Time course	Treatment	N	Liver Weight (% Body Wt.)[a]	Bile Volume (ml)	ESR Amplitude (Arbitrary Units)	Vol Corrected ESR Amplitude (Arbitrary Units)[a]
	Control	6	4.6 ± 0.3	0.15 ± 0.01	23.63 ± 3.47	3.39 ± 0.38
3 days	DEHP	6	5.4 ± 0.5[b]	0.17 ± 0.02	9.43 ± 1.34	1.57 ± 0.25
	WY	3	6.5 ± 0.9[c]	0.23 ± 0.03[c]	8.89 ± 3.52	1.94 ± 0.56
	Control	4	5.7 ± 0.5	0.18 ± 0.03	13.83 ± 2.16	2.96 ± 0.78
1 week	DEHP	5	7.1 ± 1.3	0.19 ± 0.04	14.62 ± 1.99	3.06 ± 0.98
	WY	6	8.2 ± 1.0[c]	0.44 ± 0.08[c]	12.69 ± 2.49	5.48 ± 1.64[b]
	Control	4	4.4 ± 0.3	0.17 ± 0.01	11.96 ± 0.72	1.99 ± 0.18
3 weeks	DEHP	6	6.3 ± 0.3[b]	0.19 ± 0.02	27.55 ± 1.57	5.23 ± 0.65[b]
	WY	5	11.3 ± 1.1[c]	0.76 ± 0.08[c]	10.78 ± 2.00	7.62 ± 0.57[c]

Data is represented as mean ± SEM.

[a] Bile volume was used to determine a volume corrected ESR amplitude.

[b] Denotes statistically significance from Control-fed animals ($p<0.05$).

[c] Denotes statistical significance from DEHP-treated animals ($p<0.05$).

Figure 2.1. Production of POBN radical adducts caused by peroxisome proliferators is sustained.

Representative spectra and computer simulations of radical adducts in C57BL/6J mouse liver following DEHP treatment are shown. Bile was collected for 2 hours after POBN administration (i.p.). Radical adducts in bile were detected using ESR. **(A)** ESR spectrum of radical adducts detected 2 hours following i.g. treatment with saline. **(B)** Same as A except treated with DEHP (1.2 g/kg). **(C)** Computer simulation of spectrum in panel B. **(D)** ESR spectrum of radical adducts detected following 3 weeks of feeding of NIH-07 diet. **(E)** Same as panel D, except diet contained DEHP (0.6% w/w). **(F)** Computer simulation of spectrum in panel E.

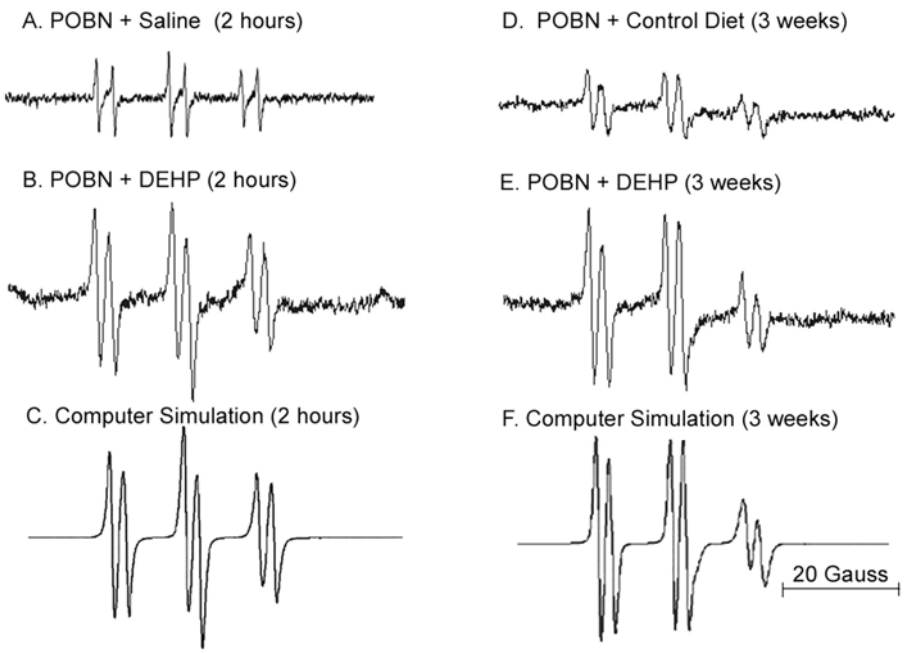

Figure 2.2. WY-14,643 causes a greater induction of POBN radical adducts in C57BL/6J mice.

Mice were fed either a DEHP (0.6% w/w)-, or WY-14,643 (0.05% w/w)-containing diet for 3 days, 1 week, or 3 weeks. Free radical adducts in bile were measured by ESR 2 hours after POBN (i.p.) administration. Statistical significance ($p<0.05$) is indicated with asterisks (*, different from Control; †, different from DEHP). N.D: No Data

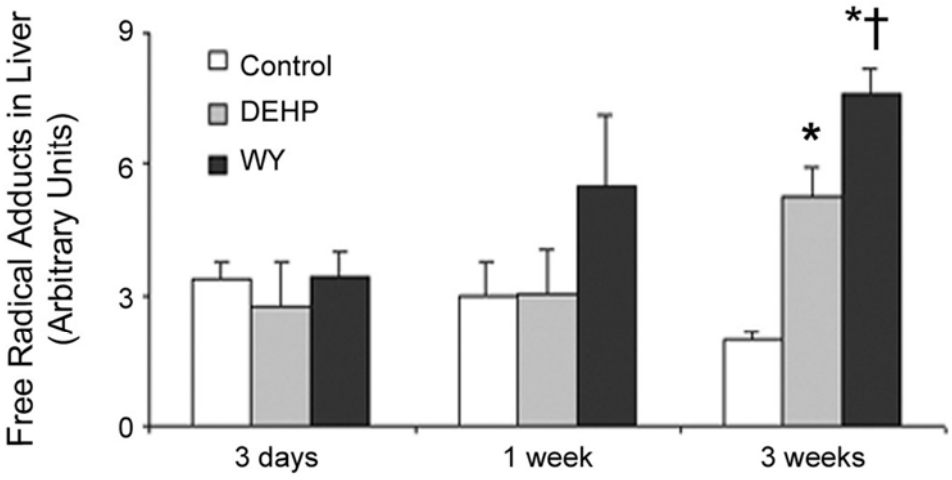

Figure 2.3. Prolonged radical species production is PPARα dependent.

PPARα-null and *p47*^{phox}-null mice were fed a WY-containing diet (0.05% w/w) for 3 weeks. Following POBN administration, bile was collected for 2 hours. POBN radical adducts were detected in bile using ESR. Statistical significance ($p<0.05$) is indicated with an asterisk as compared to the data for control diet-fed animals.

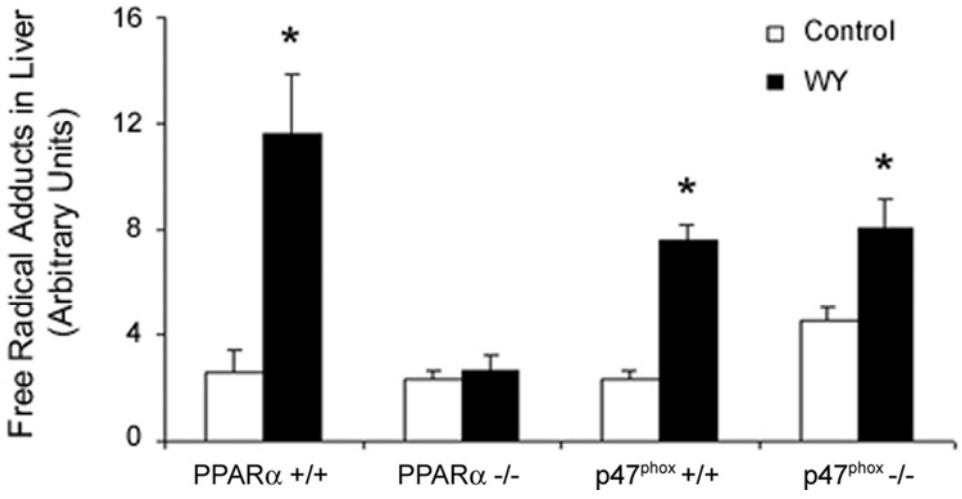

Figure 2.4. DEHP and WY-14,643 cause a sustained increase acyl-CoA oxidase activity. Mice were fed either a DEHP (0.6% w/w) or WY-14,643 (0.05% w/w)-containing diet for 3 days, 1 week, or 3 weeks. ACO activity was measured as described in the Experimental Procedures. Statistical significance ($p<0.05$) is indicated with asterisks (*, different from Control; †, different from DEHP).

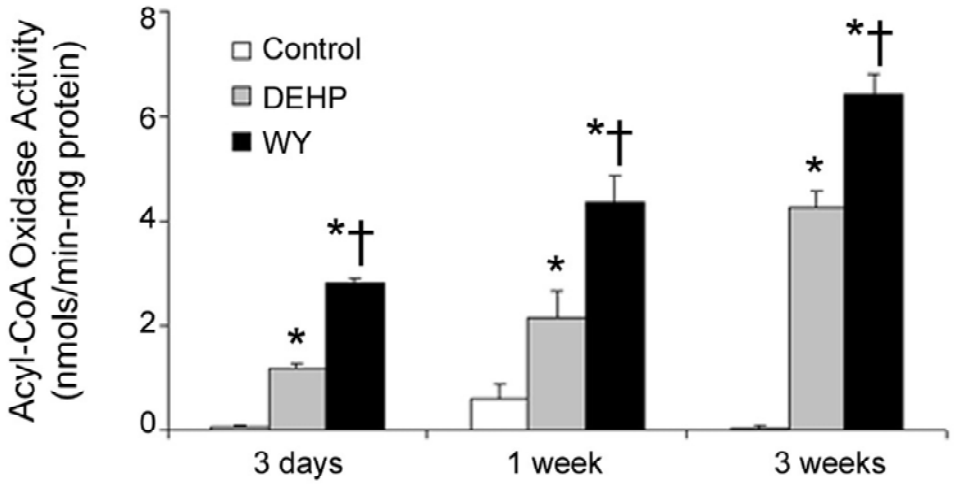

Figure 2.5. Induction of ACO correlates with peroxisome proliferator-induced radical production.

PPARα-null and *p47*^{phox}-null mice were fed WY-14,643 (0.05% w/w) containing diet for 3 weeks. (**A**) ACO activity was measured as described in the Experimental Procedures. (**B**) ACO protein expression was measured by western blot analysis. Statistical significance ($p<0.05$) is indicated with an asterisk as compared to the data for Control-fed animals.

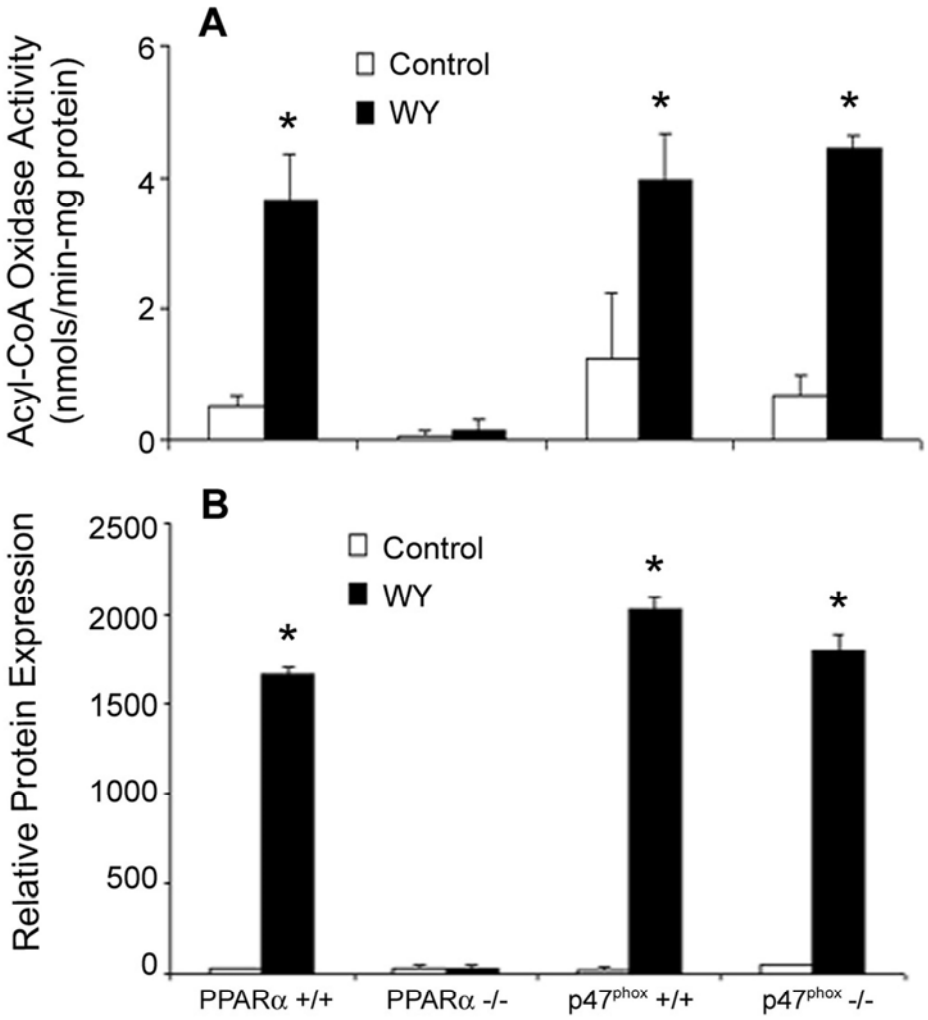

CHAPTER III

WY-14,643-induced cell proliferation and oxidative stress in mouse liver are independent of NADPH oxidase

A. ABSTRACT

Long term exposure of rodents to peroxisome proliferators leads to increases in peroxisomes, cell proliferation, oxidative damage, suppressed apoptosis, and ultimately results in the development of hepatic adenomas and carcinomas. Peroxisome proliferator activated receptor (PPAR)α was shown to be required for these pleiotropic responses; however, Kupffer cells, resident liver macrophages, were also identified as playing a role in peroxisome proliferator-induced effects, independently of PPARα. Previous studies showed that oxidants from NADPH oxidase mediate acute effects of peroxisome proliferators in rodent liver. To determine if Kupffer cell oxidants are also involved in chronic effects, NADPH oxidase-deficient (*p47*^{phox}-null) mice were fed 4-chloro-6-(2, 3-xylidino)-2-pyrimidinylthio acetic acid (WY-14,643)-containing diet (0.1% w/w) for 1 week, 5 weeks or 5 months along with *Pparα*-null and wild type mice. As expected, no change in liver size, cell replication rates or other phenotypic effects of peroxisome proliferators were observed in *Pparα* -null mice. Through 5 months of treatment, the *p47*^{phox}–null and wild type mice exhibited peroxisome proliferator-induced adverse liver effects, along with increased oxidative DNA damage and increased cell proliferation, a response that is potentially mediated through NFκB. Suppressed apoptosis caused by WY-14,643 was dependent on both NADPH oxidase and PPARα. Collectively, these findings suggest that involvement of Kupffer cells in WY-14,643-induced parenchymal cell proliferation and oxidative stress in rodent liver is an acute phenomenon that is not relevant to long-term exposure, but they are still involved in chronic apoptotic responses. These results provide new insight for understanding the mode of hepatocarcinogenic action of peroxisome proliferators.

B. INTRODUCTION

Peroxisome proliferators are a class of chemically diverse compounds such as hypolipidemic drugs, plasticizers, industrial solvents and pesticides. Peroxisome proliferators cause a number of adverse cellular and molecular changes in rodent liver, including an increase in the number and size of peroxisomes and proliferation of hepatocytes [38]. Rodents also develop hepatocellular neoplasia as a result of chronic administration of peroxisome proliferators [18,35,111]. Most of the pleiotropic effects of these agents are nuclear receptor-mediated through peroxisome proliferator-activated receptor (PPAR)α. PPARα activation is required for peroxisome proliferator-induced growth responses and for liver carcinogenesis [21]. However, a number of early events in liver that are independent of PPARα have also been reported, including Kupffer cell activation, release of reactive oxygen species and production of mitogenic cytokines [66,76,77].

Increased oxidant generation and cell proliferation, along with suppression of apoptosis, are thought to be key steps in the mode of action of non-genotoxic liver carcinogens, including peroxisome proliferators [38,60,93]. Within hepatocytes, these responses facilitate the formation and fixation of oxidative DNA lesions and clonal expansion of mutated cells, which could predispose cells to tumor development. It is well known that PPARα is required for sustained growth responses to peroxisome proliferators [21,39]; however, the chronic PPARα-independent mediators of cellular response are poorly understood. Previous studies demonstrate that Kupffer cells, the resident macrophages of the liver, are important mediators of acute phase responses to peroxisome proliferators. In particular, reactive oxygen species produced as a result of acute peroxisome proliferator treatment were shown to be Kupffer cell-derived using NADPH oxidase deficient ($p47^{phox}$-

null) mice [46,77]. Also, peroxisome proliferator-induced production of mitogenic cytokines is a result of Kupffer cell activation [66,82,112]. It has been hypothesized that mitogens, like tumor necrosis factor (TNF)α and interleukin (IL)-1 are important signaling molecules responsible for mediating cross-talk between Kupffer cells and hepatocytes that control cell proliferation and apoptosis. Kupffer cell inhibitors, glycine and methyl palmitate, were able to block acute effects of peroxisome proliferators in rodent liver [65,66]. Similar results were observed in rats treated with NADPH oxidase inhibitor, diphenyleneiodonium sulfate [97]. Furthermore, *in vitro* studies have shown that an absence of non-parenchymal cells prevents increased DNA synthesis in purified hepatocytes treated with WY-14,643 [70,71]. The importance of TNFα to peroxisome proliferator-induced changes in cell turnover was demonstrated when increased DNA synthesis and decreased apoptosis were completely blocked by pre-treatment with a TNFα antibody [41,67]. Furthermore, since Kupffer cells do not express PPARα [64] it is likely that these effects are nuclear receptor-independent.

From previous studies, it is clear that Kupffer cells play a critical role in the early events in rodent liver associated with peroxisome proliferator treatment; however, whether the role of the Kupffer cells is sustained has yet to be established. In this study, NADPH oxidase-deficient mice were used to determine if Kupffer cell-derived oxidants are necessary for prolonged peroxisome proliferator-induced pathological changes in liver. The data show that NADPH oxidase is not required for chronic proliferative response or DNA damage. We conclude that the role that Kupffer cell oxidants play in peroxisome proliferator-induced liver effects is limited and may not be a contributing factor to hepatocarcinogenesis.

C. MATERIALS AND METHODS

Animals and Diet

p47^{phox}-null male mice (C57BL/6J background; [85]), *PPARα*-null male mice (SV129 background; [33]), and corresponding wild type counterparts (6-8 weeks of age at the beginning of treatment) were used in these experiments. All animals used for this study were housed in sterilized cages in a facility with a 12-hr night/day cycle. Temperature and relative humidity were held at 22 ± 2°C and 50 ± 5%, respectively. The UNC Division of Laboratory Animal Medicine maintains these animal facilities, and veterinarians were always available to ensure animal health. All animals were given humane care in compliance with NIH and institutional guidelines and studies were performed according to protocols approved by the appropriate institutional review board. Prior to experiments, animals were maintained on standard lab chow diet and purified water *ad libitum*. 4-Chloro-6-(2,3-xylidino)-pyrimidynylthioacetic acid (WY-14,643) was obtained from Aldrich (Milwaukee, WI). NIH-07 was used as the base for the pelleted diet (prepared by Harlan Teklad, Indianapolis, IN) containing either 0% (control), or 0.1% w/w of WY-14,643. Dietary concentration of WY-14,643 was measured by high performance liquid chromatography after the pellets were made and determined to be ±18% of the target concentration. Diet was administered *ad libitum* for 1 week, 5 weeks or 5 months. Animals had free access to water throughout the study and the health status of the animals was monitored every other day.

Tissue Collection

Body weight was recorded on a weekly basis per cage, not for individual animals. Three days prior to sacrifice mice were administered bromodeoxyuridine (BrdU)-containing water (0.2 g/L). At sacrifice, mice were anesthetized with pentobarbital (100 mg/kg) and following exsanguination, livers were removed and weighed. A section from the left lateral lobe was fixed in 10% formalin. A section of the duodenum, which is a rapidly proliferating tissue, was also collected and fixed in formalin for use as a positive control in immunohistochemical staining and to confirm that mice received BrdU. The remaining tissue was placed in an eppendorf tube and snap frozen in liquid nitrogen. These samples were stored at -80ºC until assayed.

Histopathological Evaluation

A quantitative method was employed to determine the severity of necrosis, steatosis or inflammation in mouse liver. Slightly modified from the previous method [113], the scoring involves overlaying a grid on a low magnification photo of the hematoxylin/eosin-stained liver section. The necrosis index was calculated as the # of points overlapping a necrotic region/total number of points overlapping the liver section. The same procedure was followed for steatosis and inflammation indices. Grid points over portal or central veins were excluded from the calculation and in cases in which the entire liver section was too large to be captured in one photo, the average score was taken from photos of 2 or more unique fields.

BrdU Immunohistochemistry

Liver tissue sections were fixed in 10% formalin for 24 hours and transferred to 70% ethanol. Sections were embedded in paraffin and 5 μm slices were mounted onto Probe-On Plus (Fisher Scientific, Pittsburgh, PA) slides. Slides were rehydrated in serial solutions of xylene, 100%, 95%, 70%, 50% and 30% ethanol and water. For BrdU staining, the tissue was hydrolyzed in 4N HCl for 20 minutes at 37° C and permeabilized in a 0.2% pepsin/0.2N HCl solution for 15 min at 37° C. Immunostaining was performed with a monoclonal antibody against BrdU (Dako, Carpinteria, CA) diluted 1:200 in 1% BSA in PBS. Immunohistochemical detection was performed using a horseradish peroxidase labeled goat anti-mouse secondary antibody followed by staining with a 3,3'-diaminobenzidine chromogen solution. Slides were counterstained using hematoxylin. Image analysis was performed at a magnification of 200x using Bioquant Nova Prime (Bioquant Image Analysis Corp., Nashville, TN) software. A labeling index was calculated as the number of positively stained nuclei/total number of nuclei counted x 100% (at least 2000 nuclei/slide).

Preparation of Protein Extracts

Cytosolic and nuclear protein extracts were prepared by homogenizing 50 mg of liver tissue in 400 μl of buffer A, which contained 10 mM HEPES, 10 mM KCl, 0.1 mM EDTA, 0.1 mM, EGTA, 1 mM DTT and 0.5 mM PMSF, and the homogenate was placed on ice for 15 min. After adding 25 μl of NP-40, the homogenate was centrifuged at 4°C for 30 sec at 14,000 rpm. The supernatant was aliquoted as the cytosolic fraction. The remaining pellet was resuspended in 400 μl of buffer A and 25 μl of NP-40 and centrifuged at the above conditions. The supernatant was discarded and remaining cells were resuspended in 250 μl of

buffer B containing 20 mM HEPES, 0.4 M NaCl, 10 mM KCl, 1 mM EDTA, 1 mM EGTA , 1 mM DTT, 0.5 mM PMSF and 1 mM NA_3VO_4 for 30 minutes on ice. After spinning the mixture at 4°C for 5 min at 14,000 rpm, the supernatant was aliquoted as the nuclear fraction. Protein concentration of the cytsolic and nuclear extracts was determined using a BCA assay (Pierce Biotechnology Inc, Rockford, IL) prior to storing at 80°C.

Western Blot Analysis

To assess protein levels of Cyclin B1, Cdk1, Cdk2 and C-myc, nuclear protein extracts were used, while cytosolic fractions were used for measuring Caspase 8 and Caspase 9. Proteins (10 μg/lane) were separated on a 4-12% Bis-Tris gel and transferred to a nitrocellulose membrane. Immunodetection was performed by incubating membranes with the primary antibody then conjugating with a horseradish peroxidase-labeled secondary antibody (Amersham, Cleveland, OH). Bands were detected using an ECL chemiluminescence kit (Amersham). Anti-mouse primary antibodies for Cyclin B1, Cdk1, Cdk4 and C-myc were from Santa Cruz Biotechnology (Santa Cruz, CA), and Cdk2 anti-body was from Lab Vision (Fremont, CA). Antibodies for Caspase 8 and Caspase 9 were from Biovision (Mountain View, CA). Band intensity was quantified using Kodak 1D Image Analysis software (Eastman Kodak, Rochester, NY). Protein expression was normalized to β-actin (antibody from Abcam, Cambridge, MA).

Detection of Apurinic/Apyrimidinic Sites

Genomic DNA was extracted by a procedure slightly modified from the method reported previously [114]. To minimize formation of oxidative artifacts during isolation,

2,2,6,6-tetramethylpiperidinoxyl (20 mmol/L) was added to all solutions, and all procedures were performed on ice. The apurinic/apyrimidinic (AP) site assay was performed as previously described [115].

Electrophoretic Mobility Shift Assay

Electrophoretic mobility shift assay (EMSA) (Panomics Inc., Redwood City, CA) was performed according to manufacturer's instructions. Briefly, 10 μg of nuclear protein extract from liver tissue was pre-incubated with 1 μg of poly d(I-C) at room temperature. Binding buffer, 10 ng of DNA probe and water were added to the mixture and allowed to incubate for 30 minutes at 17°C. The mixture was resolved on a 6% polyacrylamide gel (Invitrogen Corp., Carlsbad, CA). After electrophoresis, protein was transferred to a Biodyne B nylon membrane (Pall Corp., East Hills, NY) then dried for 1 hour at 80°C. To reduce nonspecific binding, the membrane was placed in blocking buffer, followed by incubation with HRP-streptavidin conjugate (1:1000). The membrane was washed prior to adding ECL detection buffer and then exposed to film. Specificity of the NFκB probe was confirmed by competition assays using Hela cell nuclear extracts, whereby 2-fold excess unlabeled NFκB probe was added to the mixture prior to addition of labeled probe.

Acyl-CoA Oxidase Activity

Acyl-coA oxidase (ACO) activity and expression were measured as indicators of peroxisomal induction [87]. The activity of ACO was determined by measuring formaldehyde, which is formed from oxidation of methanol by hydrogen peroxide. Liver tissue (100 mg) was homogenized in 10 volumes of 0.25 M sucrose buffer. A volume of 1.4

ml of reaction mixture (see [66] for details) was warmed at 37°C and mixed with 100 μl of homogenate. The reaction was terminated after 5 minutes by adding 40% trichloroacetic acid. Blanks were prepared in parallel, in which 40% trichloroacetic acid was added before homogenate. Samples and blanks were centrifuged to pellet protein and 1.0 ml of the supernatant was added to 0.4 ml of Nash reagent containing acetyl acetone, which reacts with formaldehyde to form diacetyl-dihydrolutidine [88]. The concentration of formaldehyde was measured spectrophotometrically at $\lambda = 405$ nm. Protein concentration was determined using the BCA protein assay [89].

Statistical analysis

Data represented as mean values plus or minus the standard error, unless otherwise noted. Two-way ANOVA with Tukey's multiple comparison test was employed for statistical comparison between experimental groups. A p value less than 0.05 was selected prior to the study to determine statistical differences between groups.

D. RESULTS AND DISCUSSION

Liver Toxicity and Cell Proliferation Effects of WY-14,643 in Mouse Liver

To determine if Kupffer cells are involved in chronic effects of peroxisome proliferators in liver, NADPH oxidase-deficient (*p47^{phox}*-null) and C57BL/6J wild type mice were fed 4-chloro-6-(2,3-xylidino)-2-pyrimidinylthio acetic acid (WY-14,643)-containing diet (0.1% w/w) for 1 week, 5 weeks or 5 months. In parallel, *Pparα*-null and SV129 wild type mice were also treated for up to 5 months. Over the course of treatment there was a significant decline in body weight (approximately 20%) in all WY-14,643-treated mice as compared to controls, except for *Pparα*-null mice (Figure 3.1A). This effect was accompanied by significant progressive increases in absolute and relative liver weight in all WY-14,643-treated groups, except for *Pparα*-null mice (Figure 3.1B). By 5 months of treatment, the liver enlargement was most pronounced in *p47^{phox}*-null mice. The effect of WY-14,643 was much greater in C57BL/6J mice than in SV129 strain. High attrition was also observed in WY-14,643-treated mice (Figure 3.1C), particularly those on the C57BL/6J background strain.

Upon necropsy and histopathological assessment, necrotic gross liver lesions (no more than 2 mm in diameter) were found in one half of the SV129 wild type mice and all of the *p47^{phox}*-null mice treated with WY-14,643 for 5 months. Overall liver necrosis and inflammation scores in these two groups were significantly higher than in control-fed mice or C57BL/6J and *Pparα*-null mice fed WY-14,643 (Figure 3.2E and Appendix 1). Activity of serum alanine aminotransferase (ALT), a serum marker of liver injury, was significantly elevated in WY-14,643-treated wild type strains and *p47^{phox}*-nulls, but not *Pparα*-null mice (Table 1) in all time points.

Low grade lipid accumulation in hepatocytes was found in both WY-14,643-treated wild type strains and *p47*^{phox}-null mice (Figure 3.2F). Livers from control or WY-14,643-treated *Pparα*-null mice showed moderate levels of lipid accumulation (Figure 3.2C and Appendix 1). Other groups of mice fed control diet displayed normal liver morphology.

The selection of the dose of WY-14,643 for this study was based on previous acute, sub-chronic and chronic studies in the mouse. While several previous long-term dietary feeding studies with peroxisome proliferators in rodents reported relatively high attrition rates [21,116,117], we found that the survival of *p47*^{phox} –null and wild type C57BL/6J mice in our study was below 40% with pronounced temporal increases in ALT levels. This indicates that 0.1% (w/w) WY-14,643 is higher than a maximal tolerated dose in both SV129 and C57BL/6J strains. Thus, the long-term carcinogenicity studies conducted in other mouse strains with this compound may not be interpretable under the same standards as traditional 2-year cancer bioassays.

The similarities in WY-14,643-induced liver injury across strains and the disparate survival of C57BL/6J versus SV129 mice suggest that strain variations in response to WY-14,643 may not be a result of liver toxicity alone. Several studies reported significant weight loss in rodents given peroxisome proliferators chronically [21,116-118]. Excessive energy metabolism resulting in a significant reduction in fat stores is thought to be the primary contributing factor to this effect of PPARα agonists. Indeed, we also observed that WY-14,643 "responder" strains (SV129 wild type, C57BL/6J wild type and *p47*^{phox}-nulls) lost at least 20% of the body weight. However, the rate of weight loss between strains was remarkably different. C57BL/6J mice had a much higher initial rate of weight loss, a response that could be associated with high morbidity/mortality of these mice when given

WY-14,643. Given the considerable loss of body mass, it is possible that muscle wasting [119] was the contributing factor in the premature deaths.

As expected, we found that WY-14,643 causes remarkable hepatomegaly and induces cell proliferation in liver (Figure 3.3A). However, the temporality of WY-14,643-induced liver enlargement and cell proliferation patterns observed in this study is not consistent with previous reports that peroxisome proliferators cause a rapid up-and-down surge in cell proliferation in the first week of treatment [38]. In our study, all WY-14,643 "responder" mouse strains exhibited a robust elevation in BrdU labeling in liver for as long as treatment continued. While there are notable differences in our experiment and previous reports (e.g., rodent species, detection methods, etc.), we argue that the pathophysiological effects of peroxisome proliferators in rodent liver, including the robust proliferative response, extends beyond the time frame that was traditionally considered. In addition, our findings of significant liver injury may suggest that hepatocellular proliferation may be elevated, at least in part, due to compensatory liver regeneration.

NADPH oxidase deficiency does not prevent hepatocellular proliferation, but affects the decrease in apoptosis caused by WY-14,643

It was suggested that activation of Kupffer cells and resultant production of oxidants and mitogenic cytokines plays a role in acute cell proliferation response caused by peroxisome proliferators [65,66]. To determine if Kupffer cell NADPH oxidase is necessary for a sustained growth response caused by these agents, changes in liver morphology, BrdU incorporation and alterations in protein markers of cell turnover were assessed.

Histological evaluation of livers from WY-14,643-treated *p47^{phox}*-null revealed significantly hypertrophied hepatocytes, an increase in mitotic bodies and presence of binucleate hepatocytes, effects identical to those observed in C57BL/6J wild type mice. Furthermore, a significant temporal increase in hepatocellular proliferation was observed at all time points with a peak at 5 weeks in both *p47^{phox}*-null and wild type mice (Figure 3.3A). Western blot analysis of 5 month liver tissue was conducted to determine if Kupffer cell oxidants are important in cell cycle regulation of proliferation (Table 3.2). WY-14,643-induced increases in Cyclin B1, Cdk1 and Cdk4 expression were not affected by Kupffer cell NADPH oxidase deficiency. However, as previously reported [39], altered expression of these proteins caused by peroxisome proliferators was dependent on PPARα.

Suppression of apoptosis has been suggested as another key mechanism by which peroxisome proliferators may affect liver cell turnover and contribute to carcinogenesis. A number of studies have argued that reduced apoptosis after exposure to peroxisome proliferators is a TNFα-mediated (i.e., Kupffer cell-dependent) response [41,120]. To determine if, in fact, a sustained reduction of apoptosis is present during long-term feeding of these agents and whether it is dependent upon Kupffer cell NADPH oxidase, expression of Caspase 8 and Caspase 9 proteins was assessed. Treatment with WY-14,643 for 5 months led to a decrease in expression of Caspase 8 in both wild type strains (Table 3.2). Interestingly, this effect was dependent both PPARα and Kupffer cell NADPH oxidase since no reduction in Caspase 8 expression in response to WY-14,643 was observed in either knockout strain. Levels of Caspase 9, which leads to apoptosis as a result of mitochondrial stress, remained unchanged in all WY-14,643-treated animals.

To further assess the mechanism by which WY-14,643 perturbs normal cell turnover in mouse liver, NFκB binding activity was measured. This transcription factor is thought to be intimately involved in apoptosis and cell proliferation [121]. Exposure to a single dose of WY-14,643 leads to rapid activation of NFκB in Kupffer cells and then in hepatocytes [74], an effect that was shown to be dependent upon NADPH oxidase [77]. Other studies showed that NFκB activation by peroxisome proliferators in rodent liver is sustained [73] and may be important for tumor promotion by these agents [122]. Our data shows that sub-chronic treatment with WY-14,643 leads to a sustained elevation in NFκB binding activity in liver (Figure 3.3B). Furthermore, NFκB activation appears to be dependent on PPARα and is unaffected by the lack of NADPH oxidase, further supporting a temporal shift from Kupffer cell- to hepatocyte-centric effects of peroxisome proliferators. Given that NFκB activation by peroxisome proliferators is thought to be, in part, due to oxidative stress [75], it is possible that PPARα-dependent oxidant production in hepatocytes as a result of long-term WY-14,643 treatment is responsible for the continued induction of NFκB binding observed here.

Collectively, while several studies suggested that the acute effects of WY-14,643 in rodent liver are mediated through PPARα-independent activation of the Kupffer cell, this report shows that this component of the mode of action is short lived and not sustained. Indeed, *p47*^{phox}-null mice responded to sub-chronic treatment with WY-14,643 with the most pronounced hepatomegaly, increase in liver cell proliferation, and exhibited upregulation of cell cycle proteins, while *Pparα*-null mice showed no response to treatment, as expected [21,116]. The lack of a sustained effect of the Kupffer cell-mediated events suggests that activation of PPARα is the primary event responsible not only for the induction of peroxisomes, but also for cell proliferation in liver. While there is no evidence that PPARα

has a direct affect on transcription of cell cycle-regulating genes [39], there is strong evidence for transcriptional regulation by NFκB [121], further supporting the idea that WY-14,643-induced cell proliferation may be mediated by oxidant-dependent activation of NFκB that follows PPARα activation and induction of oxidant-generating enzymes in hepatocytes. In addition, a strong PPARα- and NADPH oxidase-dependent suppression of caspase 8, an initiator caspase of the death receptor pathway leading to apoptosis [123], was observed. This finding suggests that altered regulation of apoptosis by peroxisome proliferators is mediated by death receptor pathways that may include multiple signals from the Kupffer cells and from within the hepatocyte through a PPARα-mediated pathway. Regardless of the pathway, our data on cell proliferation and liver enlargement suggest that suppression of apoptosis may not play as large of a role as increased proliferation and induction of oxidant-generating peroxisomes.

PPARα, not NADPH oxidase, mediates chronic oxidative DNA damage by WY-14,643

Peroxisome proliferators induce reactive oxygen species, which are known to cause oxidative damage to cellular macromolecules [82,93,124]. Previous studies have demonstrated that early increases in reactive oxygen species by peroxisome proliferators require Kupffer cell NADPH oxidase [46]. To determine if Kupffer cell NADPH oxidase is involved in oxidative DNA damage resulting from long-term peroxisome proliferator administration, apurinic/apyrimidinic (AP) sites were measured in DNA from liver of mice fed control or WY-14,643-containing diet for 5 months. Chronic treatment with WY-14,643 caused a two-fold increase in AP sites, a response which required PPARα, but not NADPH oxidase (Figure 3.4A). To determine if peroxisomal oxidases are a potential source of

prolonged oxidant production contributing to peroxisome proliferator-induced oxidative DNA damage, acyl-coA oxidase activity was measured in liver homogenate following 5 months of WY-14,643-treatment. Activity of this peroxisome proliferation-marker protein was increased in a PPARα-dependent manner similar to that observed in peroxisome proliferator-induced DNA damage (Figure 3.4B). These findings corroborate previous reports that peroxisome proliferators cause oxidative damage [48,82,110] through a mechanism that involves oxidants from parenchymal cells.

Along with altered cell turnover, oxidative DNA damage is another mode of action that is considered to be important to peroxisome proliferator-induced carcinogenesis. Overproduction of reactive oxygen species from a number of cellular sources can lead to oxidative damage of macromolecules in absence of scavenging proteins [42,93]. Induction of microsomal and peroxisomal oxidases in hepatocytes and activation of NADPH oxidase in Kupffer cells are two potential molecular sources of peroxisome proliferator-induced oxidant production, respectively. It was previously shown that dietary administration of WY-14,643 for up to 1 month led to increased expression of base excision DNA repair genes, a marker of oxidative DNA damage *in vivo* [110]. This effect was shown to be dependent on PPARα, not Kupffer cell NADPH oxidase. In the present study we assessed oxidative DNA damage at 5 months of continuous treatment with WY-14,643 and report that oxidative DNA damage persists and continues to be dependent on PPARα, not NADPH oxidase. Taken together with the fact that the activity of acyl-coA oxidase, a PPARα target gene, was also observed to be elevated following 5 months-long WY-14,643 treatment, these data suggest that peroxisomal enzymes, not activated Kupffer cells are the likely source of reactive oxygen species that contribute to oxidative DNA damage in the mode of action of peroxisome proliferators.

In conclusion, this long term feeding study with a model peroxisome proliferator compound WY-14,643 demonstrates that PPARα, not Kupffer cell-derived oxidants are important for the key steps critical for carcinogenesis – cell proliferation and oxidative DNA damage. While activated Kupffer cells mediate acute effects of these agents on cell proliferation and production of oxidants in liver, this pathway appears to not be sustained and may play a limited, if any, role in long-term effects of peroxisome proliferators such as hepatocarcinogenesis.

Figure 3.1. WY-14,643 causes substantial changes in body and liver weight in mice and reduced survival of p47^{phox} WT and KO mice.

(A) Body weight was recorded on a weekly basis and is plotted for up to 5 months of treatment with 0.1% WY-14,643. **(B)** Liver and body weight were recorded at sacrifice. Control liver weights were averaged at 1 week, 5 weeks, and 5 months. Statistical significance ($p<0.05$) is indicated with asterisks (*, different from Control, ** different from 1 week-treated group, *** different from 5 week-treated group). **(C)** Animal survival was noted every other day**.** Kaplan-Meier method was used to plot a time course of survival rates.

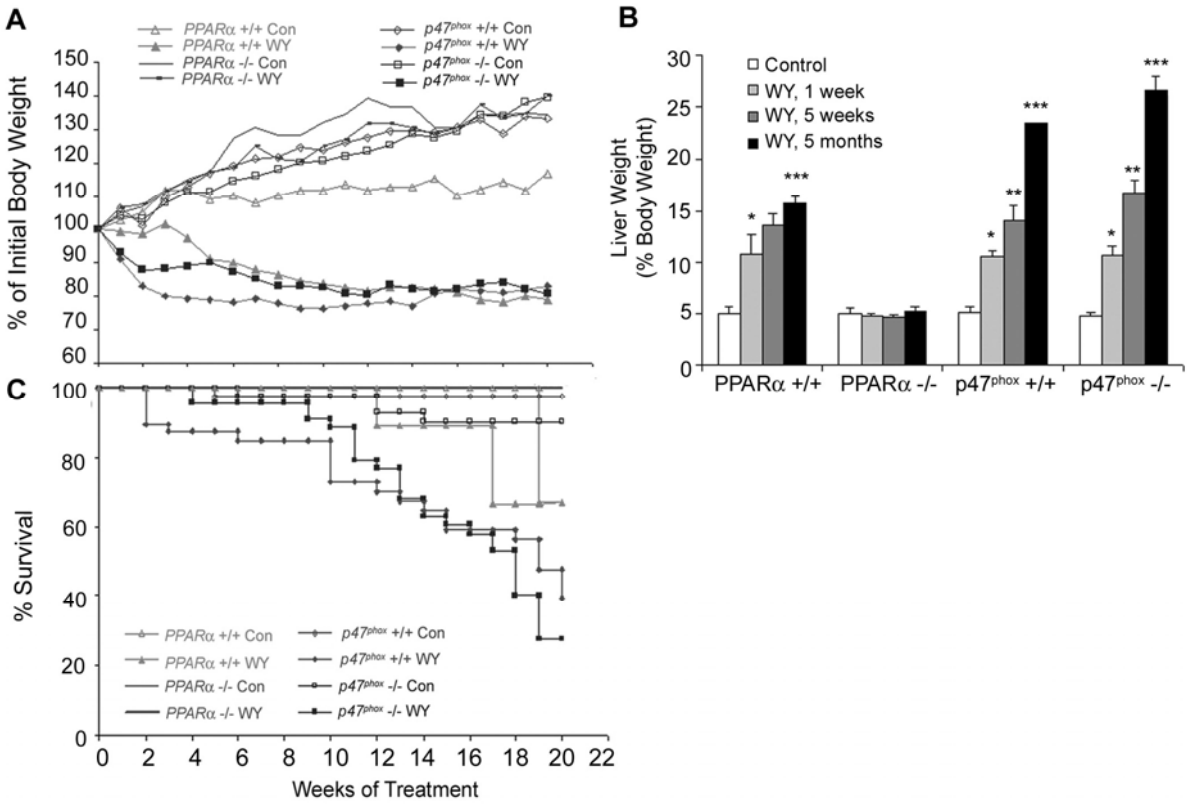

Figure 3.2. Liver histopathology in mice treated for 5 months with WY-14,643.

(A) Normal liver morphology in *PPARα* +/+ mice on the control diet. **(B)** Photomicrograph of a necro-inflammatory lesion in liver of *PPARα* +/+ mice treated with WY-14,643 (0.1%). Necrotic (n) and inflamed (i) areas are indicated. **(C)** Steatosis (s) as observed in *PPARα* -/- mice fed WY-14,643 (0.1%). **(D)** Extensive hepatocellular hypertrophy is evident in $p47^{phox}$ +/+ mice treated with WY-14,643 (0.1%). **(E)** Regions of necrosis and inflammation in liver from $p47^{phox}$ -/- mice fed WY-14,643 (0.1%). **(F)** High magnification photomicrograph shows enlarged hepatocytes, binucleate cells (b) and lipid accumulation in $p47^{phox}$ -/- mice fed WY-14,643 (0.1%). **(G)** High magnification photomicograph showing mitotic cells (m) in *PPARα* +/+ mice fed WY-14,643 (0.1%).

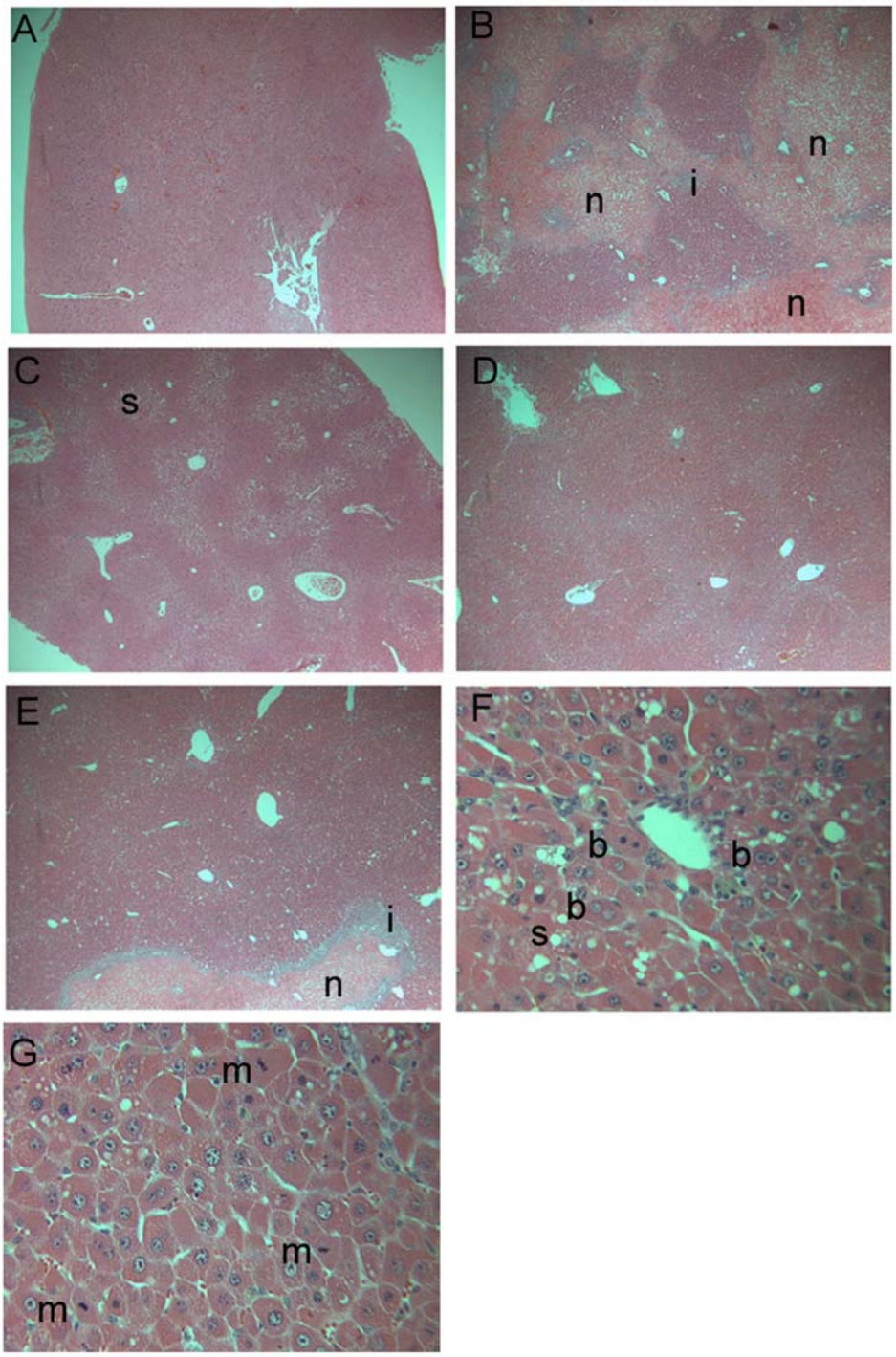
A
B
n
i
n
n
C
s
D
E
i
n
F
b
b
b
s
G
m
m
m

Table 3.1. Changes in serum ALT and triglicerides caused by WY-14, 643 in mice

	Treatment	Time course	N	[a]ALT (U/L)	[a]Triglycerides (U/L)
PPARα +/+	[b]Control		7	25.1 ± 4.9	101.4 ± 12.3
	WY-14,643 (0.1%)	1 week	3	109.7 ± 34.9*	55.0 ± 3.2*
		5 weeks	6	572.3 ± 79.7**	55.0 ± 0.0*
		5 months	6	760.7 ± 215.3**	29.8 ± 6.0**
PPARα -/-	Control		4	21.1 ± 4.1	33.0 ± 0.4
	WY-14,643 (0.1%)	1 week	3	28.6 ± 16.5	[c]N/A
		5 weeks	3	12.0 ± 1.7	131.7 ± 24.1*
		5 months	5	36.6 ± 6.2	201.8 ± 17.6**
p47^{phox} +/+	Control		17	49.6 ± 3.6	69.7 ± 6.6
	WY-14,643 (0.1%)	1 week	12	105.1 ± 13.5*	[c]N/A
		5 weeks	7	697.5 ± 89.3**	52.4 ± 10.3
		5 months	[c]N/A	[c]N/A	[c]N/A
p47^{phox} -/-	Control		3	27.8 ± 6.7	[c]N/A
	WY-14,643 (0.1%)	1 week	3	182.2 ± 51.5*	[c]N/A
		5 weeks	3	1454.0 ± 170.8**	30.5 ± 5.5
		5 months	[c]N/A	[c]N/A	[c]N/A

[a] Values represented are Mean ± SEM
[b] Control values represent average control across all time points
[c] N/A: data is Not Available
Asterisks denote statistical significance from control (*), 1 week (**) or 5 weeks (***) at a level of $p < 0.05$

Figure 3.3. Changes in cell replication caused by WY-14,643 are independent of NADPH oxidase and may be mediated by NFκB.

PPARα -/-, *p47*^{phox} -/- and WT mice were fed a WY-14,643-containing diet (0.1% w/w) for up to 5 months. **(A)** Proliferation was measured by immunohistochemical detection of BrdU in liver. Control values were averaged at 1 week, 5 weeks, and 5 months. Statistical significance ($p<0.05$) is indicated with asterisks (*, different from Control, ** different from 5 months-treated group). **(B)** DNA binding activity of NFκB was determined using EMSA as outlined in "Materials and Methods." Hela cell nuclear extracts were used as a positive control to demonstrate specificity of the NFκB probe.

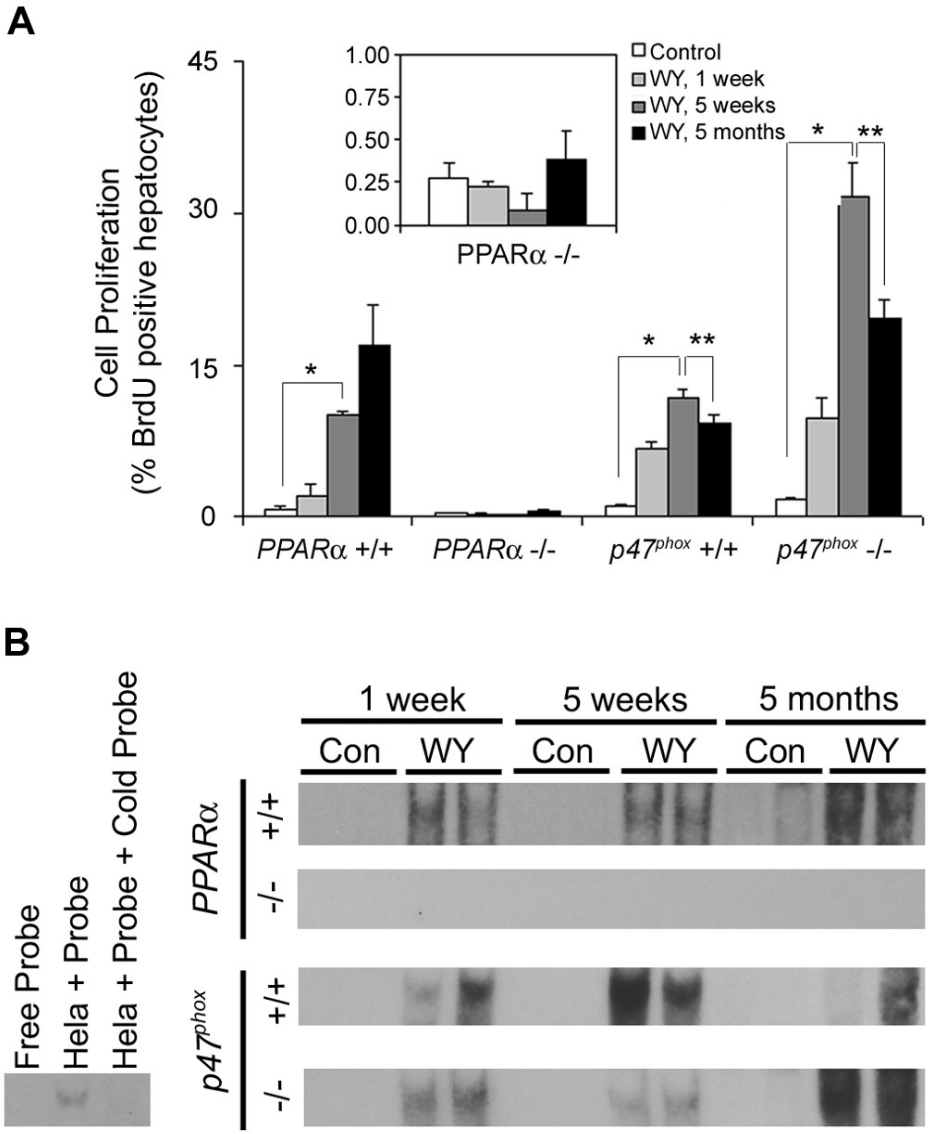
A
Cell Proliferation
(% BrdU positive hepatocytes)
45
30
15
0
1.00
0.75
0.50
0.25
0.00
PPARα -/-
Control
WY, 1 week
WY, 5 weeks
WY, 5 months
*
**
PPARα +/+
PPARα -/-
p47phox +/+
p47phox -/-
B
Free Probe
Hela + Probe
Hela + Probe + Cold Probe
1 week
5 weeks
5 months
Con
WY
PPARα
+/+
-/-
p47phox

Table 3.2. Effect of WY-14,643 on cell cycle and apoptosis-related protein expression at 5 months

	Treatment	N	[a]Cyclin B1	[a]Cdk1	[a]Cdk2	[a]Cdk4	[a]Caspase 8	[a]Caspase 9
PPARα +/+	Control	2	1.0 ± 0.1	1.0 ± 0.4	1.0 ± 0.8	1.0 ± 0.4	1.0 ± 0.7	1.0 ± 0.2
	WY-14,643	3	32.5 ± 7.9*	10.4 ± 1.4*	0.6 ± 0.1	4.7 ± 0.5*	0.0 ± 0.0*	0.6 ± 0.3
PPARα -/-	Control	3	1.0 ± 0.3	1.0 ± 0.3	1.0 ± 0.3	1.0 ± 0.7	1.0 ± 0.3	1.0 ± 0.2
	WY-14,643	3	1.4 ± 0.2	0.9 ± 0.5	0.9 ± 0.6	1.8 ± 0.6	1.1 ± 0.8	0.9 ± 0.1
$p47^{phox}$ +/+	Control	3	1.0 ± 0.5	1.0 ± 0.3	1.0 ± 0.7	1.0 ± 0.6	1.0 ± 0.6	1.0 ± 0.4
	WY-14,643	3	36.7 ± 6.4*	3.1 ± 0.6*	1.2 ± 0.6	5.7 ± 1.3*	0.1 ± 0.0*	0.7 ± 0.3
$p47^{phox}$ -/-	Control	3	1.0 ± 0.1	1.0 ± 0.3	1.0 ± 1.0	1.0 ± 0.8	1.0 ± 0.0	1.0 ± 0.3
	WY-14,643	3	19.3 ± 2.7*	4.1 ± 2.1*	2.3 ± 2.6	4.3 ± 0.2*	1.1 ± 0.5	0.6 ± 0.1

[a] Values represented are Mean ± SEM and are normalized to strain-matched control values
Asterisk (*) denotes statistical significance from control at a level of $p < 0.05$

Figure 3.4. WY-14,643 induces oxidative stress that is dependent on PPARα, not NADPH oxidase

Mice were administered Control or WY-14,643 (0.1% w/w)-containing diet for 5 months. **(A)** An apurinic/apyrimidinic (AP) site slot blot assay was performed as described in "Materials and Methods" to detect oxidative damage of DNA. **(B)** Activity of peroxisomal enzyme, Acyl-CoA oxidase was measured as described in the "Materials and Methods." Statistical significance ($p<0.05$) is indicated with an asterisk (*, different from Control).

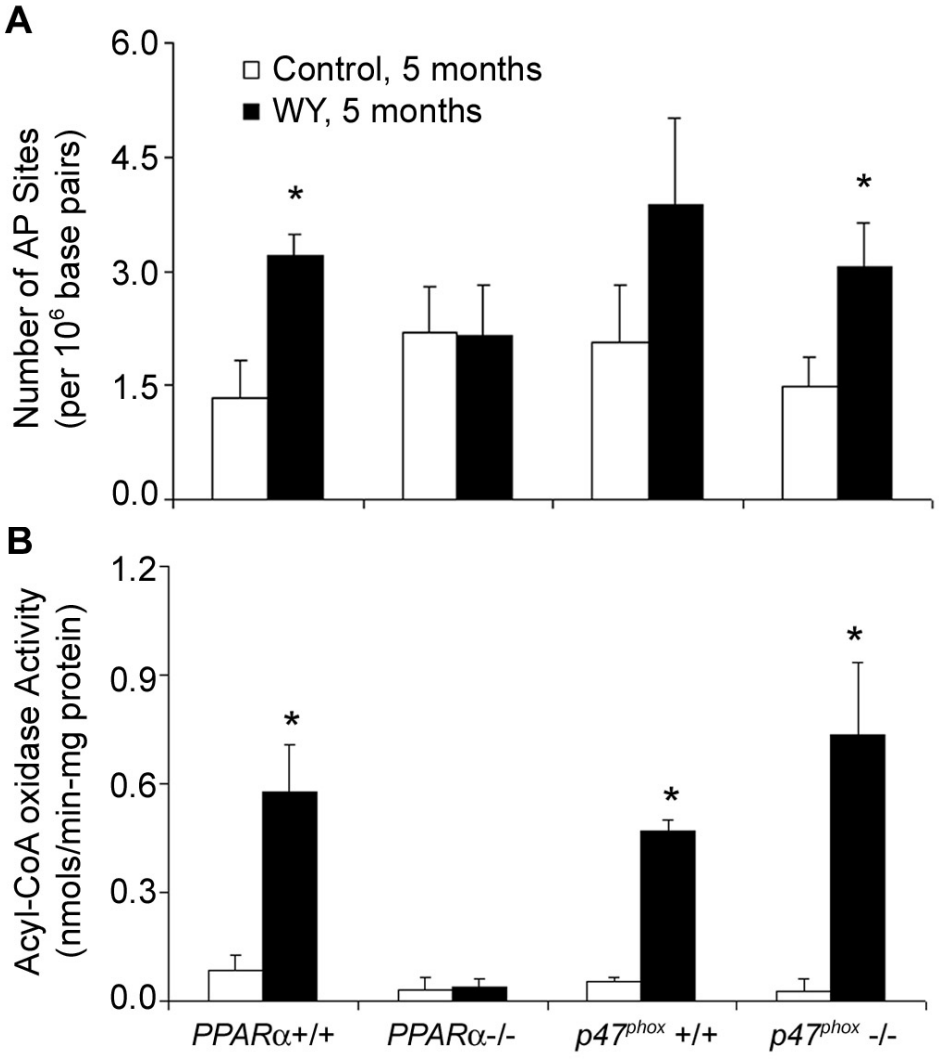

CHAPTER IV

Gene expression in mouse liver reveals a temporal shift in molecular pathways that mediate effects of peroxisome proliferators

A. ABSTRACT

Administration of peroxisome proliferators to rodents causes proliferation of peroxisomes, induction of β-oxidation enzymes, hepatocelluar hypertrophy and hyperplasia, with chronic exposure ultimately leading to hepatocellular carcinomas. Many of these and other pleiotropic responses associated with peroxisome proliferators are nuclear receptor mediated events involving peroxisome proliferator activated receptor alpha (PPARα). A significant role for nuclear receptor-independent events has also been shown, with clear evidence of Kupffer cell-mediated oxidative stress, mitogen production and cell replication following acute or sub-acute treatment with peroxisome proliferators in rodents. Recent studies have demonstrated that NADPH oxidase is not involved in the sustained proliferative effects, oxidant production or DNA damage caused by prolonged PP administration. In an effort to determine the timing of this transition from Kupffer cell- to PPARα-modulation of peroxisome proliferator effects, gene expression was assessed in liver from *PPARα* -/-, $p47^{phox}$ -/- and corresponding wild-type mice following treatment with 4-Chloro-6-(2,3-xylidino)-pyrimidynylthioacetic acid (WY-14,643) for 8 hr, 24 hr, 72 hr, 1 wk, or 4 wk. WY-14,643 -induced gene expression in $p47^{phox}$-null mouse liver differed substantially from wild-type mice at acute doses and striking differences in baseline expression of immune related genes were evident. Pathway mapping of genes that respond in a time- and dose-dependent manner corroborate existing data demonstrating suppression of immune response, cell death and signal transduction and promotion of lipid metabolism, cell cycle and DNA repair by peroxisome proliferators. Furthermore, these pathways were by in large dependent on PPARα, not NADPH oxidase demonstrating a temporal shift in response to peroxisome proliferators from Kupffer cell- to hepatocyte-centric.

B. INTRODUCTION

Peroxisome proliferators (PPs) are a chemical class comprised of a wide range of industrial, pharmaceutical and endogenous compounds. These compounds have been the subject of debate for several decades because of their carcinogenicity in rats and unknown risk to humans, who are likely exposed given the ubiquitous use of such peroxisome proliferators as phthalates. Though human health outcomes following long-term exposure to peroxisome proliferators are inconclusive, chronic administration of these agents to rats and mice leads to development of liver neoplasia by a nongenotoxic mechanism [18]. A number of peroxisome proliferartor-induced events leading up to carcinogenesis, including increased cell replication, oxidative damage and tumorigenesis itself require activation of nuclear receptor peroxisome proliferator activated receptor alpha (PPARα) [21,110]. This receptor is largely responsible for lipid metabolism through transcriptional regulation of fatty acid oxidation enzymes, apolipoproteins and transporters. Recently PPARα is also involved in glucose metabolism and inflammation [125]. Interestingly, among species there are substantial structural differences in the DNA binding element, peroxisome proliferator response element (PPRE) along with differences in basal PPARα expression, with humans exhibiting a tenth of the levels observed in rodents [28]. It is still unclear as to whether the divergent physiological observations among species in response to peroxisome proliferators (with mice and rats being the most sensitive) are solely attributed to nuclear receptor-mediated effects or if these differences are independent of PPARα.

A wide range of nuclear receptor-independent effects have been attributed to Kupffer cell activation by peroxisome proliferators. *In vitro* studies demonstrate that peroxisome proliferators stimulate superoxide and cytokine production by these liver macrophages

[66,76,77]. Studies performed *in vivo* with NADPH oxidase inhibitors and Kupffer cell inactivators corroborate that reactive oxygen species production following peroxisome proliferator treatment is derived from Kupffer cells, and that these oxidants are directly involved in signaling of mitogens which may contribute to proliferative responses [65,77]. Furthermore, studies using NADPH oxidase deficient mice ($p47^{phox}$-null) or *PPARα* –null mice demonstrated that acute oxidant production is derived from Kupffer cells, and not PPARα-mediated parenchymal sources [46]. Though key steps (enzyme induction, enhanced oxidant production and oxidative DNA damage, increased cell proliferation and suppression of apoptosis) in the mode of action of these compounds have repeatedly demonstrated with various peroxisome proliferator compounds, insight into the molecular mechanisms responsible for these events is still lacking. Understanding the role of receptor-independent events in the mode of action of peroxisome proliferators and its relevance to humans is a necessary step in predicting human health risk of cancer by these agents.

Microarray technology has served as a valuable tool for gathering mechanistic information regarding toxicants' molecular targets and temporal progression of toxicity leading to a specific disease state, both of which are important for chemical risk assessment. Genomic studies investigating the effects of peroxisome proliferators in rodent liver have largely supported phenotypic findings from traditional assays. In an effort to fill the gap in knowledge with regards to the temporal relationship between peroxisome proliferator-modulated effects and molecular mediators of these effects, gene expression analysis was conducted in liver from acute, sub-acute and sub-chronically treated $p47^{phox}$-null, *PPARα*-null and wild type mice with potent peroxisome proliferator, 4-Chloro-6-(2,3-xylidino)-pyrimidynylthioacetic acid (WY-14,643). We hypothesize that NADPH oxidase-dependent

genes which are relevant to the mechanism of hepatocarcinogenic action of peroxisome proliferators will respond to acute WY-14,643 treatment, but induction of many of these genes will diminish with sub-chronic WY-14,643 treatment. Furthermore, we expect that a strong PPARα-specific gene signature will be evident.

C. MATERIALS AND METHODS

Animals, Diet and Tissue Collection

p47^{phox}-null male mice (C57BL/6J background; [85]), *PPARα*-null male mice (SV129 background; [33]), and corresponding wild type counterparts (6-8 weeks of age at the beginning of treatment) were used in these experiments. All animals used for this study were housed in sterilized cages in a facility with a 12-hr night/day cycle. Temperature and relative humidity were held at 22 ± 2°C and 50 ± 5%, respectively. The UNC Division of Laboratory Animal Medicine maintains these animal facilities, and veterinarians were always available to ensure animal health. All animals were given humane care in compliance with NIH and institutional guidelines and studies were performed according to protocols approved by the appropriate institutional review board. Prior to experiments, animals were maintained on standard lab chow diet and purified water *ad libitum*. 4-Chloro-6-(2,3-xylidino)-pyrimidynylthioacetic acid (WY-14,643) was obtained from Aldrich (Milwaukee, WI). Acute doses were administered by a single oral gavage of 0 (control), 5 or 50 mg/kg of WY-14,643 in olive oil. Mice (n=3) were sacrificed either 8 hr, 24 hr, or 72 hr post dosing. Sub-chronic doses of WY-14,643 were administered in the diet *ad libitum*. NIH-07 was used as the base for the powdered diet containing either 0% (control), 0.005 % w/w or 0.05% w/w of WY-14,643. Mice (n=3) were sacrificed after either 1 week or 4 weeks of dietary treatment. Animals had free access to water throughout the study and the health status of the animals was monitored every other day. At sacrifice, mice were anesthetized with pentobarbital (100 mg/kg) and following exsanguination, livers were removed and weighed. A section from the

left lateral lobe was fixed in 10% formalin. The remaining tissue was placed in an eppendorf tube and snap frozen in liquid nitrogen. These samples were stored at -80ºC until assayed.

RNA Isolation

While frozen a small fragment (approximately 10 - 30 mg) was removed for each sample and homogenized for 30 sec in 600 µl RLT buffer (Qiagen, Valencia, CA) containing 1 % β-mercaptoethanol. The lysate was centrifuged for 3 min at 13000 rpm. From the resulting supernatant, total RNA was isolated using an RNeasy kit (Qiagen) as per the manufacturer's protocol. Total RNA integrity and quantification were assessed using RNA 6000 nano assay LabChips® (Agilent Technologies, Santa Clara, CA) and analysed on a 2100 Bioanalyzer (Agilent Technologies) as per the manufacturer's protocol.

cDNA Preparation and Microarray Hybridization

Preparation of cDNA and labeling was performed using reagents from the low RNA input fluorescent linear amplification kit (Agilent Technologies) based on modified version of the manufacturer's protocol. A pooled (kidney, spleen, lung, brain, and liver) RNA sample (Cogenics, RTP, NC) derived from equal amounts of RNA from each of the single organ RNA pools was used as a reference and prepared in parallel to the samples of interest [126]. Total RNA (2.5 µg) was brought to a volume of 4.5 µl with Rnase-free water and incubated for 10 min at 65°C in an eppendorf tube with the cap open so that residual ethanol (from RNA isolation) could evaporate. A T7 promoter primer (2.5 µl) was added to the mixture and allowed to incubate again for 10 min at 65°C, followed by cooling at 4°C for 5 min. To reverse transcribe cDNA from the RNA samples, a cDNA master mix containing the

following proportions was prepared: 2 µl of 5X first strand buffer, 1 µl of 0.1M DTT, 0.5 µl of 10mM dNTP mix, 0.5 µl of Rnase-free water, 0.8 µl of MMLV reverse transcriptase, and 0.2 µl of RNaseOUT. A volume of 5 µl was added to each sample, which was gently mixed and allowed to incubate for 2 hrs at 40°C, then 15 min at 65°C and cooled to 4°C for 5 min. Next, preparation of fluorescent cRNA synthesis involved addition of 1 µl of Cyanine 3-CTP (Cy3) (Perkin Elmer, Wellesley, MA) to the pooled reference sample and cyanine 5-CTP (Cy5) to the experimental samples. A transcription master mix was prepared by using the following proportion of reagents: 7.85 µl of RNase-free water, 10 µl of 4X transcription buffer, 3 µl of 0.1 M DTT, 4 µl of NTP mix, 3.2 µl of PEG, 0.25 µl of RNaseOUT, 0.3 µl of inorganic pyrophosphatase, and 0.8 µl of T7 RNA polymerase. To each cDNA sample, 29 µl of transcription master mix was added. Samples were mixed gently, followed by 2 hr incubation in the dark at 40°C and cooling at for 1 -30 min at 4°C. Finally, unincorporated dye-labeled nucleotides were removed from cRNA samples. The entire cRNA sample, along with 500 µl of PB buffer and 60 µl of RNase water was added to a spin column from a PCR Purificaiton kit (Qiagen), mixed and spun for 15 sec at 10,000 rpm. After discarding the flow-through, the column was washed with 500 µl of PE buffer and centrifuged for 15 sec at 10,000 rpm. The step was repeated using 300ul of PE buffer and centrifuging for 2 min. Finally the cRNA was eluted into a new tube by adding 50 µl of EB buffer and spinning for 1 minute. This step was repeated to produce a final volume of 100 µl. The concentration of the purified cRNA samples was then measured.

A hybridization mixture was prepared by adding 2 µg of Cy-3-labeled reference cRNA with 2 µg of Cy-5 labeled cRNA for an experimental sample, 200 µl of Rnase-free water, 8 µl of fragmentation buffer and 10 µl of 100x control targets to a fresh tube. Each

sample mixture was incubated for 30 min in the dark at 60°C before hybridizing (overnight for at least 17 hr) onto Agilent G4121A microarrays (Agilent Technologies) in a pre-heated oven at 60°C. Slides were washed in a solution containing 2X SSC/0.005% TritonX-102 followed by 0.1X SSC for 10 min each. Finally each slide was dipped into a 2:1 stabilization solution-acetonitrile solution for 10 seconds and stored in a dark box before scanning shortly after.

Microarray Data Analysis

Data was extracted from arrays using Agilent Feature Extraction 6.0 Software. Data was initially represented as $\log_2$ (Cy5/Cy3). Array quality was assessed by Feature Extraction software and genes with fewer than 70% present data across all arrays were excluded from further analysis. A total of 16,030 probes passed this data quality filter. Removal of control oligos, and RIKENs, for which little or no functional data was available reduced the list to 11,421 genes. These transcripts comprised our working data set. LOWESS normalization was performed to eliminate dye bias. A second normalization was performed to correct for basal differences in gene expression between SV129 and C57BL/6J mice or between wild-type (WT) and knockout (KO) mice on both backgrounds. For a given gene, the Cy5/Cy3 ratios were divided by the average Cy5/Cy3 ratio for their time-matched controls. Missing data points were calculated using K-nearest neighbor imputation method [127]. Average-linkage, hierarchical clustering was performed using Cluster software on median centered (by genes) data and visualization was facilitated by Treeview [128].

Differentially expressed genes were identified using either Significance Analysis of Microarrays (SAM) or EDGE software [129,130]. SAM was performed in cases where

statistical significance across only one variable (time, strain or dose) was being assessed. EDGE was preferred for identifying differentially expressed genes across two or more variables (i.e. time and dose). EDGE employs a spline –based statistic, which fits data to a curve representing the null hypothesis (no statistical difference in expression) and a curve representing the alternative hypothesis (differential expression) between two groups of interest. A statistic is calculated based on the goodness of fit of the expression data for a given gene to these two curves. The spline-based approach provides substantially more power compared to t- and F-statistics for multivariate analysis, and is well suited for timecourse array studies [131]. Q-values, which represent the false discover rate (FDR) of less than 0.05 for SAM and EDGE were selected as thresholds for differential expression. Once the list of significant genes was generated by EDGE, a t-statistic was calculated for each gene at each strain/time combination to determine statistical difference between high dose and control expression. For each strain/time combination, a list of differentially expressed genes ($P<0.05$) was submitted for functional analysis.

Functional Analysis of Significant Genes

EASE , GOMiner, or High-Throughput GOMiner were used to determine biological function of differentially expressed genes, in the context of Gene Onotology (GO) [132,133]. EASE or GOMiner was preferred for pathway analysis of genes identified in two class SAM comparisons. An EASE score or P value < 0.05 was selected as the cutoff for statistical significance EASE and GOMiner, respectively. High-Throughput GOMiner is designed to facilitate pathway mapping in cases when several gene lists are to be analyzed. High-Throughput GOMiner was used for pathway analysis of significant genes lists generated

from EDGE timecourse analysis. A Q-value, representative of the FDR, less than 0.05 and $P<0.05$ were the basis for statistical significance from this analysis. Finally, gene networks were prepared with PathwayStudio® 4.0 software (Ariadne Genomics, Rockville, MD) [134]. The software uses Medscan natural language processing to gather information from all abstracts on PubMed and other public data sources, which is extracted to assemble molecular networks.

RT-PCR

Real-time PCR assays were performed using Taqman ® (Applied Biosystems) low density arrays to probe over 300 genes of interest (Appendix 2). RNA samples from animals treated with Control or WY-14,643-containing diet for 4 weeks were used for this analysis. Preparation of cDNA and PCR were performed according to the manufacturer's protocol. Quantification of data involved determining calculating $2^{\Delta\Delta CT}$ value. The ΔC_t value for all genes were calculated relative to the average C_t value for four GAPDH probes) The $\Delta\Delta C_t$ values were calculated using WY-14,643 ΔC_t values relative to mean ΔC_t values for strain-matched controls.

D. RESULTS AND DISCUSSION

Inherent differences in gene expression between p47^{phox} WT and KO mice

The aim of this study was to investigate WY-14,643-induced temporal changes in gene expression for nuclear receptor-mediated and –independent pathways that may be important to the mechanism of action of peroxisome proliferators. In particular, differences between gene expression modulation by WY-14,643 in *p47^{phox}* – and *PPARα*-null mice were to be evaluated. First, gene expression in control-fed wild-type (WT) and knock-out (KO) mice was compared. This analysis was performed with the expectation that identifying baseline differences in WT and KO mice may help put chemical-induced gene expression changes into perspective. In addition to confirming divergent basal gene expression, putative and novel pathways associated with the KO model were revealed. Prior to normalizing with time-matched controls, Significance Analysis of Microarrays (SAM) was performed between control-fed *p47^{phox}* WT and KO mice and 2257 differentially expressed genes were identified across all time points. Following significance analysis, enriched pathways were identified using EASE. Among the several GO biological processes that were differentially expressed between *p47^{phox}* WT and KO mice were immune response, fatty acid metabolism (specifically β-oxidation), glucose metabolism and amino acid metabolism (Table 1).

Divergent expression of genes involved in innate immunity (Figure 4.1A) is not surprising given the major role that Kupffer cells play in the liver's defense response [135]. A number of lipid mediators of inflammation exhibited higher basal levels of expression in *p47^{phox}* -/- mice. These include phosopholipase A2 (*Pla2g4a*), which plays a role in arachidonic acid release and eiconsanoid biosynthesis, prostaglandin endoperoxide synthase 1 (*Ptgs1*), also known as cyclooxygenase 1 (*Cox1*), lipoprotein lipase (*Lpl*), and NADPH-

dependent enzyme leukotriene B4 dehydrogenase (*Ltb4dh*). KO mice also exhibited elevated levels of Toll-like receptor 4 (*Tlr4*), which is a well-known mediator of lipopolysaccharide (LPS)-induced inflammation. Complement 3 (*C3*) and fibronectin 1 (*Fn1*), which both promote phagocytosis were suppressed in $p47^{phox}$ -/- mice. From the heatmap, it appears that the $p47^{phox}$ -/- mice initially exhibit suppressed or balanced immune response (8 hr – 1wk), that later becomes elevated to comparable or higher levels compared to their wild-type counterparts at 4 wk. NADPH oxidase-deficient mice are highly sensitive to bacterial infections that stimulate a robust, chronic inflammatory response [85] that can not be quelled in the absence of NADPH oxidase oxidant production. The gradual increase in basal expression of inflammatory mediators in these mice after 4 weeks predicts this phenotype.

Wild-type and $p47^{phox}$-/- mice also exhibited striking differences in basal gene expression for fatty acid metabolism genes, a large number of which are PPARα –regulated genes, particularly those encoding peroxisomal and mitochondrial β-oxidation enzymes (Figure 4.1B). Because Kupffer cells do not express PPARα [64], the mechanism of suppression of PPARα-reglated genes is unclear. More than one study has connected NADPH oxidase to lipid metabolism demonstrating that reactive oxygen species in macrophages mediate low density lipoprotein (LDL) oxidation [136,137]. The oxidized LDL metabolites are PPARα active and can promote transcription of PPARα target genes. Based on this proposed mechanism of induction of PPARα by macrophages, NADPH oxidase-deficient mice would generate fewer PPARα-active metabolites, and exhibit lower basal mRNA levels of PPARα –target genes compared to WT mice, as is observed.

Interestingly, the reduced expression of fatty acid metabolism genes and induction of immune response in NADPH oxidase-deficient mice may have fewer implications for

chronic effects of PPARα-ligands than one would expect. For example, reduced basal mRNA levels of PPARα target genes in $p47^{phox}$ -/- mice may not result in reduced protein expression or enzyme activity, as previous studies have shown control levels of PPARα protein and activity of PPARα-regulated enzyme acyl-coA oxidase (ACO) to be comparable in $p47^{phox}$ WT and KO mice. Similarly, WY-14,463-induced enzyme activity was comparable int WT and KO mice as well [77,138]. Also, peroxisome proliferator-induced suppression of immune response still occurs (see below), despite the elevated expression of defense-related genes in control-fed KO mice at 4 wk.

Basal gene expression in *PPARα* WT and KO mice was also evaluated. Over 850 genes showed differential expression, with the predominant pathways distinguishing WT from KO mice being fatty acid metabolism, RNA splicing and protein-ER targeting. The disparate baseline gene expression between WT and KO mice was the motivation for time-matched control normalizations (as described in "Materials and Methods") that was performed on all subsequently discussed data.

WY-14,643-induced differences in gene expression between $p47^{phox}$ WT and KO mice

Using toxicogenomics to validate the role of Kupffer cells as an important mediator of early response to peroxisome proliferators, acute and sub-chronic changes in gene expression were assessed. In particular, genes that demonstrated an early WY-14,643-induced change in expression in WT, but not KO were identified (Figure 4.2). Within this set of genes which exhibit an early dependence on NADPH oxidase, four classifications were made: (A) WY-14,643- up-regulated or (C) down-regulated genes which are not modulated by NADPH oxidase at later time points and (B) WY-14,643-up-regulated or (D) down-

regulated genes which still appear to be modulated by NADPH oxidase following continued treatment. Pathway mapping of genes from each classification, using GOMiner was performed. Gene set A was enriched with transcripts involved in cell division, which is supported by numerous studies in which DNA synthesis or cell proliferation in response to peroxisome proliferators is abrogated as a result of inactivation of NADPH oxidase or Kupffer cells [77,139] Also, induction of cell division at later time points, independent of NADPH oxidase supports the elevated cell proliferation observed in other studies conducted in our lab (unpublished data). Within gene set B, an increase in defense response, immune cell activation and endocytosis are acute responses to WY-14,643 that diminish with long-term treatment. This gene expression signature is supported by Kupffer cell activation by peroxisome proliferators and increased phagocytosis by these cells [63]. The link between Kupffer cells and pathways identified in gene sets C and D is less clear, though several studies have reported suppression of amino acid metabolism by peroxisome proliferator [140].

Temporal changes in gene expression reveal a robust sub-chronic signature for WY-14,643 treatment

To evaluate the timing of PPARα and Kupffer cell-mediated events, a time course of gene expression in WY-14,643-fed mice was performed on array data from each WT or KO mouse strain separately using EDGE software. EDGE analysis of arrays from $p47^{phox}$ +/+ mice produced the largest set of differentially expressed genes, with over 1200 time- and dose dependent transcripts observed. Hierarchical clustering of these significant genes in all strains shows the time- and dose-dependent expression (Figure 4.3). As expected, the timing

of gene induction appears to be different among all strains, with a uniformly robust response with 1 or 4 wk of continued WY-14,643 treatment. Also, most of these genes appear to be PPARα dependent, as little to no WY-14,643-induced change in expression occurs in *PPARα* -/- null mice. Pathway analysis of the significant genes lists was performed using High-Throughput GOMiner. Many of the biological processes identified are known to be perturbed by peroxisome proliferators (Figure 4.4).

Among the processes that are down-regulated by WY-14,643 treatment are immune response, cytolysis, electron transport and signal transduction. Up-regulation of pathways traditionally associated with peroxisome proliferators, including lipid metabolism, cell division, and response to endogenous stimulus (DNA repair) was also observed. By in large, sub-chronic treatment resulted in the most substantial induction of biological processes that may be relevant to the carcinogenicity of peroxisome proliferators. As evident in Figure 4.4, a robust signature for all of these pathways is observed at 1 wk and/or 4 wk, suggesting that the acute changes, even in peroxisome proliferator-induced cell proliferation, which has historically been considered an acute/sub-acute occurrence, may be less significant to the long-term effects of these compounds. Only acyl-coA metabolism (and its GO Term ancestors) exhibits a strong acute response that is sustained with continued feeding. Interestingly, temporal pathway analysis reveals an early PPARα-independent cell replication signature (see below), which is likely not relevant to the mechanism of action given the abrogated proliferative and tumorigenic response in PPARα-null mice. Many of the gene expression changes observed at 4 wk were confirmed using RT-PCR (Appendix 3), in which increased expression of genes related to fatty acid metabolism, DNA repair, and ubiquitin-

dependent protein catabolism was observed and transcript levels for genes involved in signal transduction were down.

Gene expression profiling reveals early PPARα-mediated immunosuppression by WY-14,643

In concordance with other studies, gene expression profiles reveal immunosuppression by WY-14,643 in a manner that is dependent on PPARα (Figure 4.5) [141-143]. Furthermore we show that the earliest onset of altered immune response occurs 24 hrs post-dosing with WY-14,643 (Figure 4.4). In particular, our results corroborate previous reports demonstrating decreased complement activation. We observed reduced transcript levels of complement 1 (*C1), C2*, C5, *C8*, *C9* and serine protease mannan-binding lectin serine peptidase (*Masp1)* [144-146]. In addition to serving as important mediators of innate and adaptive immune response, complements play a major role in cell death by opsonizing apoptotic cells which are later cleared by phagocytes [147]. As a result, suppression of complement pathways would likely lead to anti-apoptotic effects, which are considered to be an important mode of action in peroxisome proliferator-induced carcinogenesis.

Altered expression was observed for transcripts encoding cytokines, such as tumor necrosis factor (TNF) and interleukin 1 (IL1) and transcription factors that are regulated by or involved in regulation of cytokine release, including necrosis factor kappa B (NFκB), E74-like factor 1 (ELF1), nuclear factor of activated T-cells 5 (NFAT5) , and interferon regulator factor 2 (IRF2). Cytokines in the liver, which are mainly produced by Kupffer cells serve as important mediators of inflammatory response, but also prime cells to proliferate or undergo apoptosis [148]. There is conflicting evidence with regards to the effects of

peroxisome proliferators on cytokine production, and their importance to hepatocarcinogenesis. While a number of studies, have shown that cytokines play a critical role in cell proliferation and apoptosis by peroxisome proliferators [41,67,120,149,150], others have refuted the that cytokines are a requisite for altered cell turnover by peroxisome proliferators [151-153,153]. Evidence of a role for NFκB, a transcription factor which both modulates and is modulated by TNFα and other cytokines is slightly more consistent with many studies demonstrating PPARα- and/or reactive oxygen species (ROS)-mediated induction of NFκB [73-75,122,154] and fewer reports of PPARα-mediated inhibition of NFκB [155]. Gene expression in this study would support the latter, but we have recently observed (data not published) elevations in NFκB-DNA binding following 5 months of WY-14,643 treatment that was PPARα-dependent. It should be noted that NFκB expression is not exlusive to Kupffer cells, though it has been shown to be preferentially activated in Kupffer cells compared to hepatocytes following acute peroxisome proliferator treatment [74]. It is very likely that as Kupffer cell-mediated effects diminish, ROS from hepatocytes mediate peroxisome proliferator-induced NFκB activation [156].

In general the mechanism by which peroxisome proliferators elicit immunosuppression is not well understood. It has been suggested that the anti-inflammatory effects of peroxisome proliferators are mediated through PPARα-dependent regulation of NFκB inhibitory protein, inhibitory kappa B alpha (IκBα), also known as nuclear factor of kappa light polypeptide gene enhancer in B-cells inhibitor α (NFKBIA) [157]. Two other hypotheses link immune response with lipid metabolism, one of which involves activation of PPARα by leukotriene B4 (LTB4) and subsequent clearance of the pro-inflammatory agent through metabolism resulting, in a negative-feedback loop that regulates inflammation [141].

The evidence supporting this hypothesis is week, as LTB4 metabolism is not increased as a result of PPARα activation. Another theory suggests that peroxisome proliferators modulate immune response by modulating serum lipids. WY-14,643 treatment causes a decrease in serum lipids, thus altering the proportion of energy from fatty acids to peripheral tissues that parcipate in the immune response (i.e., spleen, lymphatic tissue). NADPH oxidase deficiency may render mice more susceptible to a reduction in defense response caused by WY-14,643, especially considering their inherent immunocompromised state. Based on gene expression from this study, we may conclude that Kupffer cell activation by peroxisome proliferators occurs very early (8hr) and diminishes or is overshadowed by a strong PPARα-mediated suppression of other immune-related responses shortly after (24 hr).

WY-14,643-induced PPARα-independent gene expression may be mediated by other PPARs

A role for Kupffer cells in induction of cell replication by peroxisome proliferators has been demonstrated, with absence of Kupffer cells, Kupffer cell-derived oxidants or cytokines resulting in abrogation of cell proliferation [67,71,77]. It is hypothesized that mitogenic cytokines engage in cross-talk with hepatocytes to maximally induce PPARα-mediated cell proliferation. Also, it is widely known that PPARα activation is required for peroxisome proliferator-induced cell proliferation *in vivo* [21]. However, transcriptional regulation of cell cycle regulatory genes by PPARα has not yet been verified. To investigate the possibility of cell cycle regulation by mitogens or by PPARα, the PPARα-independent gene signature at 24 hr was further assessed, with particular focus on genes contributing to the "cell cycle" node (Figure 4.6A). At 24 hr, differential expression of a number of genes

largely involved in promoting mitosis was exclusive to PPARα -/- mice. The relevance of this signature is unclear given that 1) *PPARα* -/- mice do not exhibit peroxisome proliferator-induced hepatocellular proliferation, and 2) induction of these genes is diminished in *PPARα* -/- mice at 4 wks, but elevated in wild type and $p47^{phox}$ -/- mice with continued WY-14,643 treatment (Figure 4.6B). It has recently been shown that mitogens are required for passage through the G2 phase of the cell cycle into M phase [158]. Mitogen-independent progression to mitosis is possible, but not before a lengthy cell cycle arrest (~10hr). Given the suppressed state of the immune response in WY-14,643- responders (*PPARα* +/+ and $p47^{phox}$ +/+ and -/-), it is possible that reduced mitogen release can explain the less robust cell cycle signature at early time points.

EDGE analysis performed on microarray data from PPARα -/- mice revealed a short list of genes with time-and does-dependent expression that are involved in a wide range of cellular functions (Figure 4.7). Among these genes was PPARα target cytochrome P450, 4a14 (*Cyp4a14),* which exhibited WY-14,643 suppression at 1wk. WY-14,643 treatment caused a decrease in integrin beta 1 binding protein (*Itgb1bp1*) expression and an increase in *Irf2*, which inhibits transcriptional activation of interferon, suggesting that a *PPARα*-independent mechanism of immunosuppression by peroxisome proliferators may be involved. D site albumin promoter binding protein (*Dbp*) is thought to be involved in circadian rhythms, which are known to be perturbed by peroxisome proliferators and fatty acids. Cyclin-dependent kinase inhibitor 1A (*Cdkn1a*), also known as p21, which associates with p53 to prohibit cell cycle progression, is significantly up-regulated in *PPARα* -/- mice with sub-acute WY-14,643 treatment and is suppressed at later timepoints. Tubulin 2 (Tubb2), which is also important to cell cycle regulation, particularly mitosis, exhibits a

similar pattern of expression as p21. Modulation of WY-14,643-induced gene expression by other PPARs is a possibility, as Tubb2 possesses a response element for both PPARγ and PPARδ [159]. Furthermore macrophages express PPARγ at fairly high levels, but not PPARα [160]. It was recently shown that *PPARα*-null on high fat diet exhibit compensatory expression of PPARγ expression, with levels 20-fold higher than in wild-type mice [161]. Despite the fact that WY-14,643 is a weak activator of PPAR isoforms other than alpha [162], the potential for them to modulate effects of peroxisome proliferators, particularly in PPARα-null mice should not be ruled out.

Conclusions

In this microarray time course study, we have demonstrated that WY-14,643 elicits gene expression changes that contribute to a range of altered biological responses. Many of the early gene expression changes appear to be Kupffer cell-mediated. Based on our findings, modulation of cell replication by Kupffer cell-derived mitogens, independent of PPARα is not evident beyond 24 hr. Also Kupffer cell-mediated defense mechanisms are diminished early, as WY-14,643 acts a potent immunosuppressant. This effect is largely PPARα-mediated. Collectively, these data suggest that Kupffer cells do not play a critical role in chronic effects of peroxisome proliferators, but are important for early responses to these agents.

Figure 4.1. Hierarchical clustering reveals divergent expression of genes involved in immune response and fatty acid metabolism between p47^{phox} WT and KO mice.

Prior to performing time-matched control normalization, unpaired two-class SAM analysis was conducted to identify differentially expressed genes between *p47^{phox}* WT and KO mice across all time points. Significant genes (FDR <0.05) were submitted to EASE for biological pathway analysis. Hierarchical clustering was performed on genes contributing to A) immune response or B) fatty acid metabolism, both of which were identified by EASE as being enriched processes (EASE score<0.05).

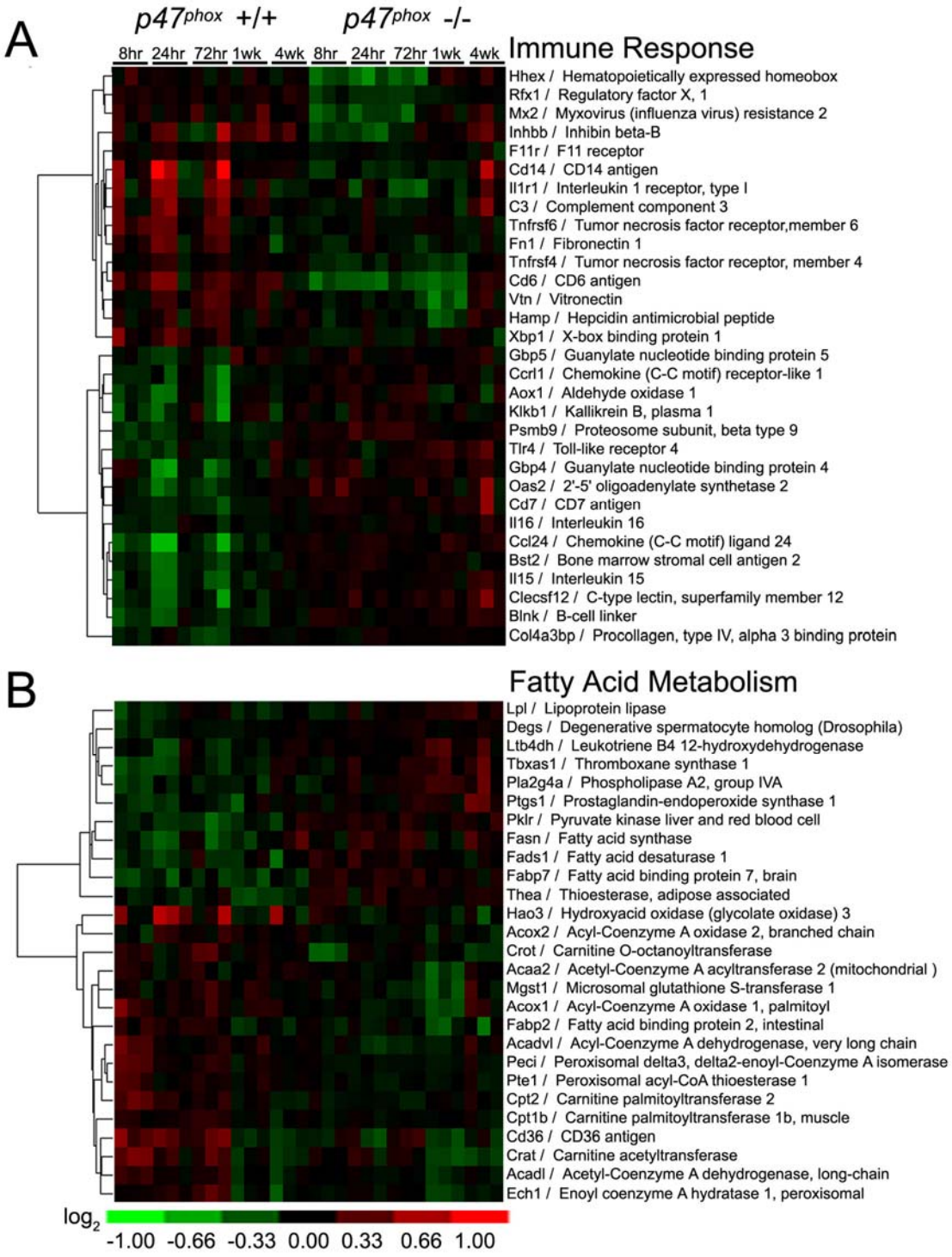
A
p47phox +/+
p47phox -/-
8hr 24hr 72hr 1wk 4wk 8hr 24hr 72hr 1wk 4wk
Immune Response
Hhex / Hematopoietically expressed homeobox
Rfx1 / Regulatory factor X, 1
Mx2 / Myxovirus (influenza virus) resistance 2
Inhbb / Inhibin beta-B
F11r / F11 receptor
Cd14 / CD14 antigen
Il1r1 / Interleukin 1 receptor, type I
C3 / Complement component 3
Tnfrsf6 / Tumor necrosis factor receptor,member 6
Fn1 / Fibronectin 1
Tnfrsf4 / Tumor necrosis factor receptor, member 4
Cd6 / CD6 antigen
Vtn / Vitronectin
Hamp / Hepcidin antimicrobial peptide
Xbp1 / X-box binding protein 1
Gbp5 / Guanylate nucleotide binding protein 5
Ccrl1 / Chemokine (C-C motif) receptor-like 1
Aox1 / Aldehyde oxidase 1
Klkb1 / Kallikrein B, plasma 1
Psmb9 / Proteosome subunit, beta type 9
Tlr4 / Toll-like receptor 4
Gbp4 / Guanylate nucleotide binding protein 4
Oas2 / 2'-5' oligoadenylate synthetase 2
Cd7 / CD7 antigen
Il16 / Interleukin 16
Ccl24 / Chemokine (C-C motif) ligand 24
Bst2 / Bone marrow stromal cell antigen 2
Il15 / Interleukin 15
Clecsf12 / C-type lectin, superfamily member 12
Blnk / B-cell linker
Col4a3bp / Procollagen, type IV, alpha 3 binding protein
B
Fatty Acid Metabolism
Lpl / Lipoprotein lipase
Degs / Degenerative spermatocyte homolog (Drosophila)
Ltb4dh / Leukotriene B4 12-hydroxydehydrogenase
Tbxas1 / Thromboxane synthase 1
Pla2g4a / Phospholipase A2, group IVA
Ptgs1 / Prostaglandin-endoperoxide synthase 1
Pklr / Pyruvate kinase liver and red blood cell
Fasn / Fatty acid synthase
Fads1 / Fatty acid desaturase 1
Fabp7 / Fatty acid binding protein 7, brain
Thea / Thioesterase, adipose associated
Hao3 / Hydroxyacid oxidase (glycolate oxidase) 3
Acox2 / Acyl-Coenzyme A oxidase 2, branched chain
Crot / Carnitine O-octanoyltransferase
Acaa2 / Acetyl-Coenzyme A acyltransferase 2 (mitochondrial)
Mgst1 / Microsomal glutathione S-transferase 1
Acox1 / Acyl-Coenzyme A oxidase 1, palmitoyl
Fabp2 / Fatty acid binding protein 2, intestinal
Acadvl / Acyl-Coenzyme A dehydrogenase, very long chain
Peci / Peroxisomal delta3, delta2-enoyl-Coenzyme A isomerase
Pte1 / Peroxisomal acyl-CoA thioesterase 1
Cpt2 / Carnitine palmitoyltransferase 2
Cpt1b / Carnitine palmitoyltransferase 1b, muscle
Cd36 / CD36 antigen
Crat / Carnitine acetyltransferase
Acadl / Acetyl-Coenzyme A dehydrogenase, long-chain
Ech1 / Enoyl coenzyme A hydratase 1, peroxisomal
log2
-1.00 -0.66 -0.33 0.00 0.33 0.66 1.00

Figure 4.2. Early differences in WY-14,643-induced response between p47^{phox} WT and KO.

Comparative t-tests were performed to identify genes in which early WY-induced expression is mediated by NADPH oxidase. Genes from various portiond of the heatmap were submitted to GOMiner to identify enriched ($P<0.05$) biological processes. **A & C)** These genes exhibit an early response to WY-14,643 that remains induced with continued treatment, but only the initial induction appears to be mediated by NADPH-oxidase. **B & D)** These genes exhibit only an early response to WY-14,643 that is NAPDH oxidase- mediated.

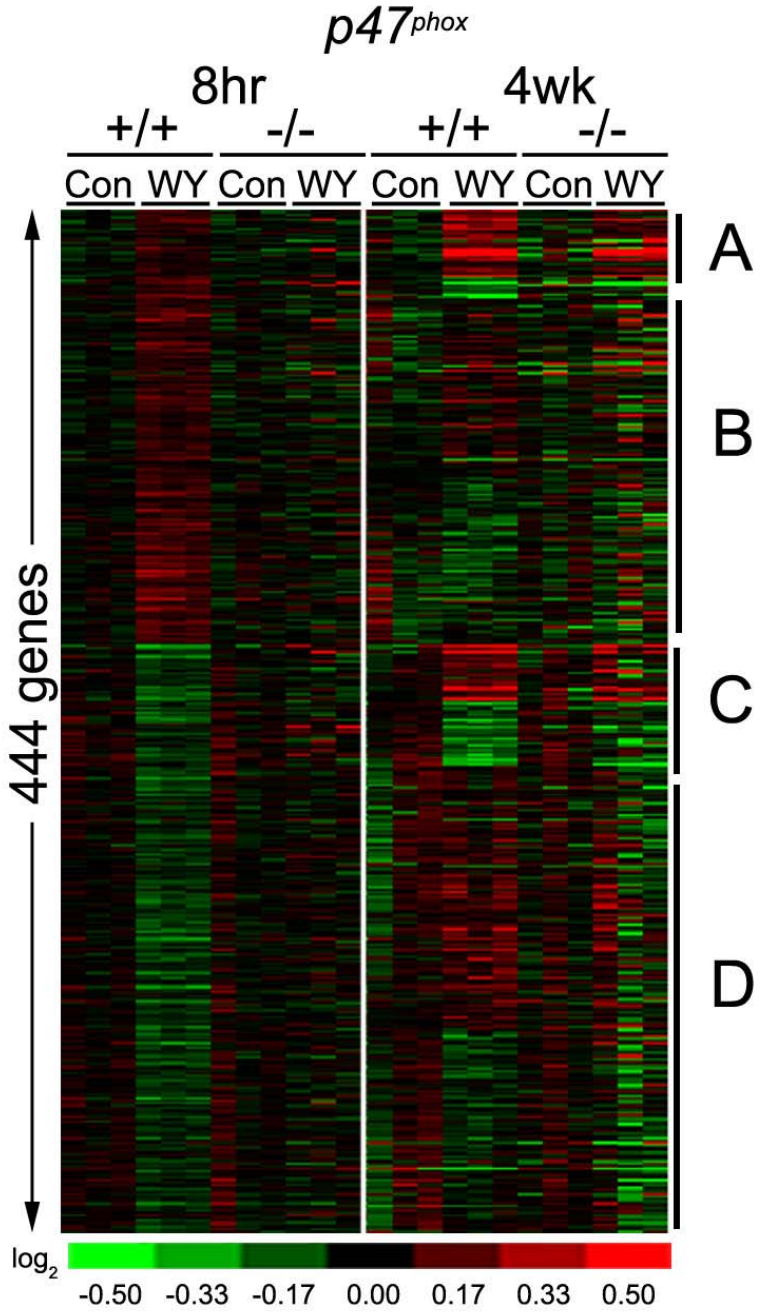

Up at 8 hr w/t WY

A. GO:0051301 Cell Division (3)
B. GO:0006952 Defense Response (11)
GO:0045321 Immune cell activation (4)
GO:0006897 Endocytosis (4)

Down at 8 hr w/t WY

C. GO:0009308 Amine metabolism (4)
D. GO:0043037 Translation (5)
GO:0030333 Antigen processing (5)

Figure 4.3. Hierarchical clustering of differentially expressed genes based on EDGE analysis.

Using EDGE software, 1294 temporal and dose dependent genes were identified in $p47^{phox}$ +/+ mice. Statistical significance was determined at $P<0.05$ and a Q (FDR) of 0.05. Hierarchical clustering of these genes in all mouse strains was performed using $\log_2$ ratios that were normalized to time-matched control arrays.

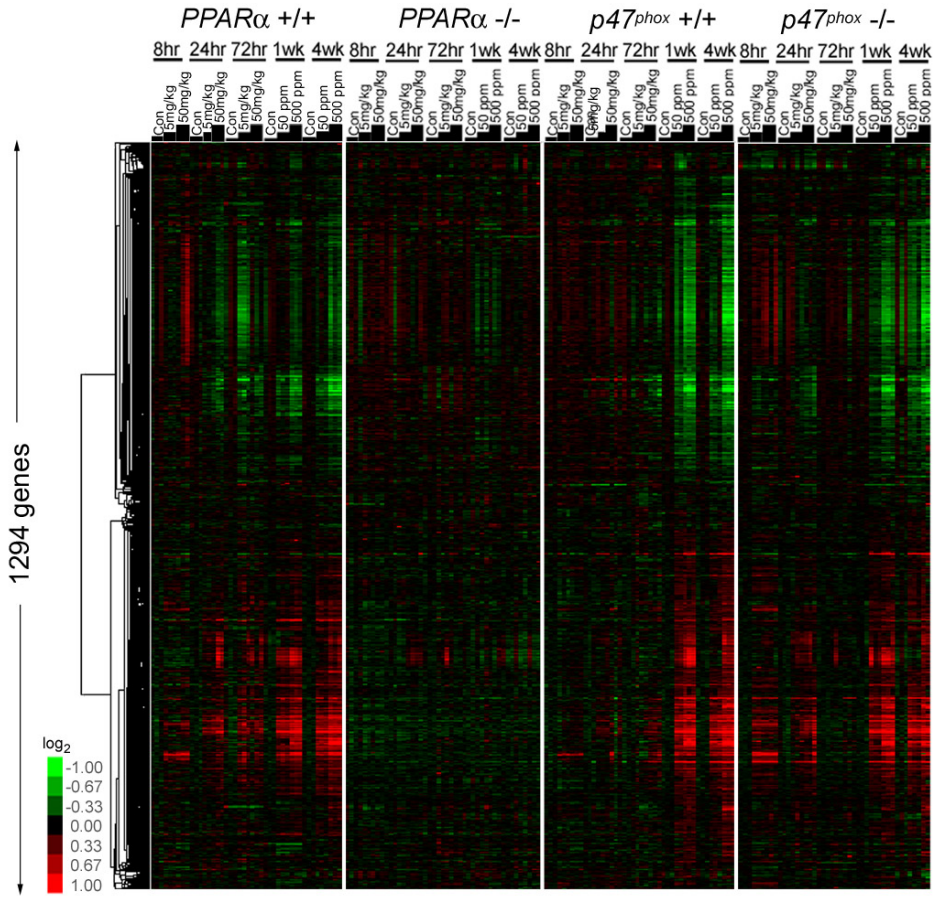

Figure 4.4. Temporal GO Pathway mapping of WY-induced biological processes.

Significant genes from EDGE analysis were submitted to High-Throughput GOMiner to identify overrepresented biological processes resulting from WY-14,643 treatment. Supervised hierarchical clustering was performed. Heatmap shading reflects the FDR for a given pathway, with darker coloring representing statistically significant pathways. The pathway ordering reflects Gene Ontology hierarchy.

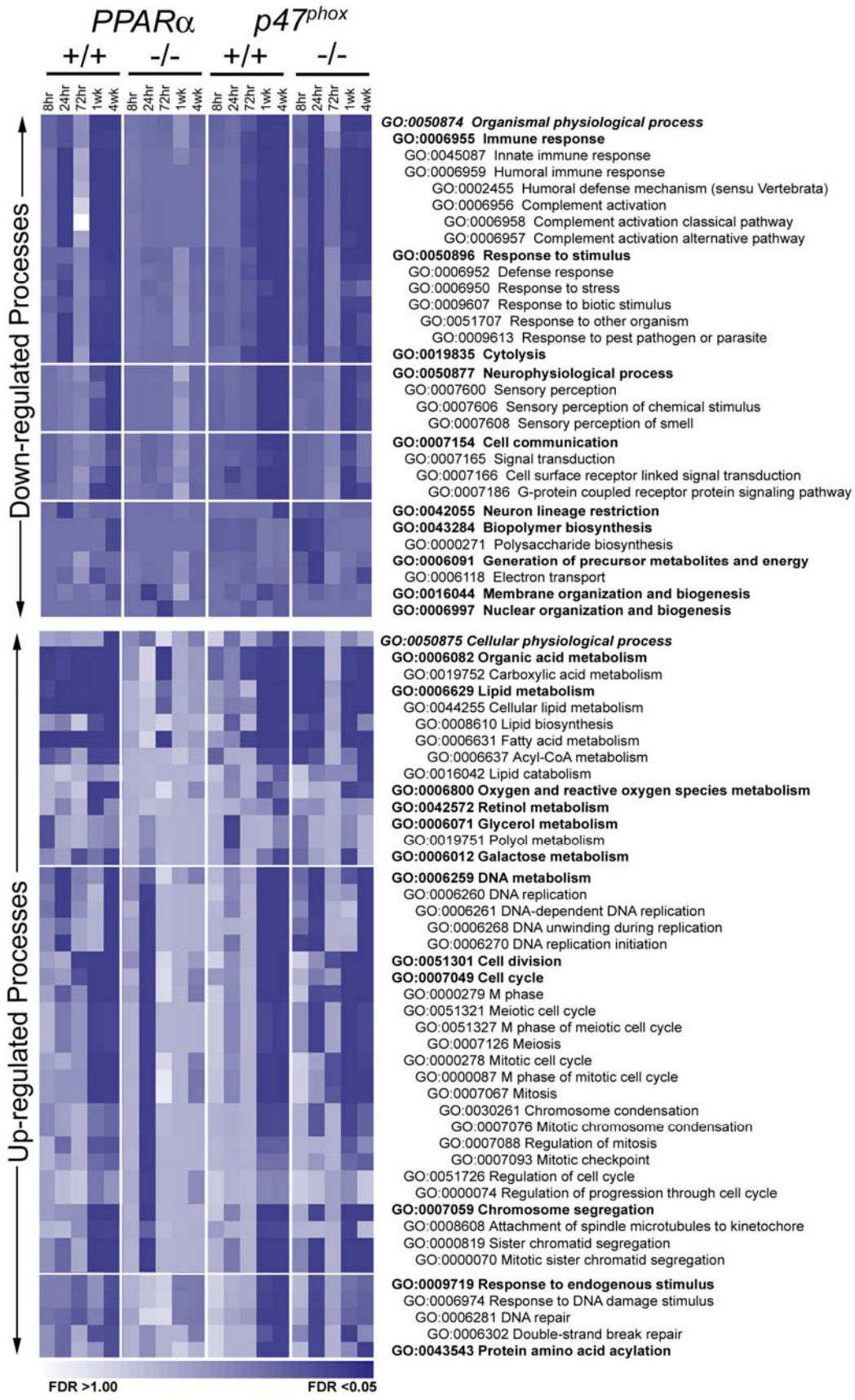
PPARα
p47phox
+/+
-/-
+/+
-/-
8hr 24hr 72hr 1wk 4wk
Down-regulated Processes
Up-regulated Processes
GO:0050874 Organismal physiological process
GO:0006955 Immune response
GO:0045087 Innate immune response
GO:0006959 Humoral immune response
GO:0002455 Humoral defense mechanism (sensu Vertebrata)
GO:0006956 Complement activation
GO:0006958 Complement activation classical pathway
GO:0006957 Complement activation alternative pathway
GO:0050896 Response to stimulus
GO:0006952 Defense response
GO:0006950 Response to stress
GO:0009607 Response to biotic stimulus
GO:0051707 Response to other organism
GO:0009613 Response to pest pathogen or parasite
GO:0019835 Cytolysis
GO:0050877 Neurophysiological process
GO:0007600 Sensory perception
GO:0007606 Sensory perception of chemical stimulus
GO:0007608 Sensory perception of smell
GO:0007154 Cell communication
GO:0007165 Signal transduction
GO:0007166 Cell surface receptor linked signal transduction
GO:0007186 G-protein coupled receptor protein signaling pathway
GO:0042055 Neuron lineage restriction
GO:0043284 Biopolymer biosynthesis
GO:0000271 Polysaccharide biosynthesis
GO:0006091 Generation of precursor metabolites and energy
GO:0006118 Electron transport
GO:0016044 Membrane organization and biogenesis
GO:0006997 Nuclear organization and biogenesis
GO:0050875 Cellular physiological process
GO:0006082 Organic acid metabolism
GO:0019752 Carboxylic acid metabolism
GO:0006629 Lipid metabolism
GO:0044255 Cellular lipid metabolism
GO:0008610 Lipid biosynthesis
GO:0006631 Fatty acid metabolism
GO:0006637 Acyl-CoA metabolism
GO:0016042 Lipid catabolism
GO:0006800 Oxygen and reactive oxygen species metabolism
GO:0042572 Retinol metabolism
GO:0006071 Glycerol metabolism
GO:0019751 Polyol metabolism
GO:0006012 Galactose metabolism
GO:0006259 DNA metabolism
GO:0006260 DNA replication
GO:0006261 DNA-dependent DNA replication
GO:0006268 DNA unwinding during replication
GO:0006270 DNA replication initiation
GO:0051301 Cell division
GO:0007049 Cell cycle
GO:0000279 M phase
GO:0051321 Meiotic cell cycle
GO:0051327 M phase of meiotic cell cycle
GO:0007126 Meiosis
GO:0000278 Mitotic cell cycle
GO:0000087 M phase of mitotic cell cycle
GO:0007067 Mitosis
GO:0030261 Chromosome condensation
GO:0007076 Mitotic chromosome condensation
GO:0007088 Regulation of mitosis
GO:0007093 Mitotic checkpoint
GO:0051726 Regulation of cell cycle
GO:0000074 Regulation of progression through cell cycle
GO:0007059 Chromosome segregation
GO:0008608 Attachment of spindle microtubules to kinetochore
GO:0000819 Sister chromatid segregation
GO:0000070 Mitotic sister chromatid segregation
GO:0009719 Response to endogenous stimulus
GO:0006974 Response to DNA damage stimulus
GO:0006281 DNA repair
GO:0006302 Double-strand break repair
GO:0043543 Protein amino acid acylation
FDR >1.00
FDR <0.05

Figure 4.5. Suppression of immune response at 4 wks is dependent on PPARα, not NADPH oxidase.

Diagrams reveal decrease in expression of genes contributing to the "Immune Response" GO pathway at 4 wks (shown in Figure 4.4), except in *PPARα* -/- mice. Interactions among gene products include regulation (gray line) and induction of expression (blue line). Networks were prepared using Pathway Studio software. Nodes shaded green are down-regulated compared to control, red nodes are up-regulated and gray nodes are molecular mediators that did not contribute to the GO analysis. No information regarding gene interactions was available for those that are not connected with arrows.

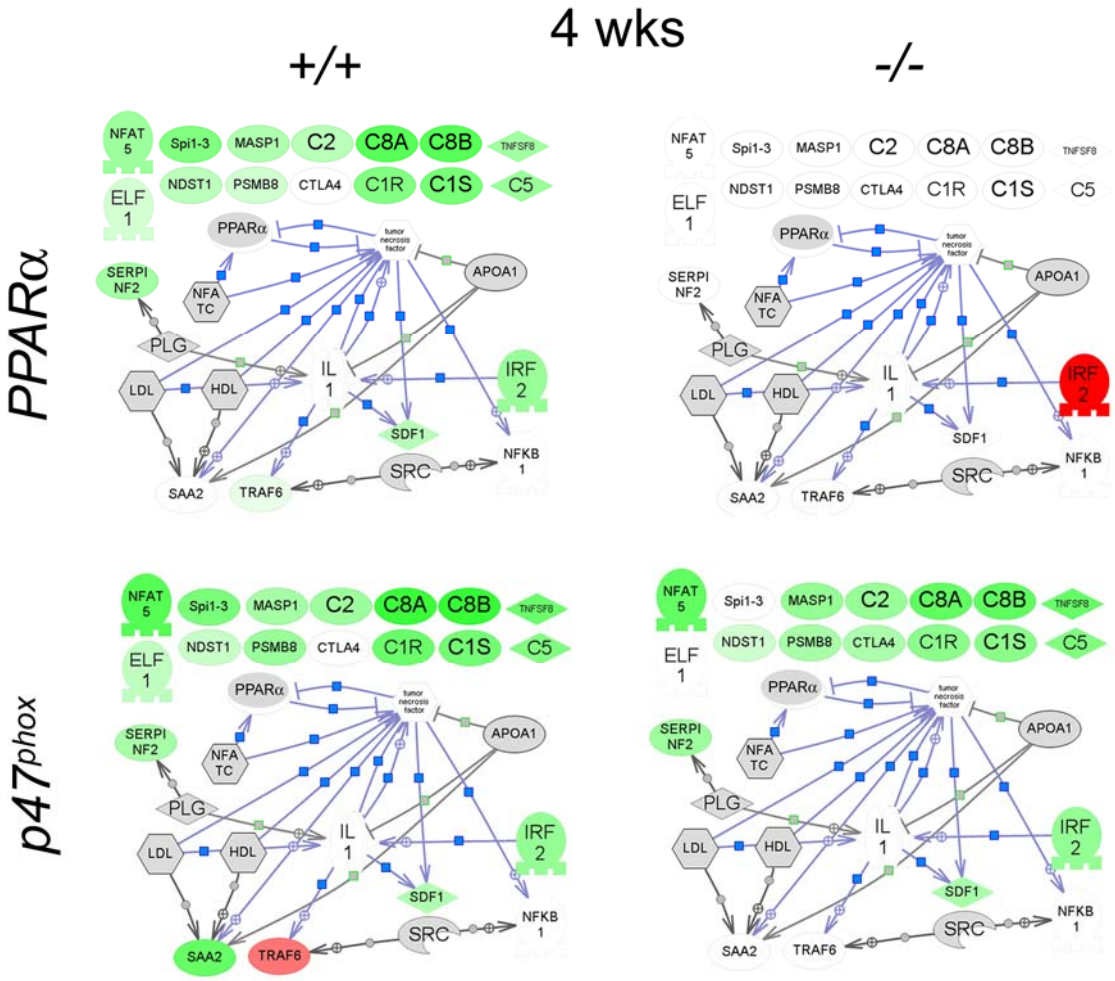

Figure 4.6. Network of genes associated with cell proliferation demonstrates shift from early PPARα-independence to PPARα-dependence after WY-14,643 treatment.

Diagrams display altered expression of genes contributing to the "Cell cycle" GO pathway (shown in Figure 4.4) at A) 24 hrs and B) 4 wks. Interactions among gene products, such as binding (purple line), direct regulation (gray line) or protein modification (green line) are represented. Networks were prepared using Pathway Studio software. Nodes shaded green are down-regulated compared to control and red nodes are up-regulated. No information was available regarding genes that are not connected with arrows.

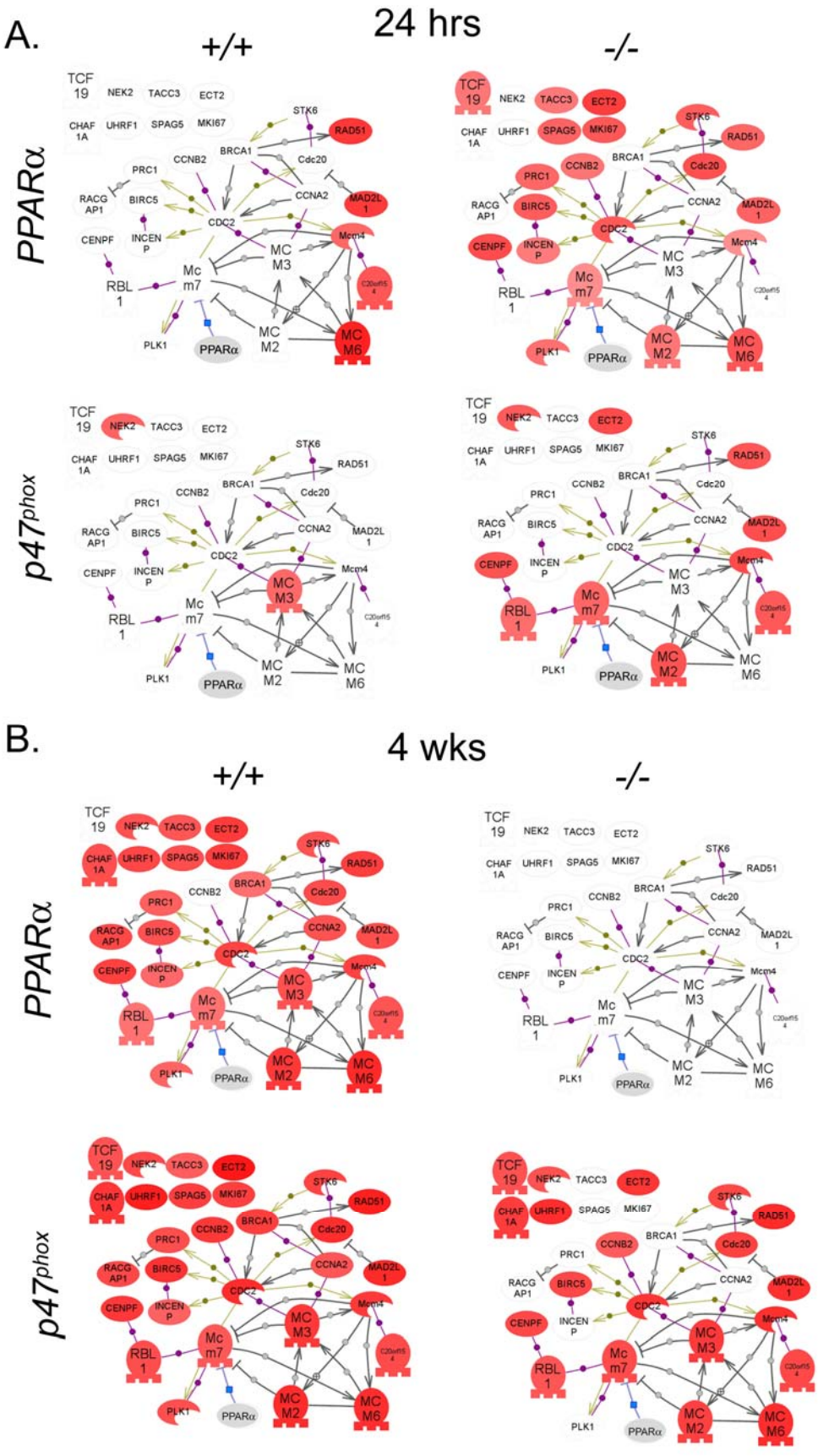
A.
24 hrs
+/+
-/-
PPARα
p47phox
B.
4 wks
+/+
-/-
PPARα
p47phox
TCF 19
NEK2
TACC3
ECT2
CHAF 1A
UHRF1
SPAG5
MKI67
STK6
RAD51
BRCA1
CCNB2
Cdc20
PRC1
RACG AP1
BIRC5
CCNA2
MAD2L 1
CDC2
CENPF
INCEN P
Mcm4
MC M3
Mc m7
RBL 1
C20orf15 4
PLK1
PPARα
MC M2
MC M6

Figure 4.7. Hierarchical clustering of temporal, dose-dependent genes in PPARα-null mice that respond to WY-14,643 treatment.

EDGE analysis on microarray data from PPARα-null mouse liver RNA samples reveals 12 differentially expressed genes (FDR<0.05) which respond in a dose dependent manner.

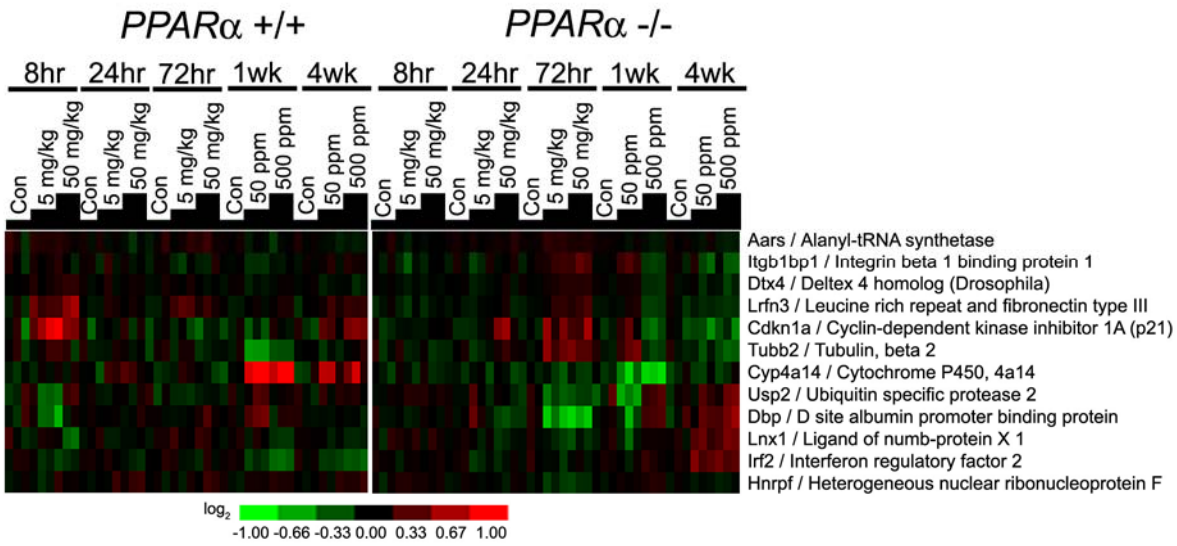

CHAPTER V

GENERAL DISCUSSION

A. SUMMARY AND CONCLUSIONS

The goal of these studies was to investigate the role of Kupffer cells in mediating long-term effects of peroxisome proliferators. Previous work has demonstrated an essential role for Kupffer cells in early oxidant production, release of mitogens and increased cell proliferation by peroxisome proliferators [97]. We show that Kupffer cell-mediated events are not sustained, but rather short-lived and thus likely do not play a role in chronic effects of peroxisome proliferators in mouse liver.

Oxidant generation has been shown to be an important, early response to peroxisome proliferator treatment with evidence that ROS contribute to NFκB activation, cytokine production and proliferation of liver parenchymal cells [94]. Previous studies show that ROS resulting from acute treatment are derived from Kupffer cells, not parenchymal cells. In chapter 2, we provide the first evidence by direct *in vivo* measurements that oxidant production is sustained for up to three weeks of peroxisome proliferator treatment [138]. Oxidant levels correlated with peroxisome proliferator carcinogenicity, with WY-14,643 inducing greater POBN-radical adduct generation than DEHP. Using *PPARα* -null and NADPH oxidase-deficient ($p47^{phox}$ –null) mice, the source of prolonged oxidant production was identified as being within parenchymal cells, not Kupffer cell. Peroxisomal enzyme, ACO was significantly elevated and the presumed source of oxidants in hepatocytes. These findings are important because they demonstrate that prolonged oxidant production in Kupffer cells is likely not involved in the mechanism of hepatocarcinogenic action of peroxisome proliferators.

In Chapter 3, we investigated the role of Kupffer cells on key events in the mode of hepatocarcinogenic action of peroxisome proliferators: cell proliferation, apoptosis and

oxidative DNA damage. With respect to these events, chronic administration of WY-14,643 had no effect on *PPARα* -null mice, as expected. In *p47^{phox}* –null and wild type mice, cell proliferation was still significantly elevated, which was far beyond the timeframe that cell proliferation has historically been shown to peak [38]. Suppression of apoptosis was observed in only wild-type mice, suggesting a role for both PPARα and Kupffer cells in this response. Furthermore, events leading to WY-14,643-induced effects on apoptosis were related to a TNFα-mediated pathway, as opposed to mitochondrial. Oxidative DNA damage by peroxisome proliferators, which has been inconsistently reported, was demonstrated in this study following chronic WY-14,643 feeding. Our findings suggest that DNA damage results from oxidant producing enzymes within parenchymal cells, not Kupffer cells. This study demonstrates that Kupffer cells play a role in the mode of action in rodent hepatocarcinogenesis, by contributing to apoptosis suppression, but not induction of cell proliferation or oxidative damage by WY-14,643.

In chapter 4, gene expression profiling in *p47^{phox}* –null, *PPARα* –null, and wild type mice confirmed most of the phenotypic responses observed in the first two studies. Up-regulation of genes involved in cell cycle, lipid metabolism and DNA repair as well as suppression of immune response and cell death were most notable following sub-chronic WY-14,643 treatment and were largely modulated by PPARα. A comparison of gene expression patterns between p47^{phox} +/+ and p47^{phox} -/- mice revealed significant inherent and WY-14,643-induced differences, many of which were related to immune response. Furthermore, these differences were most notable with acute treatment and diminished over time. The strong immunosuppression by WY-14,643 may play a partial role in suppressing apoptosis, but the relevance of altered immune response to hepatocarcinogenicity is unclear.

The mechanism for acute PPARα –independent up-regulation of cell cycle genes also remains unclear, as it did not definitively appear to be a result of mitogenic cytokines from Kupffer cells. The results of this study are important, as they demonstrate that gene expression can predict sub-chronic WY-14,643-induced phenotypes.

Collectively, the findings of these studies demonstrate that Kupffer cell activation by peroxisome proliferators is an ephemeral event that likely does not contribute to long-term effects of these agents.

B. SIGNIFICANCE OF THIS STUDY

The human health risk of peroxisome proliferators has been debated for several decades [10,96,163] Over the years, significant advances in understanding the mechanism of hepatocarcinogenicity have been made. PPARα-dependence for increased cell proliferation and tumorigenesis [21] was one of the most important findings, with regard to receptor-mediated effects of these agents. Also investigations into interspecies differences in PPARα expression and function have provided valuable insight which helps explain the disparate pathophysiological responses between the humans and rodents [28,164]. The discovery of nuclear receptor-independent targets of peroxisome proliferators has remained quite controversial but a large body of evidence has demonstrated that Kupffer cells mediate many acute pleiotropic effects of peroxisome proliferators, helping to make this concept more widely accepted [94]. Until now, studies investigating the role for Kupffer cell in chronic effects of peroxisome proliferators in mice were lacking. The overall findings of this study, that Kupffer cell derived oxidants are not required for long-term effects of peroxisome proliferators, helps to fill large gaps in our understanding of the mechanism of action of these agents and thus, should improve the human health risk assessment of these agents.

C. LIMITATIONS OF THIS STUDY

There are a number of challenges and limitations in these studies that should be brought to light for the reader. The first limitation involves use of knockout mice. The knockout mouse model provides a fairly effective way to study a specific mechanism as it relates to chemical-induced toxicity or disease. They are favored over use of chemical inhibitors, because in many cases chemical inhibitors may have non-specific targets. However, knock out mice may be no better because there is a possibility of interference of off target genes when backcrossing to produce these mouse lines. Also, knockout mice may overexpress another gene to compensate for the absent target gene. Finally, any disease or chronic conditions associated with the absent gene may confound study results.

The next challenge in interpreting results of these studies relates to our limited focus on NADPH oxidase. In addition to NADPH oxidase, inducible nitric oxide synthase (iNOS) and mitochondrial enzyme, xanthine oxidase are present in Kupffer cells and generate reactive oxygen species upon Kupffer cell activation. Oxidants could act as second messengers to signal mitogenic cytokine production, leading to increased cell proliferation. In absence of a good animal model studies on the effects of Kupffer cell-associated mechanisms remains inconclusive. Kupffer cell inactivation for chronic studies has proven unsuccessful, as extended glycine treatment failed to inhibit Kupffer cells beyond 22 weeks (Wheeler, et al, unpublished). Understanding that these studies do not take into account other ROS generated in the Kupffer cells is important.

Finally, expanding our time course to include time points before 8 hr and beyond 5 months may have significantly improved our overall understanding of Kupffer cells as a mediator of acute effects of peroxisome proliferators and their relevance to carcinogenesis.

The absence of a stronger cell proliferation signature in microarray data at 8 hr, given the historical evidence demonstrating an early peak in cell proliferation and evidence of Kupffer cell involvement in peroxisome proliferator-induced cell replication, suggests that transcriptional changes contributing to these effects may occur before 8 hr. The premature termination of our long-term feeding study and as a result, lack of a cancer endpoint limits the conclusiveness of our findings. Other studies providing evidence of reduced tumor incidence in absence of Kupffer cell-mediated events, still reported increases in cell proliferation [65] as was observed in our studies. For this reason, an 11-month WY-14,643-feeding study should still be conducted in NADPH oxidase-deficient mice to definitively determine the role of Kupffer cells in hepatocarcinogenesis by peroxisome proliferators. In fact, given that the traditional cancer bioassays are conducted over 2 years, this should be considered for subsequent long-term feeding studies in PPARα and $p47^{phox}$ –null mice.

D. FUTURE DIRECTIONS

In light of these findings disputing the role of Kupffer cells in chronic effects of peroxisome proliferators in rodent liver, the next steps in this area of research should focus on established differences between susceptible (rodents) and non-susceptible (human) species. Inter-species variability in response to peroxisome proliferator compounds is thought to be, at least in part, a result of species differences in expression of PPARα in liver parenchymal cells. In an effort to mimic this variability, one could look at genetically-encoded differences in liver PPARα expression between individuals within a single species, such as inbred mouse strains. If, in fact, expression levels of PPARα determine the peroxisome proliferator-induced phenotype, than the magnitude of peroxisome proliferator-induced responses should correlate with expression of PPARα; however, thus far we have observed little correlation between basal PPARα expression, WY-14,643-induced expression and induction of cell proliferation in liver. Thus, additional research is needed to investigate the relationship between PPARα mRNA expression, protein expression and protein-DNA binding and peroxisomal induction to determine if these correlate with peroxisome proliferator-induced hepatocellular proliferation.

In addition, humanized mouse models which express the human form of PPARα (hPPARα) have also been developed to further study receptor differences between species. It has been shown that hPPARα mice exhibit reduced hepatocelluar proliferation and tumor incidence compared to mPPARα mice when fed WY-14,643 for up to 44 weeks [165,166]. Also, increased gene expression of tumor suppressor, p53 was observed only in WY-14,643-fed hPPARα mice. Additional experimentation with hPPARα mice and investigations into the structural and functional differences between hPPARα and mPPARα may provide

additional valuable mechanistic insight for risk assessment of peroxisome proliferators. Finally, many preliminary studies investigating species differences in PPREs were conducted for only one gene, acyl-coA oxidase. With the recent completion of human and mouse genome sequencing, we now have the capability to identify sequence differences in many other peroxisome proliferator responsive genes to help further understand species differences in response to these agents.

APPENDICES

Appendix 1. Effect of WY-14,643 on histopathological changes in mouse liver following 5 months of dietary treatment

	Treatment	N	Morphology	Incidence of Non-neoplastic lesions (%)	[a]Steatosis Index	[a]Necrosis Index	[a]Inflammation Index
PPARα +/+	Control	2	Normal	0	0.0 ± 0.0	0.0 ± 0.0	0.0 ± 0.0
	WY-14,643(0.1%)	6	Hypertrophy	50	0.0 ± 0.0	2.2 ± 1.2*	4.2 ± 1.5*
PPARα -/-	Control	4	Fat deposits	0	22.5 ± 7.2	0.0 ± 0.0	0.0 ± 0.0
	WY-14,643 (0.1%)	5	Fat deposits	0	16.1 ± 14.2	0.0 ± 0.0	0.0 ± 0.0
$p47^{phox}$ +/+	Control	5	Normal	0	0.1 ± 0.1	0.0 ± 0.0	0.3 ± 0.1
	WY-14,643 (0.1%)	3	Hypertrophy	0	0.1 ± 0.1	0.0 ± 0.0	1.1 ± 0.5*
$p47^{phox}$ -/-	Control	5	Normal	0	0.0 ± 0.0	0.0 ± 0.0	0.7 ± 0.4
	WY-14,643 (0.1%)	3	Hypertrophy	100	1.5 ± 0.8*	3.3 ± 1.3*	4.1 ± 1.2*

[a]Value represents Mean ± SEM
Asterisk (*) denotes statistical significance from control at a level of $p < 0.05$

Appendix 2. Genes assayed using Low Density RT-PCR arrays

Gene Symbol	Gene Name	Assay ID	Context Sequence
Acox1	acyl-Coenzyme A oxidase 1, palmitoyl	Mm00443579_m1	GACGGCCAGGTTCTTGATGAAAATC
Acox2	acyl-Coenzyme A oxidase 2, branched chain	Mm00446408_m1	GCCTGGGGACTTGGGACGGACAGTC
Acox3	acyl-Coenzyme A oxidase 3, pristanoyl	Mm00446122_m1	CCTTCCTGGTGCAGATCCGTGACAC
Acp6	acid phosphatase 6, lysophosphatidic	Mm00480076_m1	GCTGGAGGAGCAGGTGGAGTGGAAC
Adh1	alcohol dehydrogenase 1 (class I)	Mm00507711_m1	AAGTCGCCAAGGTGACCCCAGGCTC
Adh4	alcohol dehydrogenase 4 (class II), pi polypeptide	Mm00478838_m1	TGGAAAACTCCGAAACTTCAAATAC
Adh5	alcohol dehydrogenase 5 (class III), chi polypeptide	Mm00475804_g1	GGGAGACAGCATTCGAACTGTTCTA
Adh7	alcohol dehydrogenase 7 (class IV), mu or sigma polypeptide	Mm00507750_m1	TTCGGGGAAAAGCATTCGGACTGTC
Adsl	adenylosuccinate lyase	Mm00507759_m1	GACAGTGCCAACCGACGGATCTGTT
Adss2	adenylosuccinate synthetase 2, non muscle	Mm00475827_m1	CATACCTCATTTCCCAGCAAACCAA
Akap8	A kinase (PRKA) anchor protein 8	Mm00502292_m1	CAAGGCTACGGAGGCTATGGGGCAT
Akt1	thymoma viral proto-oncogene 1	Mm00437443_m1	ACTTCTCAGTGGCACAATGCCAGCT
Alad	aminolevulinate, delta-, dehydratase	Mm00476259_m1	CGCAGAGCCGGTGCCGACATCATCA
Aldh9a1	aldehyde dehydrogenase 9, subfamily A1	Mm00480231_m1	GTTCGAGCCAGCCACCGGCCGAGTG
Ankhzn	ankyrin repeat hooked to zinc finger motif	Mm00477515_m1	GAGATAGACTTGTCAGATGCGAATC
Ap1s1	adaptor protein complex AP-1, sigma 1	Mm00475917_m1	CAAGTACTTCGGCAGCGTATGTGAG
Ap2a2	adaptor protein complex AP-2, alpha 2 subunit	Mm00475953_m1	GCACCAGTGCTGCGTCCACACCTTC
Ap4s1	adaptor-related protein complex AP-4, sigma 1	Mm00480739_m1	TCCAGCGAACAATGCTCATTCATTG
Apex1	apurinic/apyrimidinic endonuclease 1	Mm00507805_g1	GAACCCAAGTCGGAGCCAGAGACCA
Apoa1	apolipoprotein A-I	Mm00437569_m1	CCAACAGCTGAACCTGAATCTCCTG
Areg	amphiregulin	Mm00437583_m1	CACAGTGCACCTTTGGAAACGATAC
Arhd	ras homolog gene family, member D	Mm00455907_m1	GCCTTCCCAGAGAGCTACAGTCCCA
Arl2	ADP-ribosylation-like 2	Mm00480018_m1	ACTGGTGGAGGAGCGCCTGGCTGGA
Arl4	ADP-ribosylation-like 4	Mm00431857_m1	GCCCGGGAGCAATCGCGTAGCCCGA
Arntl	aryl hydrocarbon receptor nuclear translocator-like	Mm00500226_m1	TGATGCCAAGACTGGACTTCCGGTT
Arpc3	actin related protein 2/3 complex, subunit 3 (21 kDa)	Mm00480116_m1	CCCCTCGCGAGACCAAAGACACGGA
Atf4	activating transcription factor 4	Mm00515324_m1	TAAGCCATGGCGCTCTTCACGAAAT
Atp5a1	ATP synthase, H+ transporting, mitochondrial F1 complex, alpha subunit, isoform 1	Mm00431960_m1	TCAGAAGACTGGCACAGCTGAGATG
Atp6v0d1	ATPase, H+ transporting, lysosomal 38kDa, V0 subunit D isoform 1	Mm00442694_m1	GCGAGACGCTCGAGGACTTGAAGCT
Atp6v1a1	ATPase, H+ transporting, V1 subunit A, isoform 1	Mm00431979_m1	GAGACTTCCCTGAGCTCACCATGGA
Atp6v1b2	ATPase, H+ transporting, lysosomal 56/58kD, V1 subunit B, isoform 2	Mm00431987_m1	TCCTAGATCATGTGAAGTTTCCCAG
Atp6v1d	ATPase, H+ transporting, lysosomal 34kD, V1 subunit D	Mm00445832_m1	TTCCCTTCGCGAATGGCACAGACCA
Atp8a1	ATPase, aminophospholipid transporter (APLT), class I, type 8A, member 1	Mm00437712_m1	TTGGAAAGAGCCTCACGGAGAGAGC
AU041707	expressed sequence AU041707	Mm00497622_m1	TTCCTCCTGCCACTCAGGATTGCGC
Axot	axotrophin	Mm00480418_m1	CATGCAAATGAACAAGCTGAGTATG
B2m	beta-2 microglobulin	Mm00437762_m1	GCTTGTATGCTATCCAGAAAACCCC

Gene Symbol	Gene Name	Assay ID	Context Sequence
Bag1	Bcl2-associated athanogene 1	Mm00437768_m1	TCCAGCAGGGTTTTCTGGCTAAGGA
Bcap31	B-cell receptor-associated protein 31	Mm00478914_m1	CTAAAGAAGGGAGCTGCCGAGGATG
Bcap37	B-cell receptor-associated protein 37	Mm00476104_m1	GGCTCCAAAGACCTGCAGATGGTGA
Bing4	BING4 protein	Mm00517474_m1	TCTCGAACAGGGAGACACCTGGCTT
Bmp4	bone morphogenetic protein 4	Mm00432087_m1	GAGTTTCCATCACGAAGAACATCTG
Boct	organic cation transporter	Mm00480680_m1	CCTGATGCGCCTGGAGCTGTGCGAC
Brd2	bromodomain containing 2	Mm00515808_m1	CTCCCCACAAGCTCCCTGGGGAAGG
Brd7	bromodomain containing 7	Mm00478876_m1	CAATTGCAAAGAAAAGACCCAAGTG
Btc	betacellulin, epidermal growth factor family member	Mm00432137_m1	GGTCCTTGCCCTGGGTCTTGCAATT
Bzrp	benzodiazepine receptor, peripheral	Mm00437828_m1	GGCAGATGGGCTGGGCCTTGGCCGA
C1qa	complement component 1, q subcomponent, alpha polypeptide	Mm00432142_m1	GAGAGGGGAGCCAGGAGCTGCTGGC
Cacna2d3	calcium channel, voltage dependent, alpha2/delta subunit 3	Mm00486613_m1	TGTACAACAAAGATCCTGCCATTGT
Calb1	calbindin-28K	Mm00486645_m1	AGGAATTGTAGAGTTGGCTCACGTC
Calm1	calmodulin 1	Mm00486655_m1	GAGCAGATTGCTGAATTCAAGGAAG
Calu	calumenin	Mm00482945_m1	GTCGTGCAGGAAACCATGGAGGATA
Car2	carbonic anhydrase 2	Mm00501572_m1	TCAGGACAATGCAGTGCTGAAAGGA
Car4	carbonic anhydrase 4	Mm00483021_m1	TCTACTGAAGACTCAGGCTGGTGCT
Casp3	caspase 3, apoptosis related cysteine protease	Mm00438045_m1	GGGGAGCTTGGAACGCTAAGAAAAG
Casp8ap2	caspase 8 associated protein 2	Mm00516278_m1	GTCCTGCCTCTCCACTTAAAAATAA
Casp9	caspase 9	Mm00516563_m1	AGGATATTCAGCAGGCAGGATCTGG
Catnb	catenin beta	Mm00483033_m1	TTGTAGAAGCTGGTGGGATGCAGGC
Ccng	cyclin G	Mm00438084_m1	GTCTAAAATGAAGGTACAGGCGAAG
Ccs	copper chaperone for superoxide dismutase	Mm00444148_m1	GGACACTGATCGGCACCGGGGAGAT
Cd164	CD164 antigen	Mm00489798_m1	TGCCCACCGTGCTACCAGAAACCTG
Cdc25a	cell division cycle 25 homolog A (S. cerevisiae)	Mm00483162_m1	GCCCGCCCAGCTTCCATCCCAGTCT
Cdc25b	cell division cycle 25 homolog B (S. cerevisiae)	Mm00499136_m1	TGGCAGAGCGCACGTTTGAACAGGC
Cdc25c	cell division cycle 25 homolog C (S. cerevisiae)	Mm00486874_m1	AAGAAAATGCAGCGTTCCTGCTTCT
Cdc37	cell division cycle 37 homolog (S. cerevisiae)	Mm00489601_m1	TCACCAAGATCAAGACCGCTGACCA
Cdk5	cyclin-dependent kinase 5	Mm00432437_m1	AGATTGGGGAAGGCACCTATGGAAC
Cdkn1a	cyclin-dependent kinase inhibitor 1A (P21)	Mm00432448_m1	ACCAGCCTGACAGATTTCTATCACT
Cdkn1b	cyclin-dependent kinase inhibitor 1B (P27)	Mm00438167_g1	AGGAAGCGACCTGCTGCAGAAGATT
Cdkn2a	cyclin-dependent kinase inhibitor 2A	Mm00494449_m1	AAGCACGCCCAGGGCCCTGGAACTT
Cetn3	centrin 3	Mm00514305_m1	AATGAAGTTGTGACAGACTGGATAC
Ckmt1	creatine kinase, mitochondrial 1, ubiquitous	Mm00438216_m1	ATCCCCCGAGCGCTGAGTACCCAGA
Ckn1	Cockayne syndrome 1 homolog (human)	Mm00518465_m1	GGGACAACACCCTGGTGAACTATGG
Clcn3	chloride channel 3	Mm00432566_m1	ATTGGCCAAGCAGAGGGCCCTGGAT
Clcn7	chloride channel 7	Mm00442400_m1	CCTCACAGGGGCAGCGATCTGGGCA
Clk	CDC-like kinase	Mm00438249_m1	TTCACACGGGATGAAATTGTTGATA
Cln2	ceroid-lipofuscinosis, neuronal 2	Mm00487016_m1	AGCTTCCCTGCTTCCAGCCCCTATG
Clu	clusterin	Mm00442773_m1	TCCACCGTGACCACCCATTCCTCTG
Col18a1	procollagen, type XVIII, alpha 1	Mm00487131_m1	CTGGGCCACCAGGGCAATTCCCCAT

Gene Symbol	Gene Name	Assay ID	Context Sequence
Cops5	COP9 (constitutive photomorphogenic) homolog, subunit 5 (Arabidopsis thaliana)	Mm00489065_m1	CGAAACCCTGGACTAAGGATCACCA
Copz1	coatomer protein complex, subunit zeta 1	Mm00490769_m1	ACCGGGTGGCTTTGAGGGGTGAAGA
Cpt2	carnitine palmitoyltransferase 2	Mm00487202_m1	ACAGCCTGCCCAGGCTGCCTATCCC
Cri1	CREBBP/EP300 inhibitory protein 1	Mm00517974_s1	ACCGAAGAGCTCGGTTGTGATGAGA
Crlz1	charged amino acid rich leucine zipper 1	Mm00491687_s1	CGAGAGTGGGGAGGAGGATGGCGAT
Csf1	colony stimulating factor 1 (macrophage)	Mm00432688_m1	AAAGGATTCTATGCTGGGCACACAG
Csk	c-src tyrosine kinase	Mm00432751_m1	GCAGCTGGTGGAGCACTACACCACA
Ctbp1	C-terminal binding protein 1	Mm00516350_m1	TCATTGGACTAGGTCGTGTGGGCCA
Ctsh	cathepsin H	Mm00514455_m1	CACACTCAATGACGAGGCTGCAATG
Ctsl	cathepsin L	Mm00515597_m1	GCTTGTCAAGAACAGCTGGGGAAGT
Cxcl12	chemokine (C-X-C motif) ligand 12	Mm00445552_m1	TGCATCAGTGACGGTAAACCAGTCA
D7Rp2e	DNA segment, Chr 7, Roswell Park 2 complex, expressed	Mm00473613_m1	TGGGCTACCAGTGGTTGTCCCCATC
Dab2	disabled homolog 2 (Drosophila)	Mm00517751_m1	AGCTAGTCCGTGTACTTTGTGGGTT
Dap3	death associated protein 3	Mm00517732_m1	GGGTCCAGAAGTTGGACCCGAGGTG
Dbnl	drebrin-like	Mm00516526_m1	CCCGACCGACTGGGCTCTTTTTACC
Ddb1	damage specific DNA binding protein 1 (127 kDa)	Mm00497159_m1	TGCCAGCACCCAGGCCCTGTCCAGC
Ddx15	DEAD/H (Asp-Glu-Ala-Asp/His) box polypeptide 15 (RNA helicase A)	Mm00492114_m1	AATTGGAAGAAAGGTGGTGGTGTCA
Ddx25	DEAD/H (Asp-Glu-Ala-Asp/His) box polypeptide 25	Mm00600256_m1	TCGAGGAAACCGAATTCCAAGGGGC
Ddx27	DEAD/H (Asp-Glu-Ala-Asp/His) box polypeptide 27	Mm00461971_m1	CTCAAGAAGAAGCGGGCAGCCACTA
Ddx6	DEAD/H (Asp-Glu-Ala-Asp/His) box polypeptide 6	Mm00619326_m1	ATCTTGTTTGCACTGATCTGTTTAC
Ddx6	DEAD/H (Asp-Glu-Ala-Asp/His) box polypeptide 6	Mm00492142_m1	CAATCTTGTTTGCACTGATCTGTTT
Deaf1	deformed epidermal autoregulatory factor 1 (Drosophila)	Mm00516805_m1	TGACATGACTCTGAGTGGCCCTGTC
Dgka	diacylglycerol kinase, alpha (80 kDa)	Mm00444048_m1	AGATGGGGAAGAGGTTATGAAGGTG
Dhh	desert hedgehog	Mm00432820_g1	GTATCGGTCAAAGCTGATAACTCAC
Diap1	diaphanous homolog 1 (Drosophila)	Mm00492170_m1	GCCCCGGCAGGTCAACAGGAAGGCT
Dld	dihydrolipoamide dehydrogenase	Mm00432831_m1	TAGGGGAATTGAAATACCAGAAGTT
Dnaja2	DnaJ (Hsp40) homolog, subfamily A, member 2	Mm00444898_m1	ACATGATGCATCCACTAAAAGTATC
Dncic2	dynein, cytoplasmic, intermediate chain 2	Mm00494508_m1	CCGTGGGATCTAGACGAGGACCTAT
Drpla	dentatorubral pallidoluysian atrophy	Mm00492256_m1	AAAGACCAAAACCGAGCAGGAGCTC
Dsc2	desmocollin 2	Mm00516355_m1	ACCCTTGCGATCCTTGCACTTGCCT
Dtr	diphtheria toxin receptor	Mm00439307_m1	CTCCCTCTTGCAAATGCCTCCCTGG
Edr1	early development regulator 1 (homolog of polyhomeotic 1)	Mm00492282_m1	TGCAGATCAGGTGCAGAACTTGGCA
Eed	embryonic ectoderm development	Mm00469651_m1	GAGACGAAAATGACGATGCTGTCAG
Egf	epidermal growth factor	Mm00438696_m1	CCTGCAGCTCGGGTCAGTGCATCTG
Egfr	epidermal growth factor receptor	Mm00433023_m1	CCGAGCAGTTGCCCCAAATGTGATC
Eif3	eukaryotic translation initiation factor 3	Mm00468721_m1	TCTGCAACAGGTGGCACAGATTTAT
Eif4e	eukaryotic translation initiation factor 4E	Mm00725633_s1	TGTTGGGCTGCATTCCTGGCTGTCT
EIG180	ethanol induced gene product EIG180 (Interim)	Mm00504676_s1	TGGAAAGAGGTTGGGGTGAGACTCA
Emb	embigin	Mm00515881_m1	AAACCGCACAGGTTCCCATTGACGC
Emd	emerin	Mm00514704_m1	TACCTTCCATCACCAGGTGCGTGAT

Gene Symbol	Gene Name	Assay ID	Context Sequence
Entpd5	ectonucleoside triphosphate diphosphohydrolase 5	Mm00514245_m1	AACAGCAGGACAGCTCCCCTTTCTG
Epgn	epithelial mitogen	Mm00504344_m1	TAACAACACCGAAGCTGACTACATA
Ephx1	epoxide hydrolase 1, microsomal	Mm00468752_m1	CAAGATTGAAGGGCTGGACATCCAC
Eplin	epithelial protein lost in neoplasm	Mm00517749_m1	AAAACAGCGAAGAAGTTTCAGGCGC
Erbb2	v-erb-b2 erythroblastic leukemia viral oncogene homolog 2, neuro/glioblastoma derived oncogene homolog (avian)	Mm00658541_m1	CTGCACCCACTCATGTGTGGACCTG
Ercc4	excision repair cross-complementing rodent repair deficiency, complementation group 4	Mm00516619_m1	GCCGAGGAGGAATATTTTATCAATC
Ereg	epiregulin	Mm00514794_m1	CTTGACGCTGCTTTGTCTAGGTTCC
Ets1	E26 avian leukemia oncogene 1, 5 domain	Mm00468970_m1	GGCTACACAGGAAGTGGGCCGATCC
Ext2	exostoses (multiple) 2	Mm00468775_m1	CCAGAGACAGGGCACTGCTGGCTGG
Fbxw4	f-box and WD-40 domain protein 4	Mm00443559_m1	GGACCTCAACAGTGGGCAGCTGATC
Fhl1	four and a half LIM domains 1	Mm00515772_m1	TCCTGTGTGAGGTCCCTCCAGCTAT
Fkbp4	FK506 binding protein 4 (59 kDa)	Mm00487391_m1	TTGACCTGGGAAAAGGGGAGGTCAT
Fnbp4	formin binding protein 4	Mm00490113_m1	AACCCGACAGGTTCTCTTTGTAAAG
Fnta	farnesyltransferase, CAAX box, alpha	Mm00514973_m1	ACAGTGTGGCATTTTCGGAGAGTTC
Fntb	farnesyltransferase, CAAX box, beta	Mm00521491_m1	TGGACGTAAGGAGTGCATACTGTGC
Foxm1	forkhead box M1	Mm00514924_m1	CAGGAGAGCTATGCTGGTGGTGAGG
Frg1	FSHD region gene 1	Mm00516374_m1	TGTCTGACTCCAGAATTGCCCTGAA
Fzd7	frizzled homolog 7 (Drosophila)	Mm00433409_s1	TAGGGAGAGAACTGCTGGGTGGGGG
Gaa	glucosidase, alpha, acid	Mm00484581_m1	AGCCGCCTCCACTTCAAGATCAAAG
Gab1	growth factor receptor bound protein 2-associated protein 1	Mm00491216_m1	TGAAGCGTTATGCGTGGAAGAGAAG
Gapd	glyceraldehyde-3-phosphate dehydrogenase	Mm99999915_g1	TGAACGGATTTGGCCGTATTGGGCG
Gcm1	glial cells missing homolog 1 (Drosophila)	Mm00492310_m1	TTTTCCAGTCCAAAGGCGAGCATGA
Gcm2	glial cells missing homolog 2 (Drosophila)	Mm00492312_m1	TGACCCACAGATGCCTCAGGAACCA
Gcs1	glucosidase 1	Mm00498596_g1	AGCATGGCAGCTACAATGTCTTCTG
Gng3	guanine nucleotide binding protein (G protein), gamma 3 subunit	Mm00494686_g1	CCGGATAAAGGTGTCCAAGGCAGCA
Gnpat	glyceronephosphate O-acyltransferase	Mm00464931_m1	CTCCTCTATGCGAAAGACCTCAAAA
Golga4	golgi autoantigen, golgin subfamily a, 4	Mm00516938_m1	AGCCCCTGCTCAGGCTTCCTCCAGC
Gpd2	glycerol phosphate dehydrogenase 1, mitochondrial	Mm00439082_m1	CACGAGTTTCTGCAGCTGATGAGCG
Gpx3	glutathione peroxidase 3	Mm00492427_m1	AGAGAAGTCTAAGACAGACTGCCAT
Gstm5	glutathione S-transferase, mu 5	Mm00515890_m1	CAATTCTAACCACGAAAACCTGAAG
Gtf2i	general transcription factor II I	Mm00494826_m1	TGCAAGAAATTTGCCGAGGCCTTGG
Gtpbp2	GTP binding protein 2	Mm00517163_m1	CTGCCCCCAGAGGCTGAAGATGGAA
Gus	beta-glucuronidase	Mm00446953_m1	AGCCGCTACGGGAGTCGGGCCCAGT
H1f0	H1 histone family, member 0	Mm00515079_s1	CAAGGCCTCCAAACCCAAGAAGGCC
Hiat1	hippocampus abundant gene transcript 1	Mm00468642_m1	TCAGCCCGTGGTGGTACTTTGCTGT
Hip2	huntingtin interacting protein 2	Mm00516776_m1	AAGATCAATGGGCAGCAGCAATGAC
Hnf4	hepatic nuclear factor 4	Mm00433964_m1	GGAGATGCTTCTCGGAGGGTCTGCC
Hoxa2	homeo box A2	Mm00439361_m1	CGGCCACAAAGAATCCCTGGAAATA
Hsd17b12	hydroxysteroid (17-beta) dehydrogenase 12	Mm00479916_m1	GTTTGCAAGGTGACACGCTTGGTGC
Hspa4	heat shock 70 kDa protein 4	Mm00434038_m1	CGCTGCACGCCGGCATGTGTTTCTT
Ifrg15	interferon alpha responsive gene, 15 kDa	Mm00499068_m1	CCTGGCTGGAAATTGTGTGTGACGC

Gene Symbol	Gene Name	Assay ID	Context Sequence
Igf2	insulin-like growth factor 2	Mm00439563_m1	CCCGACCTTCGGCCTTGTGGTACCA
Igfbp4	insulin-like growth factor binding protein 4	Mm00494922_m1	CTTCCACCCCAAACAGTGTCACCCC
Il6st	interleukin 6 signal transducer	Mm00439668_m1	ACACCAAAGTTCGCTCAAGGAGAAA
Imp4a	importin 4a	Mm00502820_m1	AGAACAATCCTGAGCAGGTTGTGGA
Iqgap1	IQ motif containing GTPase activating protein 1	Mm00443860_m1	GTATCCACGCCCTCAGTTTGTACCT
Irf6	interferon regulatory factor 6	Mm00516797_m1	ACATCAACGGTTCTCCCATGGCGCC
Itgb7	integrin beta 7	Mm00442916_m1	GGCTGCCCTCTGCCAGGAACAGATT
Itm2b	integral membrane protein 2B	Mm00515213_m1	TGGATTGCAAGGACCCGGGTGACGT
Itm2c	integral membrane protein 2C	Mm00499081_m1	TCCTTGCTCAGCTGGCCCGAGATAA
Kcnd2	potassium voltage-gated channel, Shal-related family, member 2	Mm00498065_m1	GAGAAAACCACGAACCATGAGTTTG
Kcnj9	potassium inwardly-rectifying channel, subfamily J, member 9	Mm00434622_m1	ATTTGAAGCAAAACCAGACCCCGCA
Khdrbs1	KH domain containing, RNA binding, signal transduction associated 1	Mm00516130_m1	ATGAGAGACAAAGCCAAGGAGGAAG
Kpna1	karyopherin (importin) alpha 1	Mm00434700_m1	TTCAGACACAGGTAATTTTGAATTG
Laptm4a	lysosomal-associated protein transmembrane 4A	Mm00493224_m1	TCTGGATCAGTTGCCTGATTTCCCA
Lasp1	LIM and SH3 protein 1	Mm00464946_m1	TGGATAAGTACTGGCATAAAGCATG
Lig1	ligase I, DNA, ATP-dependent	Mm00495331_m1	ACGGAGAGTCCCTGGTTCGCCAGCC
Lig3	ligase III, DNA, ATP-dependent	Mm00521933_m1	TTTTCAGCAGCAAAACCCAACAACT
Limd1	LIM domains containing 1	Mm00522167_m1	GCAGCCTGCAGCAGGAAGTTAAGAG
Lin7c	lin 7 homolog c (C. elegans)	Mm00457063_m1	GCAACTGCAAAGGCTACTGTTGCTG
Lrrfip1	leucine rich repeat (in FLII) interacting protein 1	Mm00521802_m1	AGGCGCAAAGACTGGCGGAGGCCAG
Lyst	lysosomal trafficking regulator	Mm00465000_m1	GTGACTCAGCTGGCGGGGGCAGTGA
Madh4	MAD homolog 4 (Drosophila)	Mm00484724_m1	GATGGACGACTTCAGGTGGCTGGTC
Man1b	mannosidase 1, beta	Mm00487564_m1	TCAGGAGAGGAAATATTCAAGACTA
Map2k1	mitogen activated protein kinase kinase 1	Mm00435940_m1	GACCAGCTCGGCCGAGACCAACCTG
Map2k2	mitogen activated protein kinase kinase 2	Mm00445688_m1	CGCCTCTGAGGCAAACCTGGTGGAC
Map2k3	mitogen activated protein kinase kinase 3	Mm00435950_m1	AGACCAAAGGAAAATCCAAAAGGAA
Mark2	MAP/microtubule affinity-regulating kinase 2	Mm00433039_m1	GGGACACGGAGCAGCCCACCTTGGG
Mark3	MAP/microtubule affinity-regulating kinase 3	Mm00522364_m1	GGTACAGTGACCACGCTGGACCAGC
Mbd3	methyl-CpG binding domain protein 3	Mm00488961_m1	TGACGACATCAGGAAGCAGGAGGAG
Mcrs1	microspherule protein 1	Mm00522246_m1	GATGGACAAAGATTCTCAGGGGCTG
Mfng	manic fringe homolog (Drosophila)	Mm00434941_m1	CAAAAAACCGCACGAAGCTGGTGCG
MGC18745	hypothetical protein MGC18745 (Interim)	Mm00523039_m1	GCGGCCCGCGGCAATGGCACGAGCA
Mgmt	0-6-methylguanine-DNA methyltransferase	Mm00485014_m1	GAAGCAATCCGGTCCCCATCCTCAT
Minpp1	multiple inositol polyphosphate histidine phosphatase 1	Mm00487691_m1	CCCGACGTCTCAGATATGGAGTGTG
Mpg	N-methylpurine-DNA glycosylase	Mm00447872_m1	CATTTCTGGGACAGGTTCTTGTCCG
Mpv17	Mpv17 transgene, kidney disease mutant	Mm00485133_m1	CCAGGTTCTGACAGCTGGATCACTG
Mtap4	microtubule-associated protein 4	Mm00485247_m1	TACAGCCAGCAACAGAGCTCTCCAA
Mttp	microsomal triglyceride transfer protein	Mm00435015_m1	AAAAATCGGGTGGCTGTGGTGATAA
Muc1	mucin 1, transmembrane	Mm00449604_m1	GAGGAGGTTTCGGCAGGTAATGGCA
Myd116	myeloid differentiation primary response gene 116	Mm00435119_m1	GACGTGCAGCCCGCCGCCCAGACAC
Myt1	myelin transcription factor 1	Mm00456190_m1	CTGAGGAGTCAGAGCCAGCAGCACA

Gene Symbol	Gene Name	Assay ID	Context Sequence
Naglu	alpha-N-acetylglucosaminidase (Sanfilippo disease IIIB)	Mm00479175_m1	GCCATCACCAGGGTGTTTCCACAGG
Nap1l1	nucleosome assembly protein 1-like 1	Mm00450101_m1	AATGGCGATCTGGATGATGATGCTG
Ncoa1	nuclear receptor coactivator 1	Mm00447958_m1	TGGAGTCCCAGAGCCAGTTTACAGC
Ncoa2	nuclear receptor coactivator 2	Mm00500749_m1	AAGAGGAAGGCGAAGATTTGCAGTC
Ncoa3	nuclear receptor coactivator 3	Mm00500775_m1	CAGGACCGAGTTCTCTGGGTTTGCG
Ndr3	N-myc downstream regulated 3	Mm00443491_m1	CCTCCTTCCCCACAGGGTACCAGTA
Nfe2l2	nuclear, factor, erythroid derived 2, like 2	Mm00477784_m1	AGTCCCAGCAGGACATGGATTTGAT
Nid1	nidogen 1	Mm00477827_m1	GTGGATGCAGGCACCCATAGGGCAG
Ninj1	ninjurin 1	Mm00479014_m1	CCCCCGACGCCTTGCCACCCCGCTG
Nr1d2	nuclear receptor subfamily 1, group D, member 2	Mm00441730_m1	AGCTGAACGCAGGAGGTGTGATTGC
Nr1h3	nuclear receptor subfamily 1, group H, member 3	Mm00443454_m1	GCCAAAGCAGGGCTGCAGGTGGAGT
Nr1i3	nuclear receptor subfamily 1, group I, member 3	Mm00437986_m1	GCTCCAAAGTCGGTTTCTGTATGCA
Nras	neuroblastoma ras oncogene	Mm00477878_g1	CACTTTGAAGCTGCACTGATGCCCT
Nsf	N-ethylmaleimide sensitive fusion protein	Mm00435390_m1	GTTCAGCTTGCCTCAGCGAAAATGG
Nsmaf	neutral sphingomyelinase (N-SMase) activation associated factor	Mm00448040_m1	GATGTCAGCGTCAATACTATCAATT
Nthl1	nth (endonuclease III)-like 1 (E.coli)	Mm00476559_m1	CATATCAGGCATAGCAGTGGACACA
Nucb2	nucleobindin 2	Mm00450268_m1	CTGAAGATGAGGTGGAGGATCATCC
Ogg1	8-oxoguanine DNA-glycosylase 1	Mm00501781_m1	TCTGGACAGTCCTTCCGGTGGAAGG
Orc4l	origin recognition complex, subunit 4-like (S. cerevisiae)	Mm00457224_m1	GCTTGACTGGGAGAGGATTTGAATT
Osbpl1a	oxysterol binding protein-like 1A	Mm00498542_m1	CAAGACCCAGCCCAGAACAAGCCTG
Osp94	osmotic stress protein 94 kDa	Mm00495441_m1	CAGGTGCACGCCGGCCTGTATATCT
Papss1	3-phosphoadenosine 5-phosphosulfate synthase 1	Mm00442283_m1	TCTTCAGGAACGGGACATCGTCCCT
Pbx2	pre B-cell leukemia transcription factor 2	Mm00479560_m1	GGCCCAGGCCAAGAAACATGCCCTA
Pcmt1	protein-L-isoaspartate (D-aspartate) O-methyltransferase 1	Mm00476600_m1	AACCTCCGCAAGAATGGAATCATCA
Pcna	proliferating cell nuclear antigen	Mm00448100_g1	CAACTTGGAATCCCAGAACAGGAGT
Pcolce	procollagen C-proteinase enhancer protein	Mm00476608_m1	CACTTCGGGCACTGAGCACCAGTTT
Pcsk7	proprotein convertase subtilisin/kexin type 7	Mm00476621_m1	ATGCTGCGGAGCATTGTGACCACTG
Pcyt1a	phosphate cytidylyltransferase 1, choline, alpha isoform	Mm00447774_m1	GAACTCCGTGTGAGCGGCCTGTGAG
Pdcd6ip	programmed cell death 6 interacting protein	Mm00478032_m1	CGCAAGGTTGCAGCACGCAGCAGAA
Pde8a	phosphodiesterase 8A	Mm00501020_m1	GCTGCTGGCTTCACACGGAGGTTTA
Perp	p53 apoptosis effector related to Pmp22	Mm00480750_m1	CCTCATGGAGTACGCATGGGGACGA
Pfkl	phosphofructokinase, liver, B-type	Mm00435587_m1	GGCGGTGATGCGCAAGGTATGAATG
Pias1	protein inhibitor of activated STAT 1	Mm00497998_m1	AGCCCACCAGTCTAGCTTCAGACAA
Pik3ca	phosphatidylinositol 3-kinase, catalytic, alpha polypeptide	Mm00435669_m1	TTTAAAAATGGCGACGACTTACGGC
Pl6	PL6 protein	Mm00480010_m1	GCGCAGAAGGCAACTAGCCCTAAAG
Pla2g7	phospholipase A2 group VII (platelet-activating factor acetylhydrolase, plasma)	Mm00479105_m1	TCTCGGAGCCTTCAGGACGATTTAT
Plod3	procollagen-lysine, 2-oxoglutarate 5-dioxygenase 3	Mm00478798_m1	AGATTATGAGGGAGGCGGCTGCCGC
Pmscl2	polymyositis/scleroderma autoantigen 2	Mm00479342_m1	TCTGCCTCAAGAAATTTGTCAAGCC

Gene Symbol	Gene Name	Assay ID	Context Sequence
Podxl	podocalyxin-like	Mm00449829_m1	AGAGGAAGGACCAGCAACGGCTCAC
Pold1	polymerase (DNA directed), delta 1, catalytic subunit (125kDa)	Mm00448253_m1	CCCTAAAGGTGGACCGCTTCCCTTT
Pole	polymerase (DNA directed), epsilon	Mm00448288_m1	TCATGCGCAAAGGAGCTCGCTGGTA
Polg	polymerase (DNA directed), gamma	Mm00450527_m1	TCCCCCTCGGCCTGGTATTCCTGGT
Polg2	polymerase (DNA directed), gamma 2, accessory subunit	Mm00450161_m1	CTCTTCTTCACGGTGCCTTGGAGCA
Polh	polymerase (DNA directed), eta (RAD 30 related)	Mm00453168_m1	ATCGAAATGATAATGACCGCGTGGC
Poli	polymerase (DNA directed), iota	Mm00449480_m1	CGGCGGGCAGCTCGCGGGCAGTTTG
Polm	polymerase (DNA directed), mu	Mm00450512_m1	CAGAAAGCAGGGCTCCAATATTACC
Pon3	paraoxonase 3	Mm00447161_m1	ATTGAGGGCCTCGAGAATGGCTCTG
Ppara	peroxisome proliferator activated receptor alpha	Mm00440939_m1	GTGGAGATCGGCCTGGCCTTCTAAA
Pparbp	peroxisome proliferator activated receptor binding protein	Mm00501992_m1	AAAGAAGATTCTCCTGGGCTCCTCC
Pparg	peroxisome proliferator activated receptor gamma	Mm00440945_m1	CAGTGGAGACCGCCCAGGCTTGCTG
Ppib	peptidylprolyl isomerase B	Mm00478295_m1	TCACAGTCAAGGTATACTTTGATTT
Ppm1g	protein phosphatase 1G (formerly 2C), magnesium-dependent, gamma isoform	Mm00446988_m1	CTCCATGGAGGATGCTCACAACTGT
Prim1	DNA primase, p49 subunit	Mm00477089_m1	CATCCCAAGACAGGTCGGATTTCTG
Prkcl	protein kinase C, lambda	Mm00435769_m1	GAAAAGGAGGCAATGAACACCAGGG
Prkcsh	protein kinase C substrate 80K-H	Mm00447244_m1	CTGTGGGAAGAGCAGCAAGCTGCTG
Procr	protein C receptor, endothelial	Mm00440992_m1	AACTCCGATGGCTCCCAAAGCCTGC
Psa	puromycin-sensitive aminopeptidase	Mm00477144_m1	CATATGGCGGTGAAGACTGTCCTCA
Psma6	proteasome (prosome, macropain) subunit, alpha type 6	Mm00478827_m1	GAACAGACAGTGGAAACTGCAATTA
Psma7	proteasome (prosome, macropain) subunit, alpha type 7	Mm00478829_m1	CACCGCGGTTGGTGTTCGAGGAAAG
Psmb2	proteasome (prosome, macropain) subunit, beta type 2	Mm00449477_m1	GTCTTCGGAGTCGGACCCCATATCA
Psmd7	proteasome (prosome, macropain) 26S subunit, non-ATPase, 7	Mm00477746_m1	AGTGGAGGAAGTTCATGACGATGGG
Pte2a	peroxisomal acyl-CoA thioesterase 2A	Mm00652967_m1	ACCTGCTCAGTCACCCTCAGGTAAC
Pte2b	peroxisomal acyl-CoA thioesterase 2B	Mm00506680_m1	ATCCAAAGGTAAAAGGCCCAGACAT
Pten	phosphatase and tensin homolog	Mm00477210_m1	GGAACTTGCAATCCTCAGTTTGTGG
Pter	phosphotriesterase related	Mm00447265_m1	GTCAGTGGAGCAGCTTACAGATGTC
Ptprk	protein tyrosine phosphatase, receptor type, K	Mm00436070_m1	CTGATGAAGATGTGCCCGGGCCTGT
Pts	6-pyruvoyl-tetrahydropterin synthase	Mm00478494_m1	ACCGGCTGCACAGCCCATCTCTGAG
Pvrl2	poliovirus receptor-related 2	Mm00436144_m1	CTCTGTGCGCTACCCTCCAGAAGTA
Pxmp2	peroxisomal membrane protein 2, 22 kDa	Mm00477269_m1	AAGCAGTCAGCAGCGGCATTTTGTC
Rab1	RAB1, member RAS oncogene family	Mm00485436_g1	CACAACAGCAAAGGAATTTGCAGAT
Rab10	RAB10, member RAS oncogene family	Mm00489481_m1	GACATCCTCCGAAAGACCCCTGTAA
Rab18	RAB18, member RAS oncogene family	Mm00441057_m1	GCAAGTCCAGCCTGCTCCTGAGGTT
Rab2	RAB2, member RAS oncogene family	Mm00445482_m1	CTAATGTAGAGGAGGCATTTATTAA
Rab6	RAB6, member RAS oncogene family	Mm00445868_m1	AGGATAGAACCGTGCGATTGCAATT
Rabggta	Rab geranylgeranyl transferase, a subunit	Mm00490374_m1	ACCTGGCTCACAAGGATCTCACAGT
Rabggtb	RAB geranylgeranyl transferase, b subunit	Mm00599962_m1	AGACGCGAGAAGTTACCAGATGTGT
Rad1	RAD1 homolog (S. pombe)	Mm00487885_m1	TGACAAGCCCTATTTCAGGTTGTCT
Rad50	RAD50 homolog (S. cerevisiae)	Mm00485504_m1	AGACTCTTGACCAAGCAATTATGAA

Gene Symbol	Gene Name	Assay ID	Context Sequence
Ralb	v-ral simian leukemia viral oncogene homolog B (ras related)	Mm00469677_m1	GTTCAGGGAACAGATTCTCCGAGTC
Rasa3	RAS p21 protein activator 3	Mm00436272_m1	GCTGCACGCATCTTCGAGTGCCAGG
Rbbp9	retinoblastoma binding protein 9	Mm00489397_m1	CCATCGCAGCCATGAGGTATGCAGA
Rbl2	retinoblastoma-like 2	Mm00487954_m1	ATTTTAAAGGCCTGTCCGAGGACTG
Rce1	Ras and a-factor-converting enzyme 1 homolog (S. cerevisiae)	Mm00491708_m1	TTGTCCTGGCCCCTCGTTCTTGGGC
Rcn2	reticulocalbin 2	Mm00488777_m1	GTTCAGGCAGCTTCATCTAAAGGAT
Rdx	radixin	Mm00501337_m1	TGAGTGGCAGCACAAAGCTTTTGCA
Recc1	replication factor C, 140 kDa	Mm00488021_m1	TGCCCACCCAGGCCATCTATGCCAG
Rfc2	replication factor C (activator 1) 2 (40kD)	Mm00451399_m1	CCACTACGAGCTGCCGTGGGTTGAA
Rfx1	vregulatory factor X, 1 (influences HLA class II expression)	Mm00501349_m1	AAGTGCGGAGAAGCCGAGGAAGAGG
Rnf14	ring finger protein 14	Mm00451391_m1	GCCGGAAGATGGCAGACTTTCTGTA
Rock1	Rho-associated coiled-coil forming kinase 1	Mm00485745_m1	GGAGACCTTCAAGCACGAATTACAT
Rps6ka1	ribosomal protein S6 kinase polypeptide 1	Mm00436395_m1	CACACCCAGGGATTCGCCAGGCATC
Rw1	RW1 protein	Mm00502154_m1	TACAGGAACAGCGCTCATCCACTGC
S100a13	S100 calcium binding protein A13	Mm00477273_m1	TGCCTCATTTGCTCAAGGACGTGGG
Satb1	special AT-rich sequence binding protein 1	Mm00485916_m1	GGTTCCACGCCTGATTCTGGCAGGT
Scamp2	secretory carrier membrane protein 2	Mm00452165_m1	TAACTTGGGGACCAGTGGTTGGCTT
Scd2	stearoyl-Coenzyme A desaturase 2	Mm00485951_g1	CACATACTGCAAGAGATCTCTGGCG
Sdc1	syndecan 1	Mm00448918_m1	CTCTGGCTCTGGCACAGGTGCTTTG
Sec61a	SEC61, alpha subunit (S. cerevisiae)	Mm00489804_m1	AAGCCAGAGAGAAAGATTCAGTTTA
Selel	selectin, endothelial cell, ligand	Mm00486029_m1	GCCAACAGGCGCTTCAGACACTGAT
Sepr	selenoprotein R	Mm00489121_m1	CACTTCGAGCCAGGTGTCTACGTGT
Sh3d2b	SH3 domain protein 2B	Mm00489003_m1	TCTACAAGGCGAGCCAGCTGGTCAG
Shc1	src homology 2 domain-containing transforming protein C1	Mm00468940_m1	GAGACCCTGGACATGAACAAGCTGA
Shyc	selective hybridizing clone	Mm00488194_m1	AAGTATTTCAAGCAGCTGCAGGTGG
Skd3	suppressor of K+ transport defect 3	Mm00486168_g1	CCGACCCATCTTGAAAGCTCACTTC
Slc16a1	solute carrier family 16 (monocarboxylic acid transporters), member 1	Mm00436566_m1	TGTTATTGGAGGTCTTGGGCTTGCT
Slc20a1	solute carrier family 20, member 1	Mm00489378_m1	ATCCTCCGTAAGGCAGATCCGGTTC
Slc4a1	solute carrier family 4 (anion exchanger), member 1	Mm00441492_m1	GACCCAGAAGCTCTTCCCACAGAGC
Slc7a8	solute carrier family 7 (cationic amino acid transporter, y+ system), member 8	Mm00444250_m1	TCCTCCCGGCTGTTCTTTGCTGGAG
Slc9a1	solute carrier family 9 (sodium/hydrogen exchanger), member 1	Mm00444270_m1	CGGGTGCTGGGTGTCCTGGTCCTGA
Smpd1	sphingomyelin phosphodiesterase 1, acid lysosomal	Mm00488318_m1	CACACCCTAAGAATTGGGGGCTTCT
Soat1	sterol O-acyltransferase 1	Mm00486279_m1	AGAACCACAGAGCCAAAGATCTGAG
Sorbs1	sorbin and SH3 domain containing 1	Mm00501490_m1	TGAGCCCACAGCAACCTCAAGCCCA
Sos1	Son of sevenless homolog 1, (Drosophila)	Mm00436712_m1	TTCAGATGTGGAGGAACGTGTTCAA
Sparcl1	SPARC-like 1 (mast9, hevin)	Mm00447780_m1	GCCACCTCTCCGCAGATCTAGCCAG
Sptlc1	serine palmitoyltransferase, long chain base subunit 1	Mm00447343_m1	ACAACATCGTGTCCGGCCCTCCAAC
Sqle	squalene epoxidase	Mm00436772_m1	AGCTGGGCCTTGGAGATACAGTAGA
Src	Rous sarcoma oncogene	Mm00436783_m1	GAAGGTGGATGTCAGAGAGGGAGAC

Gene Symbol	Gene Name	Assay ID	Context Sequence
Star	steroidogenic acute regulatory protein	Mm00441558_m1	CAGTATTGACCTGAAGGGGTGGCTG
Stip1	stress-induced phosphoprotein 1	Mm00489584_m1	GGCCAGGCTATGGAGCAGGTGAATG
Stmn3	stathmin-like 3	Mm00456285_m1	TGGCCAGCACCGTATCTGCCTACAA
Stx5a	syntaxin 5A	Mm00502335_m1	CGATTCAGAGGATCGACGAGAATGT
Stx7	syntaxin 7	Mm00444002_m1	GCAGACTATCAGCGCAAATCCAGGA
Supt5h	suppressor of Ty 5 homolog (S. cerevisiae)	Mm00449743_m1	GGCGGAGGAGGCCGAGGTTGAGGAA
Tacstd2	tumor-associated calcium signal transducer 2	Mm00498401_s1	CAGACCTCGGTGTGCTGGTGCGTAA
Tceb3	transcription elongation factor B (SIII), polypeptide 3 (110kD)	Mm00496800_m1	TCCAGTAGAGCGAAATAGTGAGGCC
Tcfl4	transcription factor-like 4	Mm00448970_m1	CAACAGCCTGGATCCTGGGCTTTTT
Tde1	tumor differentially expressed 1	Mm00449549_m1	TCCCTCGCCAGCTGGGTCCCGTGCC
Tdo2	tryptophan 2,3-dioxygenase	Mm00451266_m1	CCAAAATGGCCATGTCAGGGATGAG
Tex261	testis expressed gene 261	Mm00493609_m1	TCCTGTCATGCGGGCTAGTGGTGGT
Tgfa	transforming growth factor alpha	Mm00446231_m1	GCTAGCGCTGGGTATCCTGTTAGCT
Tgfb1	transforming growth factor, beta 1	Mm00441724_m1	GTGGACCGCAACAACGCCATCTATG
Tgfb2	transforming growth factor, beta 2	Mm00436952_m1	CACCTCCCCTCCGAAAATGCCATCC
Tgfbi	transforming growth factor, beta induced, 68 kDa	Mm00493634_m1	GGTCGCCAGCACGGCCCCAATGTAT
Th1l	TH1-like homolog (Drosophila)	Mm00498553_m1	GACGGCGGCCAGCATCAGGAAGATG
Tjp1	tight junction protein 1	Mm00493699_m1	TCTGAGGGGAAGGCGGATGGTGCTA
Tnf	tumor necrosis factor	Mm00443258_m1	AAAGGGATGAGAAGTTCCCAAATGG
Tnfaip2	tumor necrosis factor, alpha-induced protein 2	Mm00447578_m1	GAACCTCTACCCCAATGATATTCTC
Tom1	target of myb1 homolog (chicken)	Mm00495692_m1	CTCCTGAGCAGATTGGGAAGCTGCG
Tpp2	tripeptidyl peptidase II	Mm00447609_m1	TCCCAAGCCAATAAACTAATCAAGG
Tra1	tumor rejection antigen gp96	Mm00441926_m1	TCCTGCTGACCTTCGGGTTCGTCAG
Trap100	thyroid hormone receptor-associated protein 100 kDa	Mm00501920_m1	CATTAGTTCCCAGATGGTGTCCTGC
Trp53	transformation related protein 53	Mm00441964_g1	GGGAGCGCAAAGAGAGCGCTGCCCA
Tssc4	tumor-suppressing subchromosomal transferable fragment 4	Mm00502351_g1	TAGTGGAGGTGGGACGGGTGTCAGG
Ttc3	tetratricopeptide repeat domain	Mm00493917_m1	CACCTCCAAGTCAGCCTCCAAGACA
Ttr	transthyretin	Mm00443267_m1	ATGAATTCGCGGATGTGGTTTTCAC
Txn2	thioredoxin 2	Mm00444931_m1	ACTTTCATGCACAGTGGTGTGGCCC
Txnip	thioredoxin interacting protein	Mm00452393_m1	AGAGCAGCCTACAGGTGAGAACGAG
Uchl5	ubiquitin carboxyl-terminal esterase L5	Mm00497950_m1	TTTTGCCAAGCAGGTAATTAATAAT
Ulk2	Unc-51 like kinase 2 (C. elegans)	Mm00497023_m1	AGGCACTCCTCAGGTTCTCCAGTGC
Unc5h3	unc5 homolog (C. elegans) 3	Mm00494093_m1	ACAATGGGAGGATGTTGTGGTGGTT
Ung	uracil-DNA glycosylase	Mm00449156_m1	GACATCCGAGATGTGAAGGTTGTCA
Usf1	upstream transcription factor 1	Mm00447694_m1	GTCGTTCTCGGGCAAGGACTTAGCA
Usp14	ubiquitin specific protease 14	Mm00458097_m1	CAACCGCTATGGAATTGCCATGTGG
Usp21	ubiquitin specific protease 21	Mm00450059_m1	TGACAAGATGGCTCACCACACACTG
Usp4	ubiquitin specific protease 4 (proto-oncogene)	Mm00495954_m1	GTTCCCAGTCAGAGCTCTGAACATG
Usp5	ubiquitin specific protease 5 (isopeptidase T)	Mm00496731_m1	CACGCCGGAGTCTGAGGGTGGCCTC
Vamp8	vesicle-associated membrane protein 8	Mm00450314_m1	TTGGAAGCCACGTCTGAACACTTCA
Vapb	vesicle-associated membrane protein, associated protein B and C	Mm00498148_m1	CAAGTTCCGAGGTCCCTTCACTGAT
Vps29	vacuolar protein sorting 29 (S. pombe)	Mm00451139_m1	ACAGGATGTTGGTGTTGGTACTAGG
Wbp1	WW domain binding protein 1	Mm00497419_m1	GCAACAGCAGCAGAGTCCGGCAGCA

Gene Symbol	Gene Name	Assay ID	Context Sequence
Wee1	wee 1 homolog (S. pombe)	Mm00494175_m1	ACGAATACTGTAATGGTGGGAGTTT
Wisp2	WNT1 inducible signaling pathway protein 2	Mm00497471_m1	GTGCTGTGTGCCTCTTCGAAGAGGA
Xpa	xeroderma pigmentosum, complementation group A	Mm00457111_m1	ATGAACCAGGGCCCGTCATGGAGTT
Xpc	xeroderma pigmentosum, complementation group C	Mm00456378_m1	AGGAGAGCGTTGCGGATGACTTTGA
Xrcc1	X-ray repair complementing defective repair in Chinese hamster cells 1	Mm00494229_m1	CTGCCCTCCCGGAGGTACCTCATGG
0610009M14 Rik	RIKEN cDNA 0610009M14 gene	Mm00470231_m1	GCGATGACGATAGTGGTTCCGGAAG
0610040D20 Rik	RIKEN cDNA 0610040D20 gene	Mm00480910_m1	GGACCGCCCAACTCGAGAGCATACA
0710008N11 Rik	RIKEN cDNA 0710008N11 gene	Mm00458268_m1	TCGGCCTGCAGTTTCAGGCCTGTCG
1110021H02 Rik	RIKEN cDNA 1110021H02 gene	Mm00502923_m1	AATATCAGTCCCTGATCCGGTATGT
2610203K23Rik	RIKEN cDNA 2610203K23 gene	Mm00508088_m1	GAGAGAACGCTGACGGTTCATGAGA
5830483C08Rik	RIKEN cDNA 5830483C08 gene	Mm00724022_m1	GAAGCCCCACCTCAGGAACCTATTT

Appendix 3. Hierarchical clustering or RT-PCR data demonstrates PPARα-dependence of WY-14,643 modulated genes involved in processes similarly identified by microarray analysis.

Over 300 genes were probed using RT-PCR low-density arrays. $\Delta\Delta C_T$ quantification was performed as described in "Materials and Methods." Genes that are visually differentially expressed in the heatmap were submitted to GOMiner for pathway analysis.

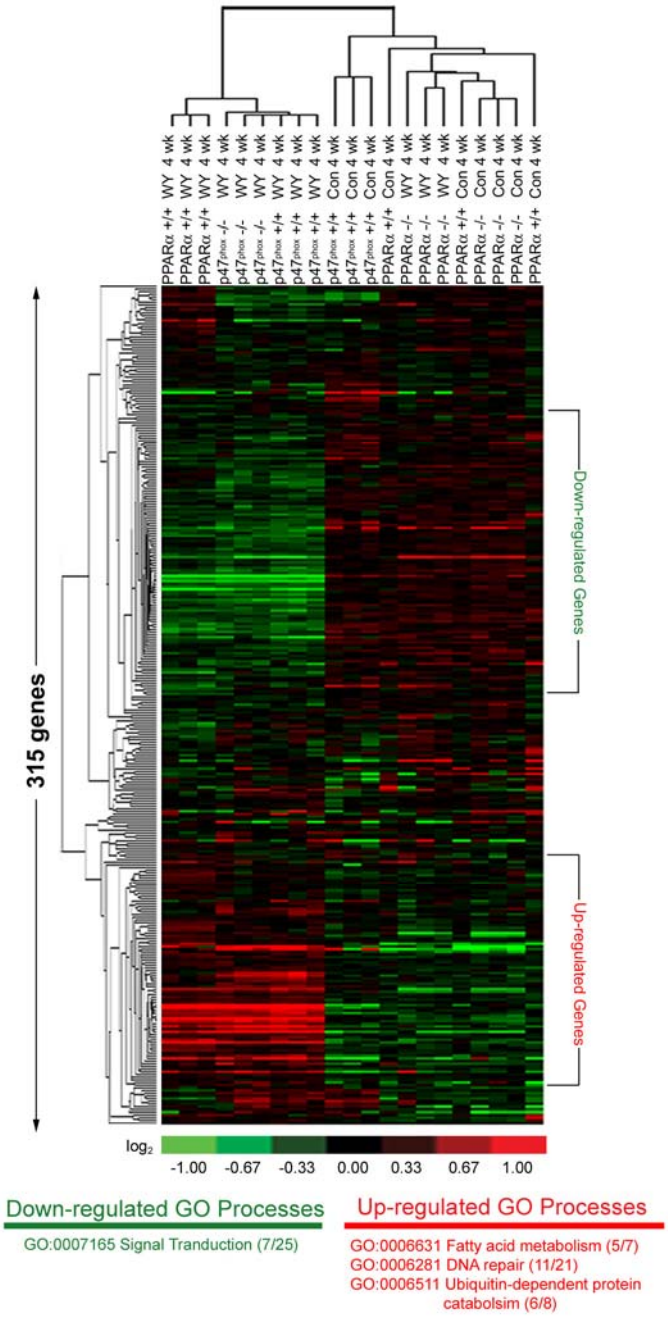
PPARα +/+ WY 4 wk
PPARα +/+ WY 4 wk
PPARα +/+ WY 4 wk
p47phox -/- WY 4 wk
p47phox -/- WY 4 wk
p47phox -/- WY 4 wk
p47phox +/+ WY 4 wk
p47phox +/+ WY 4 wk
p47phox +/+ WY 4 wk
p47phox +/+ Con 4 wk
p47phox +/+ Con 4 wk
p47phox +/+ Con 4 wk
PPARα +/+ Con 4 wk
PPARα -/- WY 4 wk
PPARα -/- WY 4 wk
PPARα -/- WY 4 wk
PPARα +/+ Con 4 wk
PPARα -/- Con 4 wk
PPARα -/- Con 4 wk
PPARα -/- Con 4 wk
PPARα +/+ Con 4 wk
315 genes
Down-regulated Genes
Up-regulated Genes
log2
-1.00 -0.67 -0.33 0.00 0.33 0.67 1.00
Down-regulated GO Processes
GO:0007165 Signal Tranduction (7/25)
Up-regulated GO Processes
GO:0006631 Fatty acid metabolism (5/7)
GO:0006281 DNA repair (11/21)
GO:0006511 Ubiquitin-dependent protein catabolsim (6/8)

REFERENCES

[1] Gonzalez, F. J.; Peters, J. M.; Cattley, R. C. Mechanism of action of the nongenotoxic peroxisome proliferators: role of the peroxisome proliferator-activator receptor alpha. *J. Natl. Cancer Inst.* **90**:1702-1709; 1998.

[2] Huber, W. W.; Grasl-Kraupp, B.; Schulte-Hermann, R. Hepatocarcinogenic potential of di(2-ethylhexyl)phthalate in rodents and its implications on human risk. *Crit. Rev. Toxicol.* **26**:365-481; 1996.

[3] Wilkinson, C. F.; Lamb, J. C. The potential health effects of phthalate esters in children's toys: a review and risk assessment. *Regul. Toxicol. Pharmacol.* **30**:140-155; 1999.

[4] International Agency for Research on Cancer Peroxisome proliferation and its role in carcinogenesis. *IARC Technical Report* **24**: 2000.

[5] Frick, M. H.; Elo, O.; Haapa, K.; Heinonen, O. P.; Heinsalmi, P.; Helo, P.; Huttunen, J. K.; Kaitaniemi, P.; Koskinen, P.; Manninen, V.; . Helsinki Heart Study: primary-prevention trial with gemfibrozil in middle-aged men with dyslipidemia. Safety of treatment, changes in risk factors, and incidence of coronary heart disease. *N Engl J Med* **317**:1237-1245; 1987.

[6] Huttunen, J. K.; Heinonen, O. P.; Manninen, V.; Koskinen, P.; Hakulinen, T.; Teppo, L.; Manttari, M.; Frick, M. H. The Helsinki Heart Study: an 8.5-year safety and mortality follow-up. *J. Intern. Med.* **235**:31-39; 1994.

[7] Thiess, A. M.; Fleig, I. [Chromosome studies in workers exposed to di-2-ethylhexyl phthalate]. *Zentralbl. Arbeitsmed. Arbeitsschutz. Prophyl.* **28**:351-355; 1978.

[8] Issemann, I.; Green, S. Activation of a member of the steroid hormone receptor superfamily by peroxisome proliferators. *Nature* **347**:645-650; 1990.

[9] Reddy, J. K.; Krishnakantha, T. P. Hepatic peroxisome proliferation: induction by two novel compounds structurally unrelated to clofibrate. *Science* **190**:787-789; 1975.

[10] Klaunig, J. E.; Babich, M. A.; Baetcke, K. P.; Cook, J. C.; Corton, J. C.; David, R. M.; Deluca, J. G.; Lai, D. Y.; McKee, R. H.; Peters, J. M.; Roberts, R. A.; Fenner-Crisp, P. A. PPARalpha agonist-induced rodent tumors: modes of action and human relevance. *Crit Rev. Toxicol.* **33**:655-780; 2003.

[11] Cattley, R. C.; DeLuca, J.; Elcombe, C.; Fenner-Crisp, P.; Lake, B. G.; Marsman, D. S.; Pastoor, T. A.; Popp, J. A.; Robinson, D. E.; Schwetz, B.; Tugwood, J.; Wahli, W. Do peroxisome proliferating compounds pose a hepatocarcinogenic hazard to humans? *Regul. Toxicol. Pharmacol.* **27**:47-60; 1998.

[12] Staels, B.; Dallongeville, J.; Auwerx, J.; Schoonjans, K.; Leitersdorf, E.; Fruchart, J. C. Mechanism of action of fibrates on lipid and lipoprotein metabolism. *Circulation* **98**:2088-2093; 1998.

[13] Awasthi, Y. C.; Singh, S. V.; Goel, S. K.; Reddy, J. K. Irreversible inhibition of hepatic glutathione S-transferase by ciprofibrate, a peroxisome proliferator. *Biochem. Biophys. Res. Commun.* **123**:1012-1018; 1984.

[14] Hoivik, D. J.; Qualls, C. W., Jr.; Mirabile, R. C.; Cariello, N. F.; Kimbrough, C. L.; Colton, H. M.; Anderson, S. P.; Santostefano, M. J.; Morgan, R. J.; Dahl, R. R.; Brown, A. R.; Zhao, Z.; Mudd, P. N., Jr.; Oliver, W. B., Jr.; Brown, H. R.; Miller, R. T. Fibrates induce hepatic peroxisome and mitochondrial proliferation without overt evidence of cellular proliferation and oxidative stress in cynomolgus monkeys. *Carcinogenesis* **25**:1757-1769; 2004.

[15] Muerhoff, A. S.; Griffin, K. J.; Johnson, E. F. The peroxisome proliferator-activated receptor mediates the induction of CYP4A6, a cytochrome P450 fatty acid omega-hydroxylase, by clofibric acid. *J. Biol. Chem.* **267**:19051-19053; 1992.

[16] Reddy, J. K.; Rao, S.; Moody, D. E. Hepatocellular carcinomas in acatalasemic mice treated with nafenopin, a hypolipidemic peroxisome proliferator. *Cancer Res* **36**:1211-1217; 1976.

[17] Kluwe, W. M.; Haseman, J. K.; Douglas, J. F.; Huff, J. E. The carcinogenicity of dietary di(2-ethylhexyl) phthalate (DEHP) in Fischer 344 rats and B6C3F1 mice. *J Toxicol. Environ. Health* **10**:797-815; 1982.

[18] Lalwani, N. D.; Reddy, M. K.; Qureshi, S. A.; Reddy, J. K. Development of hepatocellular carcinomas and increased peroxisomal fatty acid beta-oxidation in rats fed [4-chloro-6-(2,3-xylidino)-2-pyrimidinylthio] acetic acid (Wy-14,643) in the semipurified diet. *Carcinogenesis* **2**:645-650; 1981.

[19] Reddy, J. K.; Azarnoff, D. L.; Hignite, C. E. Hypolipidaemic hepatic peroxisome proliferators form a novel class of chemical carcinogens. *Nature* **283**:397-398; 1980.

[20] Grasl-Kraupp, B.; Ruttkay-Nedecky, B.; Mullauer, L.; Taper, H.; Huber, W.; Bursch, W.; Schulte-Hermann, R. Inherent increase of apoptosis in liver tumors: implications for carcinogenesis and tumor regression. *Hepatology* **25**:906-912; 1997.

[21] Peters, J. M.; Cattley, R. C.; Gonzalez, F. J. Role of PPAR alpha in the mechanism of action of the nongenotoxic carcinogen and peroxisome proliferator Wy-14,643. *Carcinogenesis* **18**:2029-2033; 1997.

[22] Fan, C. Y.; Pan, J.; Usuda, N.; Yeldandi, A. V.; Rao, M. S.; Reddy, J. K. Steatohepatitis, spontaneous peroxisome proliferation and liver tumors in mice lacking peroxisomal fatty acyl-CoA oxidase. Implications for peroxisome proliferator-activated receptor alpha natural ligand metabolism. *J. Biol. Chem.* **273**:15639-15645; 1998.

[23] Rao, M. S.; Lalwani, N. D.; Scarpelli, D. G.; Reddy, J. K. The absence of gamma-glutamyl transpeptidase activity in putative preneoplastic lesions and in

hepatocellular carcinomas induced in rats by the hypolipidemic peroxisome proliferator Wy-14,643. *Carcinogenesis* **3**:1231-1233; 1982.

[24] Rao, M. S.; Reddy, J. K. Hepatocarcinogenesis of peroxisome proliferators. *Ann N Y. Acad Sci* **804**:573-587; 1996.

[25] Chu, R.; Lim, H.; Brumfield, L.; Liu, H.; Herring, C.; Ulintz, P.; Reddy, J. K.; Davison, M. Protein profiling of mouse livers with peroxisome proliferator-activated receptor alpha activation. *Mol. Cell Biol.* **24**:6288-6297; 2004.

[26] Reddy, J. K.; Lalwani, N. D.; Qureshi, S.; Reddy, M. K.; Moehle, C. M. Induction of hepatic peroxisome proliferation in nonrodent species, including primates. *Am. J. Pathol.* **114**:171-183; 1984.

[27] James, N. H.; Roberts, R. A. Species differences in response to peroxisome proliferators correlate in vitro with induction of DNA synthesis rather than suppression of apoptosis. *Carcinogenesis* **17**:1623-1632; 1996.

[28] Palmer, C. N.; Hsu, M. H.; Griffin, K. J.; Raucy, J. L.; Johnson, E. F. Peroxisome proliferator activated receptor-alpha expression in human liver. *Mol. Pharmacol.* **53**:14-22; 1998.

[29] Hsu, M. H.; Savas, U.; Griffin, K. J.; Johnson, E. F. Identification of peroxisome proliferator-responsive human genes by elevated expression of the peroxisome proliferator-activated receptor alpha in HepG2 cells. *J Biol. Chem* **276**:27950-27958; 2001.

[30] Lawrence, J. W.; Li, Y.; Chen, S.; Deluca, J. G.; Berger, J. P.; Umbenhauer, D. R.; Moller, D. E.; Zhou, G. Differential gene regulation in human versus rodent hepatocytes by peroxisome proliferator-activated receptor (PPAR) alpha. PPAR alpha fails to induce peroxisome proliferation-associated genes in human cells independently of the level of receptor expresson. *J Biol. Chem* **276**:31521-31527; 2001.

[31] Woodyatt, N. J.; Lambe, K. G.; Myers, K. A.; Tugwood, J. D.; Roberts, R. A. The peroxisome proliferator (PP) response element upstream of the human acyl CoA oxidase gene is inactive among a sample human population: significance for species differences in response to PPs. *Carcinogenesis* **20**:369-372; 1999.

[32] Ito, Y.; Yokota, H.; Wang, R.; Yamanoshita, O.; Ichihara, G.; Wang, H.; Kurata, Y.; Takagi, K.; Nakajima, T. Species differences in the metabolism of di(2-ethylhexyl) phthalate (DEHP) in several organs of mice, rats, and marmosets. *Arch Toxicol.* **79**:147-154; 2005.

[33] Lee, S. S.; Pineau, T.; Drago, J.; Lee, E. J.; Owens, J. W.; Kroetz, D. L.; Fernandez-Salguero, P. M.; Westphal, H.; Gonzalez, F. J. Targeted disruption of the alpha isoform of the peroxisome proliferator- activated receptor gene in mice results in

abolishment of the pleiotropic effects of peroxisome proliferators. *Mol. Cell Biol.* **15**:3012-3022; 1995.

[34] Zhang, X.; Tanaka, N.; Nakajima, T.; Kamijo, Y.; Gonzalez, F. J.; Aoyama, T. Peroxisome proliferator-activated receptor alpha-independent peroxisome proliferation. *Biochem Biophys. Res Commun.* **346**:1307-1311; 2006.

[35] Reddy, J. K.; Rao, M. S.; Azarnoff, D. L.; Sell, S. Mitogenic and carcinogenic effects of a hypolipidemic peroxisome proliferator, [4-chloro-6-(2,3-xylidino)-2-pyrimidinylthio]acetic acid (Wy-14, 643), in rat and mouse liver. *Cancer Res.* **39**:152-161; 1979.

[36] Yeldandi, A. V.; Milano, M.; Subbarao, V.; Reddy, J. K.; Rao, M. S. Evaluation of liver cell proliferation during ciprofibrate-induced hepatocarcinogenesis. *Cancer Lett.* **47**:21-27; 1989.

[37] Moody, D. E.; Reddy, J. K.; Lake, B. G.; Popp, J. A.; Reese, D. H. Peroxisome proliferation and nongenotoxic carcinogenesis: commentary on a symposium. *Fundam. Appl. Toxicol.* **16**:233-248; 1991.

[38] Marsman, D. S.; Cattley, R. C.; Conway, J. G.; Popp, J. A. Relationship of hepatic peroxisome proliferation and replicative DNA synthesis to the hepatocarcinogenicity of the peroxisome proliferators di(2-ethylhexyl)phthalate and [4-chloro-6-(2,3-xylidino)-2- pyrimidinylthio]acetic acid (Wy-14,643) in rats. *Cancer Res.* **48**:6739-6744; 1988.

[39] Peters, J. M.; Aoyama, T.; Cattley, R. C.; Nobumitsu, U.; Hashimoto, T.; Gonzalez, F. J. Role of peroxisome proliferator-activated receptor alpha in altered cell cycle regulation in mouse liver. *Carcinogenesis* **19**:1989-1994; 1998.

[40] Roberts, R. A.; Soames, A. R.; Gill, J. H.; James, N. H.; Wheeldon, E. B. Non-genotoxic hepatocarcinogens stimulate DNA synthesis and their withdrawal induces apoptosis, but in different hepatocyte populations. *Carcinogenesis* **16**:1693-1698; 1995.

[41] Rolfe, M.; James, N. H.; Roberts, R. A. Tumour necrosis factor alpha (TNF alpha) suppresses apoptosis and induces DNA synthesis in rodent hepatocytes: a mediator of the hepatocarcinogenicity of peroxisome proliferators? *Carcinogenesis* **18**:2277-2280; 1997.

[42] Yeldandi, A. V.; Rao, M. S.; Reddy, J. K. Hydrogen peroxide generation in peroxisome proliferator-induced oncogenesis. *Mutat. Res.* **448**:159-177; 2000.

[43] Gueraud, F.; Alary, J.; Costet, P.; Debrauwer, L.; Dolo, L.; Pineau, T.; Paris, A. In vivo involvement of cytochrome P450 4A family in the oxidative metabolism of the lipid peroxidation product trans-4-hydroxy-2-nonenal, using PPARalpha-deficient mice. *J Lipid Res* **40**:152-159; 1999.

[44] Nemali, M. R.; Reddy, M. K.; Usuda, N.; Reddy, P. G.; Comeau, L. D.; Rao, M. S.; Reddy, J. K. Differential induction and regulation of peroxisomal enzymes: predictive value of peroxisome proliferation in identifying certain nonmutagenic carcinogens. *Toxicol. Appl. Pharmacol.* **97**:72-87; 1989.

[45] Milton, M. N.; Elcombe, C. R.; Gibson, G. G. On the mechanism of induction of microsomal cytochrome P450IVA1 and peroxisome proliferation in rat liver by clofibrate. *Biochem Pharmacol.* **40**:2727-2732; 1990.

[46] Rusyn, I.; Kadiiska, M. B.; Dikalova, A.; Kono, H.; Yin, M.; Tsuchiya, K.; Mason, R. P.; Peters, J. M.; Gonzalez, F. J.; Segal, B. H.; Holland, S. M.; Thurman, R. G. Phthalates rapidly increase production of reactive oxygen species in vivo: role of Kupffer cells. *Mol. Pharmacol.* **59**:744-750; 2001.

[47] Reddy, J. K.; Goel, S. K.; Nemali, M. R.; Carrino, J. J.; Laffler, T. G.; Reddy, M. K.; Sperbeck, S. J.; Osumi, T.; Hashimoto, T.; Lalwani, N. D.; . Transcription regulation of peroxisomal fatty acyl-CoA oxidase and enoyl-CoA hydratase/3-hydroxyacyl-CoA dehydrogenase in rat liver by peroxisome proliferators. *Proc. Natl. Acad. Sci. U. S. A* **83**:1747-1751; 1986.

[48] Tomaszewski, K. E.; Heindel, S. W.; Jenkins, W. L.; Melnick, R. L. Induction of peroxisomal acyl CoA oxidase activity and lipid peroxidation in primary rat hepatocyte cultures. *Toxicology* **65**:49-60; 1990.

[49] Akbiyik, F.; Cinar, K.; Demirpence, E.; Ozsullu, T.; Tunca, R.; Haziroglu, R.; Yurdaydin, C.; Uzunalimoglu, O.; Bozkaya, H. Ligand-induced expression of peroxisome proliferator-activated receptor alpha and activation of fatty acid oxidation enzymes in fatty liver. *Eur. J Clin. Invest* **34**:429-435; 2004.

[50] Soliman, M. S.; Cunningham, M. L.; Morrow, J. D.; Roberts, L. J.; Badr, M. Z. Evidence against peroxisome proliferation-induced hepatic oxidative damage. *Biochem. Pharmacol.* **53**:1369-1374; 1997.

[51] Kasai, H.; Okada, Y.; Nishimura, S.; Rao, M. S.; Reddy, J. K. Formation of 8-hydroxydeoxyguanosine in liver DNA of rats following long-term exposure to a peroxisome proliferator. *Cancer Res.* **49**:2603-2605; 1989.

[52] Takagi, A.; Sai, K.; Umemura, T.; Hasegawa, R.; Kurokawa, Y. Significant increase of 8-hydroxydeoxyguanosine in liver DNA of rats following short-term exposure to the peroxisome proliferators di(2- ethylhexyl)phthalate and di(2-ethylhexyl)adipate. *Jpn. J. Cancer Res.* **81**:213-215; 1990.

[53] Cattley, R. C.; Glover, S. E. Elevated 8-hydroxydeoxyguanosine in hepatic DNA of rats following exposure to peroxisome proliferators: Relationship to carcinogenesis and nuclear localization. *Carcinogenesis* **14**:2495-2499; 1993.

[54] Hegi, M. E.; Ulrich, D.; Sagelsdorff, P.; Richter, C.; Lutz, W. K. No measurable increase in thymidine glycol or 8-hydroxydeoxyguanosine in liver DNA of rats

treated with nafenopin or choline-devoid low- methionine diet. *Mutat. Res.* **238**:325-329; 1990.

[55] Hardwick, J. P.; Song, B. J.; Huberman, E.; Gonzalez, F. J. Isolation, complementary DNA sequence, and regulation of rat hepatic lauric acid omega-hydroxylase (cytochrome P-450LA omega). Identification of a new cytochrome P-450 gene family. *J Biol. Chem* **262**:801-810; 1987.

[56] Johnson, E. F.; Palmer, C. N.; Griffin, K. J.; Hsu, M. H. Role of the peroxisome proliferator-activated receptor in cytochrome P450 4A gene regulation. *FASEB J* **10**:1241-1248; 1996.

[57] Peters, J. M.; Hennuyer, N.; Staels, B.; Fruchart, J. C.; Fievet, C.; Gonzalez, F. J.; Auwerx, J. Alterations in lipoprotein metabolism in peroxisome proliferator-activated receptor alpha-deficient mice. *J Biol. Chem* **272**:27307-27312; 1997.

[58] Mehendale, H. M. PPAR-alpha: a key to the mechanism of hepatoprotection by clofibrate. *Toxicol. Sci* **57**:187-190; 2000.

[59] Wheeler, M. D.; Smutney, O. M.; Check, J. F.; Rusyn, I.; Schulte-Hermann, R.; Thurman, R. G. Impaired Ras membrane association and activation in PPARalpha knockout mice after partial hepatectomy. *Am. J. Physiol Gastrointest. Liver Physiol* **284**:G302-G312; 2003.

[60] Bayly, A. C.; Roberts, R. A.; Dive, C. Suppression of liver cell apoptosis in vitro by the non-genotoxic hepatocarcinogen and peroxisome proliferator nafenopin. *J Cell Biol.* **125**:197-203; 1994.

[61] Oberhammer, F. A.; Qin, H. M. Effect of three tumour promoters on the stability of hepatocyte cultures and apoptosis after transforming growth factor-beta 1. *Carcinogenesis* **16**:1363-1371; 1995.

[62] Roberts, R. A.; James, N. H.; Woodyatt, N. J.; Macdonald, N.; Tugwood, J. D. Evidence for the suppression of apoptosis by the peroxisome proliferator activated receptor alpha. *Carcinogenesis* **19**:43-48; 1998.

[63] Bojes, H. K.; Thurman, R. G. Peroxisome proliferators activate Kupffer cells *in vivo*. *Cancer Res.* **56**:1-4; 1996.

[64] Peters, J. M.; Rusyn, I.; Rose, M. L.; Gonzalez, F. J.; Thurman, R. G. Peroxisome proliferator-activated receptor alpha is restricted to hepatic parenchymal cells, not Kupffer cells: implications for the mechanism of action of peroxisome proliferators in hepatocarcinogenesis. *Carcinogenesis* **21**:823-826; 2000.

[65] Rose, M. L.; Germolec, D.; Arteel, G. E.; Schoonhoven, R.; Thurman, R. G. Dietary glycine prevents increases in hepatocyte proliferation caused by the peroxisome proliferator WY-14,643. *Chem. Res. Toxicol.* **10**:1198-1204; 1997.

[66] Rose, M. L.; Germolec, D. R.; Schoonhoven, R.; Thurman, R. G. Kupffer cells are causally responsible for the mitogenic effect of peroxisome proliferators. *Carcinogenesis* **18**:1453-1456; 1997.

[67] Bojes, H. K.; Germolec, D. R.; Simeonova, P.; Bruccoleri, A.; Schoonhoven, R.; Luster, M. I.; Thurman, R. G. Antibodies to tumor necrosis factor alpha prevent increases in cell replication in liver due to the potent peroxisome proliferator, WY-14,643. *Carcinogenesis* **18**:669-674; 1997.

[68] Heller, R. A.; Kronke, M. Tumor necrosis factor receptor-mediated signaling pathways. *J. Cell Biol.* **126**:5-9; 1994.

[69] Decker, K. Biologically active products of stimulated liver macrophages (Kupffer cells). *Eur. J. Biochem.* **192**:245-261; 1990.

[70] Hasmall, S. C.; James, N. H.; Hedley, K.; Olsen, K.; Roberts, R. A. Mouse hepatocyte response to peroxisome proliferators: dependency on hepatic nonparenchymal cells and peroxisome proliferator receptor α (PPARα). *Arch. Toxicol.* **75**:357-361; 2001.

[71] Parzefall, W.; Berger, W.; Kainzbauer, E.; Teufelhofer, O.; Schulte-Hermann, R.; Thurman, R. G. Peroxisome proliferators do not increase DNA synthesis in purified rat hepatocytes. *Carcinogenesis* **22**:519-523; 2001.

[72] Baldwin, A. S., Jr. The NF-kappa B and I kappa B proteins: new discoveries and insights. *Annu. Rev. Immunol.* **14**:649-683; 1996.

[73] Li, Y.; Leung, L. K.; Glauert, H. P.; Spear, B. T. Treatment of rats with the peroxisome proliferator ciprofibrate results in increased liver NF-kappaB activity. *Carcinogenesis* **17**:2305-2309; 1996.

[74] Rusyn, I.; Tsukamoto, H.; Thurman, R. G. WY-14,643 rapidly activates nuclear factor kappaB in Kupffer cells before hepatocytes. *Carcinogenesis* **19**:1217-1222; 1998.

[75] Calfee-Mason, K. G.; Spear, B. T.; Glauert, H. P. Effects of vitamin E on the NF-kappaB pathway in rats treated with the peroxisome proliferator, ciprofibrate. *Toxicol. Appl. Pharmacol.* **199**:1-9; 2004.

[76] Rose, M. L.; Rivera, C. A.; Bradford, B. U.; Graves, L. M.; Cattley, R. C.; Schoonhoven, R.; Swenberg, J. A.; Thurman, R. G. Kupffer cell oxidant production is central to the mechanism of peroxisome proliferators. *Carcinogenesis* **20**:27-33; 1999.

[77] Rusyn, I.; Yamashina, S.; Segal, B. H.; Schoonhoven, R.; Holland, S. M.; Cattley, R. C.; Swenberg, J. A.; Thurman, R. G. Oxidants from nicotinamide adenine dinucleotide phosphate oxidase are involved in triggering cell proliferation in the liver due to peroxisome proliferators. *Cancer Res.* **60**:4798-4803; 2000.

[78] Lake, B. G. Peroxisome proliferation: current mechanisms relating to nongenotoxic carcinogenesis. *Toxicol. Lett.* **82-83**:673-681; 1995.

[79] Reddy, J. K.; Azarnoff, D. L.; Hignite, C. E. Hypolipidaemic hepatic peroxisome proliferators form a novel class of chemical carcinogens. *Nature* **283**:397-398; 1980.

[80] Reddy, J. K.; Rao, M. S. Peroxisome proliferation and hepatocarcinogenesis. *IARC Sci. Publ.* 225-235; 1992.

[81] Peters, J. M.; Cheung, C.; Gonzalez, F. J. Peroxisome proliferator-activated receptor-alpha and liver cancer: where do we stand? *J Mol. Med* **83**:774-785; 2005.

[82] Conway, J. G.; Tomaszewski, K. E.; Olson, M. J.; Cattley, R. C.; Marsman, D. S.; Popp, J. A. Relationship of oxidative damage to the hepatocarcinogenicity of the peroxisome proliferators di(2-ethylhexyl)phthalate and Wy-14,643. *Carcinogenesis* **10**:513-519; 1989.

[83] Suzuki, Y. J.; Forman, H. J.; Sevanian, A. Oxidants as stimulators of signal transduction. *Free Radic. Biol. Med* **22**:269-285; 1997.

[84] Akiyama, T. E.; Nicol, C. J.; Fievet, C.; Staels, B.; Ward, J. M.; Auwerx, J.; Lee, S. S.; Gonzalez, F. J.; Peters, J. M. Peroxisome proliferator-activated receptor-alpha regulates lipid homeostasis, but is not associated with obesity: studies with congenic mouse lines. *J Biol. Chem* **276**:39088-39093; 2001.

[85] Jackson, S. H.; Gallin, J. I.; Holland, S. M. The $p47^{phox}$ mouse knock-out model of chronic granulomatous disease. *J. Exp. Med.* **182**:751-758; 1995.

[86] Zhong, Z.; Froh, M.; Connor, H. D.; Li, X.; Conzelmann, L. O.; Mason, R. P.; Lemasters, J. J.; Thurman, R. G. Prevention of hepatic ischemia-reperfusion injury by green tea extract. *Am. J Physiol Gastrointest. Liver Physiol* **283**:G957-G964; 2002.

[87] Tomaszewski, K. E.; Derks, M. C.; Melnick, R. L. Acyl CoA oxidase is the most suitable marker for hepatic peroxisomal changes caused by treatment of F344 rats with di(2-ethylhexyl)phthalate. *Toxicol. Lett.* **37**:203-212; 1987.

[88] NASH, T. The colorimetric estimation of formaldehyde by means of the Hantzsch reaction. *Biochem J* **55**:416-421; 1953.

[89] Smith, P. K.; Krohn, R. I.; Hermanson, G. T.; Mallia, A. K.; Gartner, F. H.; Provenzano, M. D.; Fujimoto, E. K.; Goeke, N. M.; Olson, B. J.; Klenk, D. C. Measurement of protein using bicinchoninic acid. *Anal. Biochem* **150**:76-85; 1985.

[90] Dikalova, A. E.; Kadiiska, M. B.; Mason, R. P. An in vivo ESR spin-trapping study: free radical generation in rats from formate intoxication--role of the Fenton reaction. *Proc. Natl. Acad. Sci. U. S. A* **98**:13549-13553; 2001.

[91] Hayashi, Y.; Ueda, Y.; Nakajima, A.; Mitsuyama, Y. EPR evidence of hydroxyl radical generation as an initiator of lipid peroxidation in amyloid beta-protein-stimulated PC12 cells. *Brain Res* **1025**:29-34; 2004.

[92] Rusyn, I.; Denissenko, M. F.; Wong, V. A.; Butterworth, B. E.; Cunningham, M. L.; Upton, P. B.; Thurman, R. G.; Swenberg, J. A. Expression of base excision repair enzymes in rat and mouse liver is induced by peroxisome proliferators and is dependent upon carcinogenic potency. *Carcinogenesis* **21**:2141-2145; 2000.

[93] Reddy, J. K.; Rao, M. S. Oxidative DNA damage caused by persistent peroxisome proliferation: its role in hepatocarcinogenesis. *Mutat. Res.* **214**:63-68; 1989.

[94] Rusyn, I.; Rose, M. L.; Bojes, H. K.; Thurman, R. G. Novel role of oxidants in the molecular mechanism of action of peroxisome proliferators. *Antiox Redox Signal* **2**:607-621; 2000.

[95] Nemali, M. R.; Usuda, N.; Reddy, M. K.; Oyasu, K.; Hashimoto, T.; Osumi, T.; Rao, M. S.; Reddy, J. K. Comparison of constitutive and inducible levels of expression of peroxisomal beta-oxidation and catalase genes in liver and extrahepatic tissues of rat. *Cancer Res.* **48**:5316-5324; 1988.

[96] Rusyn, I.; Peters, J. M.; Cunningham, M. L. Modes of action and species-specific effects of di-(2-ethylhexyl)phthalate in the liver. *Crit Rev. Toxicol.* **36**:459-479; 2006.

[97] Rose, M. L.; Rusyn, I.; Bojes, H. K.; Belyea, J.; Cattley, R. C.; Thurman, R. G. Role of Kupffer cells and oxidants in signaling peroxisome proliferator- induced hepatocyte proliferation. *Mutat. Res.* **448**:179-192; 2000.

[98] Fridovich, I. Biological effects of the superoxide radical. *Arch Biochem Biophys.* **247**:1-11; 1986.

[99] Dunford, H. B. Free radicals in iron-containing systems. *Free Radic. Biol. Med* **3**:405-421; 1987.

[100] Towner, R. A.; Qian, S. Y.; Kadiiska, M. B.; Mason, R. P. In vivo identification of aflatoxin-induced free radicals in rat bile. *Free Radic. Biol. Med* **35**:1330-1340; 2003.

[101] Nichols, P.; Schonbaum, G. R. Catalases. In Boyer, P. D. eds. *The Enzymes*. New York: Academic Press; 1963:147-225.

[102] Handler, J. A.; Thurman, R. G. Catalase-dependent ethanol oxidation in perfused rat liver. Requirement for fatty-acid-stimulated H2O2 production by peroxisomes. *Eur. J. Biochem.* **176**:477-484; 1988.

[103] Handler, J. A.; Seed, C. B.; Bradford, B. U.; Thurman, R. G. Induction of peroxisomes by treatment with perfluorooctanoate does not increase rates of H_2O_2 production in intact liver. *Toxicol. Lett.* **60**:61-68; 1992.

[104] Klucis, E.; Crane, D. I.; Hughes, J. L.; Poulos, A.; Masters, C. J. Identification of a catalase-negative sub-population of peroxisomes induced in mouse liver by clofibrate. *Biochim. Biophys. Acta* **1074**:294-301; 1991.

[105] Oikawa, I.; Novikoff, P. M. Catalase-negative peroxisomes: transient appearance in rat hepatocytes during liver regeneration after partial hepatectomy. *Am J Pathol.* **146**:673-687; 1995.

[106] Powanda, M. C.; Blackburn, B. S.; Bostian, K. A.; Fowler, J. P.; Hauer, E. C.; Pekarek, R. S. Clofibrate-induced alterations in zinc, iron and copper metabolism. *Biochem Pharmacol.* **27**:125-127; 1978.

[107] Huang, H. L.; Shaw, N. S. Role of hypolipidemic drug clofibrate in altering iron regulatory proteins IRP1 and IRP2 activities and hepatic iron metabolism in rats fed a low-iron diet. *Toxicol. Appl. Pharmacol.* **180**:118-128; 2002.

[108] Fischer, J. G.; Glauert, H. P.; Yin, T.; Sweeney-Reeves, M. L.; Larmonier, N.; Black, M. C. Moderate iron overload enhances lipid peroxidation in livers of rats, but does not affect NF-kappaB activation induced by the peroxisome proliferator, Wy-14,643. *J Nutr.* **132**:2525-2531; 2002.

[109] Hertz, R.; Seckbach, M.; Zakin, M. M.; Bar-Tana, J. Transcriptional suppression of the transferrin gene by hypolipidemic peroxisome proliferators. *J Biol. Chem.* **271**:218-224; 1996.

[110] Rusyn, I.; Asakura, S.; Pachkowski, B.; Bradford, B. U.; Denissenko, M. F.; Peters, J. M.; Holland, S. M.; Reddy, J. K.; Cunningham, M. L.; Swenberg, J. A. Expression of base excision DNA repair genes is a sensitive biomarker for in vivo detection of chemical-induced chronic oxidative stress: Identification of the molecular source of radicals responsible for DNA damage by peroxisome proliferators. *Cancer Res.* **64**:1050-1057; 2004.

[111] Reddy, J. K.; Moody, D. E.; Azarnoff, D. L.; Rao, M. S. Di-(2-ethylhexyl)phthalate: an industrial plasticizer induces hypolipidemia and enhances hepatic catalase and carnitine acetyltransferase activities in rat and mice. *Life Sci.* **18**:941-945; 1976.

[112] Bojes, H. K.; Rose, M. L.; Keller, B. J.; Germolec, D. R.; Simeonova, P.; Luster, M. I.; Thurman, R. G. Mitogenic actions of peroxidase proliferators: involvement of protein kinase C and tumor necrosis factor alpha. *Drug Metab Rev.* **29**:235-260; 1997.

[113] Mauton, P. R. Principles and Practices of Unbiased Stereology: An Introduction for Bioscientists: Baltimore, MD The Johns Hopkins University Press; 2002.

[114] Nakamura, J.; La, D. K.; Swenberg, J. A. 5'-nicked apurinic/apyrimidinic sites are resistant to β-elimination by β-polymerase and are persistent in human cultured cells after oxidative stress. *J. Biol. Chem.* **275**:5323-5328; 2000.

[115] Nakamura, J.; Swenberg, J. A. Endogenous apurinic/apyrimidinic sites in genomic DNA of mammalian tissues. *Cancer Res.* **59**:2522-2526; 1999.

[116] Ward, J. M.; Peters, J. M.; Perella, C. M.; Gonzalez, F. J. Receptor and nonreceptor-mediated organ-specific toxicity of di(2-ethylhexyl)phthalate (DEHP) in peroxisome proliferator-activated receptor alpha-null mice. *Toxicol. Pathol.* **26**:240-246; 1998.

[117] Torrey, C. E.; Campbell, J. A.; Hoivik, D. J.; Miller, R. T.; Allen, J. S.; Mann, P. C.; Selinger, K.; Rickert, D.; Savina, P. M.; Santostefano, M. J. Evaluation of the carcinogenic potential of clofibrate in the p53+/- mouse. *Int. J Toxicol.* **24**:289-299; 2005.

[118] Hurtt, M. E.; Elliott, G. S.; Cook, J. C.; Obourn, J. D.; Frame, S. R.; Biegel, L. B. Induction of coagulation effects by Wyeth-14,643 in Crl:CD BR rats. *Drug Chem Toxicol.* **20**:1-10; 1997.

[119] Johnson, T. E.; Zhang, X.; Shi, S.; Umbenhauer, D. R. Statins and PPARalpha agonists induce myotoxicity in differentiated rat skeletal muscle cultures but do not exhibit synergy with co-treatment. *Toxicol. Appl. Pharmacol.* **208**:210-221; 2005.

[120] Hasmall, S. C.; James, N. H.; Macdonald, N.; Gonzalez, F. J.; Peters, J. M.; Roberts, R. A. Suppression of mouse hepatocyte apoptosis by peroxisome proliferators: role of PPARalpha and TNFalpha. *Mutat. Res* **448**:193-200; 2000.

[121] Guttridge, D. C.; Albanese, C.; Reuther, J. Y.; Pestell, R. G.; Baldwin, A. S., Jr. NF-kappaB controls cell growth and differentiation through transcriptional regulation of cyclin D1. *Mol. Cell Biol.* **19**:5785-5799; 1999.

[122] Glauert, H. P.; Eyigor, A.; Tharappel, J. C.; Cooper, S.; Lee, E. Y.; Spear, B. T. Inhibition of Hepatocarcinogenesis by the Deletion of the p50 Subunit of NF-{kappa}B in Mice Administered the Peroxisome Proliferator Wy-14,643. *Toxicol. Sci* **90**:331-336; 2006.

[123] Varfolomeev, E. E.; Schuchmann, M.; Luria, V.; Chiannilkulchai, N.; Beckmann, J. S.; Mett, I. L.; Rebrikov, D.; Brodianski, V. M.; Kemper, O. C.; Kollet, O.; Lapidot, T.; Soffer, D.; Sobe, T.; Avraham, K. B.; Goncharov, T.; Holtmann, H.; Lonai, P.; Wallach, D. Targeted disruption of the mouse Caspase 8 gene ablates cell death induction by the TNF receptors, Fas/Apo1, and DR3 and is lethal prenatally. *Immunity.* **9**:267-276; 1998.

[124] Deutsch, W. A.; Kukreja, A.; Shane, B.; Hegde, V. Phenobarbital, oxazepam and Wyeth 14,643 cause DNA damage as measured by the Comet assay. *Mutagenesis* **16**:439-442; 2001.

[125] Berger, J. P.; Akiyama, T. E.; Meinke, P. T. PPARs: therapeutic targets for metabolic disease. *Trends Pharmacol. Sci.* **26**:244-251; 2005.

[126] Bammler, T.; Beyer, R. P.; Bhattacharya, S.; Boorman, G. A.; Boyles, A.; Bradford, B. U.; Bumgarner, R. E.; Bushel, P. R.; Chaturvedi, K.; Choi, D.; Cunningham, M. L.; Deng, S.; Dressman, H. K.; Fannin, R. D.; Farin, F. M.; Freedman, J. F.; Fry, R. C.; Harper, A.; Humble, M. C.; Hurban, P.; Kavanagh, T. J.; Kaufmann, W. K.; Kerr, K. F.; Jing, L.; Lapidus, J. A.; Lasarev, M. R.; Li, J.; Li, Y. J.; Lobenhofer, E. K.; Lu, X.; Malek, R. L.; Milton, S.; Nagalla, S. R.; O'Malley, J. P.; Palmer, V. S.; Pattee, P.; Paules, R. S.; Perou, C. M.; Phillips, K.; Qin, L.; Qiu, Y.; Quigley, S. D.; Rodland, M.; Rusyn, I.; Samson, L. D.; Schwartz, D. A.; Shi, Y.; Shin, J. L.; Sieber, S. O.; Slifer, S.; Speer, M. C.; Spencer, P. S.; Sproles, D. I.; Swenberg, J. A.; Suk, W. A.; Sullivan, R. C.; Tian, R.; Tennant, R. W.; Todd, S. A.; Tucker, C. J.; Houten, B. V.; Weis, B. K.; Xuan, S.; Zarbl, H.; Members of the Toxicogenomics Research Consortium Standardizing global gene expression analysis between laboratories and across platforms. *Nat. Methods* **2**:351-356; 2005.

[127] Troyanskaya, O.; Cantor, M.; Sherlock, G.; Brown, P.; Hastie, T.; Tibshirani, R.; Botstein, D.; Altman, R. B. Missing value estimation methods for DNA microarrays. *Bioinformatics.* **17**:520-525; 2001.

[128] Eisen, M. B.; Spellman, P. T.; Brown, P. O.; Botstein, D. Cluster analysis and display of genome-wide expression patterns. *Proc. Natl. Acad. Sci. U. S. A* **95**:14863-14868; 1998.

[129] Leek, J. T.; Monsen, E.; Dabney, A. R.; Storey, J. D. EDGE: extraction and analysis of differential gene expression. *Bioinformatics* **22**:507-508; 2006.

[130] Tusher, V. G.; Tibshirani, R.; Chu, G. Significance analysis of microarrays applied to the ionizing radiation response. *Proc. Natl. Acad. Sci. U. S. A* **98**:5116-5121; 2001.

[131] Storey, J. D.; Xiao, W.; Leek, J. T.; Tompkins, R. G.; Davis, R. W. Significance analysis of time course microarray experiments. *Proc. Natl. Acad Sci U. S. A* **102**:12837-12842; 2005.

[132] Zeeberg, B. R.; Qin, H.; Narasimhan, S.; Sunshine, M.; Cao, H.; Kane, D. W.; Reimers, M.; Stephens, R. M.; Bryant, D.; Burt, S. K.; Elnekave, E.; Hari, D. M.; Wynn, T. A.; Cunningham-Rundles, C.; Stewart, D. M.; Nelson, D.; Weinstein, J. N. High-Throughput GoMiner, an 'industrial-strength' integrative gene ontology tool for interpretation of multiple-microarray experiments, with application to studies of Common Variable Immune Deficiency (CVID). *BMC. Bioinformatics* **6**:168; 2005.

[133] Hosack, D. A.; Dennis, G., Jr.; Sherman, B. T.; Lane, H. C.; Lempicki, R. A. Identifying biological themes within lists of genes with EASE. *Genome Biol.* **4**:R70; 2003.

[134] Nikitin, A.; Egorov, S.; Daraselia, N.; Mazo, I. Pathway studio--the analysis and navigation of molecular networks. *Bioinformatics* **19**:2155-2157; 2003.

[135] Li, Z.; Diehl, A. M. Innate immunity in the liver. *Curr. Opin. Gastroenterol.* **19**:565-571; 2003.

[136] Teissier, E.; Nohara, A.; Chinetti, G.; Paumelle, R.; Cariou, B.; Fruchart, J. C.; Brandes, R. P.; Shah, A.; Staels, B. Peroxisome proliferator-activated receptor alpha induces NADPH oxidase activity in macrophages, leading to the generation of LDL with PPAR-alpha activation properties. *Circ. Res* **95**:1174-1182; 2004.

[137] Bey, E. A.; Cathcart, M. K. In vitro knockout of human p47phox blocks superoxide anion production and LDL oxidation by activated human monocytes. *J Lipid Res* **41**:489-495; 2000.

[138] Woods, C. G.; Burns, A. M.; Maki, A.; Bradford, B. U.; Cunningham, M. L.; Connor, H. D.; Kadiiska, M. B.; Mason, R. P.; Peters, J. M.; Rusyn, I. Sustained formation of alpha-(4-pyridyl-1-oxide)-N-tert-butylnitrone radical adducts in mouse liver by peroxisome proliferators is dependent upon peroxisome proliferator-activated receptor-alpha, but not NADPH oxidase. *Free Radic. Biol. Med.* doi:10.1016/j.freeradbiomed.2006.10.053; 2006.

[139] Rose, M. L.; Rusyn, I.; Bojes, H. K.; Germolec, D. R.; Luster, M.; Thurman, R. G. Role of Kupffer cells in peroxisome proliferator-induced hepatocyte proliferation. *Drug Metab Rev.* **31**:87-116; 1999.

[140] Kersten, S.; Mandard, S.; Escher, P.; Gonzalez, F. J.; Tafuri, S.; Desvergne, B.; Wahli, W. The peroxisome proliferator-activated receptor alpha regulates amino acid metabolism. *FASEB J* **15**:1971-1978; 2001.

[141] Devchand, P. R.; Keller, H.; Peters, J. M.; Vazquez, M.; Gonzalez, F. J.; Wahli, W. The PPARalpha-leukotriene B4 pathway to inflammation control. *Nature* **384**:39-43; 1996.

[142] Yang, Q.; Xie, Y.; Alexson, S. E.; Nelson, B. D.; DePierre, J. W. Involvement of the peroxisome proliferator-activated receptor alpha in the immunomodulation caused by peroxisome proliferators in mice. *Biochem Pharmacol.* **63**:1893-1900; 2002.

[143] Cunard, R.; DiCampli, D.; Archer, D. C.; Stevenson, J. L.; Ricote, M.; Glass, C. K.; Kelly, C. J. WY14,643, a PPAR alpha ligand, has profound effects on immune responses in vivo. *J Immunol.* **169**:6806-6812; 2002.

[144] Currie, R. A.; Bombail, V.; Oliver, J. D.; Moore, D. J.; Lim, F. L.; Gwilliam, V.; Kimber, I.; Chipman, K.; Moggs, J. G.; Orphanides, G. Gene ontology mapping as an unbiased method for identifying molecular pathways and processes affected by toxicant exposure: application to acute effects caused by the rodent non-genotoxic carcinogen diethylhexylphthalate. *Toxicol. Sci.* **86**:453-469; 2005.

[145] Cariello, N. F.; Romach, E. H.; Colton, H. M.; Ni, H.; Yoon, L.; Falls, J. G.; Casey, W.; Creech, D.; Anderson, S. P.; Benavides, G. R.; Hoivik, D. J.; Brown, R.; Miller, R. T. Gene expression profiling of the PPAR-alpha agonist ciprofibrate in the cynomolgus monkey liver. *Toxicol. Sci* **88**:250-264; 2005.

[146] Yamazaki, K.; Kuromitsu, J.; Tanaka, I. Microarray analysis of gene expression changes in mouse liver induced by peroxisome proliferator- activated receptor alpha agonists. *Biochem Biophys. Res Commun.* **290**:1114-1122; 2002.

[147] Fishelson, Z.; Attali, G.; Mevorach, D. Complement and apoptosis. *Mol. Immunol.* **38**:207-219; 2001.

[148] Ramadori, G.; Armbrust, T. Cytokines in the liver. *Eur. J Gastroenterol. Hepatol.* **13**:777-784; 2001.

[149] Hasmall, S. C.; West, D. A.; Olsen, K.; Roberts, R. A. Role of hepatic non-parenchymal cells in the response of rat hepatocytes to the peroxisome proliferator nafenopin in vitro. *Carcinogenesis* **21**:2159-2165; 2000.

[150] West, D. A.; James, N. H.; Cosulich, S. C.; Holden, P. R.; Brindle, R.; Rolfe, M.; Roberts, R. A. Role for tumor necrosis factor alpha receptor 1 and interleukin-1 receptor in the suppression of mouse hepatocyte apoptosis by the peroxisome proliferator nafenopin. *Hepatology* **30**:1417-1424; 1999.

[151] Anderson, S. P.; Dunn, C. S.; Cattley, R. C.; Corton, J. C. Hepatocellular proliferation in response to a peroxisome proliferator does not require TNFalpha signaling. *Carcinogenesis* **22**:1843-1851; 2001.

[152] Ledda-Columbano, G. M.; Curto, M.; Piga, R.; Zedda, A. I.; Menegazzi, M.; Sartori, C.; Shinozuka, H.; Bluethmann, H.; Poli, V.; Ciliberto, G.; Columbano, A. In vivo hepatocyte proliferation is inducible through a TNF and IL-6-independent pathway. *Oncogene* **17**:1039-1044; 1998.

[153] Alsarra, I. A.; Brockmann, W. G.; Cunninghamn, M. L.; Badr, M. Hepatocellular proliferation in response to agonists of peroxisome proliferator-activated receptor alpha: a role for kupffer cells? *Journal of Carcinogenesis* doi:10.1186/1477-3163-5-26; 2006.

[154] Tharappel, J. C.; Nalca, A.; Owens, A. B.; Ghabrial, L.; Konz, E. C.; Glauert, H. P.; Spear, B. T. Cell proliferation and apoptosis are altered in mice deficient in the NF-kappaB p50 subunit after treatment with the peroxisome proliferator ciprofibrate. *Toxicol. Sci* **75**:300-308; 2003.

[155] Delerive, P.; De Bosscher, K.; Besnard, S.; Vanden Berghe, W.; Peters, J. M.; Gonzalez, F. J.; Fruchart, J. C.; Tedgui, A.; Haegeman, G.; Staels, B. Peroxisome proliferator-activated receptor alpha negatively regulates the vascular inflammatory gene response by negative cross-talk with transcription factors NF-kappaB and AP-1. *J Biol. Chem* **274**:32048-32054; 1999.

[156] Li, Y.; Tharappel, J. C.; Cooper, S.; Glenn, M.; Glauert, H. P.; Spear, B. T. Expression of the hydrogen peroxide-generating enzyme fatty acyl CoA oxidase activates NF-kappaB. *DNA Cell Biol.* **19**:113-120; 2000.

[157] Delerive, P.; Gervois, P.; Fruchart, J. C.; Staels, B. Induction of IkappaBalpha expression as a mechanism contributing to the anti-inflammatory activities of peroxisome proliferator-activated receptor-alpha activators. *J Biol. Chem* **275**:36703-36707; 2000.

[158] Foijer, F.; Te, R. H. Restriction beyond the restriction point: mitogen requirement for G2 passage. *Cell Div.* **1**:8; 2006.

[159] White, I. R.; Man, W. J.; Bryant, D.; Bugelski, P.; Camilleri, P.; Cutler, P.; Hayes, W.; Holbrook, J. D.; Kramer, K.; Lord, P. G.; Wood, J. Protein expression changes in the Sprague Dawley rat liver proteome following administration of peroxisome proliferator activated receptor alpha and gamma ligands. *Proteomics.* **3**:505-512; 2003.

[160] Castrillo, A.; Tontonoz, P. Nuclear receptors in macrophage biology: at the crossroads of lipid metabolism and inflammation. *Annu. Rev. Cell Dev. Biol.* **20**:455-480; 2004.

[161] Patsouris, D.; Reddy, J. K.; Muller, M.; Kersten, S. Peroxisome proliferator-activated receptor alpha mediates the effects of high-fat diet on hepatic gene expression. *Endocrinology* **147**:1508-1516; 2006.

[162] Kliewer, S. A.; Forman, B. M.; Blumberg, B.; Ong, E. S.; Borgmeyer, U.; Mangelsdorf, D. J.; Umesono, K.; Evans, R. M. Differential expression and activation of a family of murine peroxisome proliferator-activated receptors. *Proc. Natl. Acad Sci U. S. A* **91**:7355-7359; 1994.

[163] Reddy, J. K.; Lalwani, N. D. Carcinogenesis by hepatic peroxisome proliferators: Evaluation of the risk of hypolipidemic drugs and industrial plasticizers in humans. *CRC Crit Rev Toxicol* **12**:1-58; 1983.

[164] Lambe, K. G.; Woodyatt, N. J.; Macdonald, N.; Chevalier, S.; Roberts, R. A. Species differences in sequence and activity of the peroxisome proliferator response element (PPRE) within the acyl CoA oxidase gene promoter. *Toxicol. Lett.* **110**:119-127; 1999.

[165] Cheung, C.; Akiyama, T. E.; Ward, J. M.; Nicol, C. J.; Feigenbaum, L.; Vinson, C.; Gonzalez, F. J. Diminished hepatocellular proliferation in mice humanized for the nuclear receptor peroxisome proliferator-activated receptor alpha. *Cancer Res* **64**:3849-3854; 2004.

[166] Morimura, K.; Cheung, C.; Ward, J. M.; Reddy, J. K.; Gonzalez, F. J. Differential susceptibility of mice humanized for peroxisome proliferator-activated receptor {alpha} to Wy-14,643-induced liver tumorigenesis. *Carcinogenesis* 2006.